

Project Proposal Reference Number: 45S_BE_3289

Design & Development of fixed wing multirotor UAV for quick medical response

A Project sponsored by



KARNATAKA STATE COUNCIL FOR SCIENCE AND TECHNOLOGY

**INDIAN INSTITUTE OF SCIENCE CAMPUS
BENGALURU -560012**

In partial fulfilment

Submitted by

ARUN V	1KG19ME402
KOUSHIK K	1KG19ME405
RALLAPALLI CHANUKYA	1KG19ME409
YASHWANTH B S	1KG19ME414

Under the Guidance of

Dr. Balaji B
Professor and HOD
Dept. of Mechanical Engineering
KSSEM, Bengaluru



Department of Mechanical Engineering
K.S. School of Engineering and Management
No. 15, Mallasandra, off Kanakapura Road, Bengaluru – 560109
2021-22

Design & Development Of Fixed Wing Multirotor UAV For Quick Medical Response

Project Work submitted to



VISVESVARAYA TECHNOLOGICAL UNIVERSITY

in partial fulfillment of the requirements
for the award of degree of

BACHELOR OF ENGINEERING
in
MECHANICAL ENGINEERING

Submitted by

ARUN V	1KG19ME402
KOUSHIK K	1KG19ME405
RALLAPALLI CHANUKYA	1KG19ME409
YASHWANTH B S	1KG19ME414

Under the Guidance of

Dr. Balaji B

Professor and HOD

Dept. of Mechanical Engineering

K S School of Engineering and Management



Department of Mechanical Engineering
K.S. School of Engineering and Management
No. 15, Mallasandra, off Kanakapura Road, Bengaluru-560109
2021-2022



**K.S. SCHOOL OF ENGINEERING AND MANAGEMENT
MECHANICAL ENGINEERING**

CERTIFICATE

This is to certify that the project work entitled **Design & Development Of Fixed Wing Multicopter UAV For Quick Medical Response** is a bonafide work carried out by

ARUN V 1KG19ME402

KOUSHIK K 1KG19ME405

RALLAPALLI CHANUKYA 1KG19ME409

YASHWANTH B S 1KG19ME414

in partial fulfillment for the award of **Bachelor of Engineering in Mechanical Engineering** of **Visvesvaraya Technological University, Belagavi**, during the year 2021-2022. It is certified that all the suggestions indicated during internal assessment have been incorporated in the report and this report satisfies the academic requirement with respect to **Project Work (18MEP83)** prescribed for the degree.

Guide

Head of the Department

Principal

Dr. Balaji B
Professor & HOD
Dept. of ME

Dr. Balaji B
Professor & HOD
Dept. of ME

Dr. K. Rama Narasimha
KSSEM

Examiners

Name and Signature of Examiner-1

Name and Signature of Examiner-2

International Competition of Youth Business Projects & Start-ups (stage-1)



Participated in "International Competition of youth Business Projects & Start-ups (stage -1) – organized by Acharya institute of Technology , soladevanahalli – Bangalore. In association with Society of Ambient Intelligence (Ukraine – Uzbekistan – Lavtvia – Portugal) on 5th March 2022. An we won first place for the Air-eL UAM logistics business proposition.



KSSEM Project Exhibition



**Secured FIRST place in the Project Exhibition
2022**





Kammavari Sangham (R) - 1952

K.S. SCHOOL OF ENGINEERING AND MANAGEMENT

(Affiliated to VTU, Belagavi & Approved by AICTE, New Delhi, Accredited by NAAC)
#15, Mallasandra, Off Kanakapura Road, Bengaluru-560109

Department of Mechanical Engineering

CERTIFICATE

This is to certify that Mr./MS. ARUN. V has secured FIRST place in the Project Exhibition held on 21st June, 2022.

Dr. B Balaji
Professor and Head

Dr. K Rama Narasimha
Principal/Director



Kammavari Sangham (R) - 1952

K.S. SCHOOL OF ENGINEERING AND MANAGEMENT

(Affiliated to VTU, Belagavi & Approved by AICTE, New Delhi, Accredited by NAAC)
#15, Mallasandra, Off Kanakapura Road, Bengaluru-560109

Department of Mechanical Engineering

CERTIFICATE

This is to certify that Mr./MS. KOUSHIK. K has secured FIRST place in the Project Exhibition held on 21st June, 2022.

Dr. B Balaji
Professor and Head

Dr. K Rama Narasimha
Principal/Director



Kammavari Sangham (R) - 1952

K.S. SCHOOL OF ENGINEERING AND MANAGEMENT

(Affiliated to VTU, Belagavi & Approved by AICTE, New Delhi, Accredited by NAAC)
#15, Mallasandra, Off Kanakapura Road, Bengaluru-560109

Department of Mechanical Engineering

CERTIFICATE

This is to certify that Mr./MS. CHANUKYA. R has secured FIRST place in the Project Exhibition held on 21st June, 2022.

Dr. B Balaji
Professor and Head

Dr. K Rama Narasimha
Principal/Director



Kammavari Sangham (R) - 1952

K.S. SCHOOL OF ENGINEERING AND MANAGEMENT

(Affiliated to VTU, Belagavi & Approved by AICTE, New Delhi, Accredited by NAAC)
#15, Mallasandra, Off Kanakapura Road, Bengaluru-560109

Department of Mechanical Engineering

CERTIFICATE

This is to certify that Mr./MS. YASHWANTH. B. S. has secured FIRST place in the Project Exhibition held on 21st June, 2022.

Dr. B Balaji
Professor and Head

Dr. K Rama Narasimha
Principal/Director

ACKNOWLEDGEMENT

We would like to express our heartfelt thanks to our guide **Dr. Balaji B**, Professor & HOD, Department of Mechanical Engineering, K S School of Engineering and Management, Bangalore, who has been our main Inspiration and Motivation to carry out this project work and who has always been there for us to clarify our doubts and give his valuable suggestions throughout this project process.

Words fall short to express our gratitude towards **Dr. K Rama Narasimha**, Principal/Director, K S School of Engineering and Management, Bangalore, for his constant support and guidance throughout our project work.

We would like to thank all the teaching and non-teaching staff of Department of Mechanical Engineering, K S School of Engineering and Management, Bangalore, for supporting us throughout our project process.

This project would not have been possible if we were not supported by our parents and friends for all their love and encouragement. They were our source of an inspiration and their support has always been there morally and financially for us. Thanking them with full heart for their motivation.

Words always fail to express the gratitude towards those who have helped in disguise and we are very much grateful to people who have directly or indirectly helped us towards the completion of the thesis.

ARUN V	1KG19ME402
KOUSHIK K	1KG19ME405
RALLAPALLI CHANUKYA	1KG19ME409
YASHWANTH B S	1KG19ME414

ABSTRACT

The present automotive industries are focusing on developing such aerial vehicle which operates with minimal human interaction and in a more stable manner.

VTOL is one of the technologies which fulfils these requirements. Due to their high payload capacity and automation with sensors make them more suitable for applications like military, rescue tasks, delivery task and aerial photography. The use of these UAVs is more economic than using a manned aircraft for a certain application.

In this project we are focusing on, a VTOL UAV system design, build, and fly a quadcopter mode and aircraft mode considered for transportation of medicines & health care products through the developed UAV. Providing a quick medical response.

TABLE OF CONTENTS

Contents

International Competition of Youth Business Projects & Start-ups (stage-1)	i
ACKNOWLEDGEMENT	iv
ABSTRACT	v
TABLE OF CONTENTS	vi
LIST OF FIGURES	viii
Chapter – 1	10
<i>Introduction to Drone Technology</i>	<i>10</i>
<i>AERODYNAMIC PRINCIPLES OF FUNCTIONING OF A QUADCOPTER</i>	<i>11</i>
<i>Level flight</i>	<i>12</i>
<i>Forward and backward pitch (forward and reverse)</i>	<i>12</i>
<i>TYPES OF CHASSIS OR FRAMES</i>	<i>17</i>
<i>PROPELLERS</i>	<i>18</i>
<i>BRUSHLESS DC MOTORS (BLDC) OR ELECTRONIC SWITCHING ENGINES</i>	<i>23</i>
<i>Principle of operation: electronic switching</i>	<i>26</i>
<i>SPEED VARIABLES or ESCs (Electronic Speed Controllers)</i>	<i>29</i>
<i>BEC AND UBEC POWER SUPPLY SYSTEMS (Battery Elimination Circuits)</i>	<i>32</i>
<i>SELECTING BATTERIES</i>	<i>32</i>
<i>GLOBAL TRACTION AND CONTROL SYSTEM: ELECTRICAL DIAGRAM</i>	<i>36</i>
<i>Connections</i>	<i>37</i>
<i>Power Distribution Board</i>	<i>38</i>
<i>Flight Controller</i>	<i>39</i>
<i>Inertial measurement unit</i>	<i>39</i>
<i>Accelerometer</i>	<i>40</i>
<i>Gyroscope</i>	<i>41</i>
<i>Magnetometer</i>	<i>41</i>
<i>Wireless Communication Modules</i>	<i>42</i>
<i>Electrical Parameters</i>	<i>43</i>
<i>Anti-Spark System</i>	<i>45</i>
<i>Calculation of parameters at maximum efficiency</i>	<i>47</i>
<i>ORIENTATION OF A BODY IN THE SPACE</i>	<i>47</i>
<i>THEORETICAL MODEL</i>	<i>49</i>
<i>Aerodynamics of the quadrotor</i>	<i>49</i>

<i>Rotational cinematic kinematics</i>	50
<i>Dynamics of the quadrotor</i>	50
THE CONTROL SYSTEM OF A CUADRICOPTER	53
Chapter 2	56
Literature Review	56
<i>Selection of Airframe Configuration</i>	57
<i>Propulsion Systems</i>	59
Chapter 3	60
Requirements Specifications	60
<i>Mission Profile</i>	60
<i>Objectives</i>	60
<i>Methodology</i>	60
<i>Scope for Future Work</i>	61
Chapter 4	62
DESIGN	62
<i>Design Statement</i>	62
<i>Design Methodology</i>	62
<i>Assumptions for the design</i>	62
1. Sizing of the UAV	62
2. Power system selection	63
3. Performance of B-1800	63
4. Summary	63
5. Future Scope of Work	63
<i>Preliminary wing analysis</i>	66
<i>Bending Moment</i>	66
<i>Aerodynamic characteristics of 5 m Span wing</i>	67
<i>Wing Sizing (Main wing)</i>	67
<i>Bending Moment Diagram</i>	70
References	93

LIST OF FIGURES

Fig. 1 History of rotary wing aircrafts	10
Fig. 2 Conventional aircraft with 3-axes of displacement.....	11
Fig. 3 Quad copter Axes of Motion	12
Fig. 4 Angular motion of a quadcopter	14
Fig. 5 Right & Left wrapping	14
Fig. 6 Motor Rotation Directions.....	16
Fig. 7 Types of frame	17
Fig. 8 Sections of Propeller	18
Fig. 9 Profile of a propeller	18
Fig. 10 General Propeller	19
Fig. 11 Pusher Propeller	19
Fig. 12 Aerodynamic forces acting of a airfoil section.....	20
Fig. 13 Effective & Geometric Pitching.....	21
Fig. 14 Vertices of airflow.....	22
Fig. 15 Electrical circuit of a BLDC motor.....	23
Fig. 16 In runner BLDC motor	24
Fig. 17 In runner BLDC Motor - inner view	24
Fig. 18 Out runner BLDC Motor	25
Fig. 19 Out runner BLDC Motor schematic.....	25
Fig. 20 BLDC Inrunner Motor Anatomy	25
Fig. 22Characteristic curve of a BLDC Motor	28

Chapter – 1

Introduction to Drone Technology

Rotating wing aircraft with multi-rotors began to design, and even fly successfully, at the beginning of the last century. They were, however, firstly replaced by the autogyro, whose main rotor is not motorized and subsequently by helicopters given the inherent instability of multiple rotor structures. In the following figures you can see the first known quadcopter and some aircraft with this configuration of the mid-20th century.

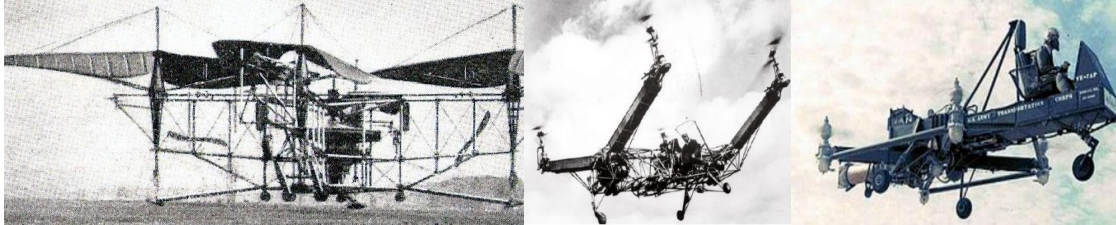


Fig. 1 History of rotary wing aircrafts

If the stability of the cells (structures of the aircraft) with multiple rotating wings is significantly more complex than the one of the helicopters one could ask what advantages they bring and the reason for their current boom. In a helicopter the tail rotor is used to compensate for the reaction torque (Newton's third law) produced by the movement of the main rotor. By varying the thrust supplied, the helicopter is also allowed to rotate over the vertical axis passing through the center of the main rotor (yaw movement). In these conditions the power consumed by the tail rotor is not used to obtain vertical, lateral or forward thrust. However, it is simple to understand that 4 rotors with opposite turns that compensate the pairs of reaction pairs with each other will take full advantage of the power to get vertical thrust. From this point of view the efficiency of the multi copter is superior to that of the conventional helicopter. The disadvantages caused by the instability of multiple rotating wing structures were solved with the appearance of solid state gyroscopes, accelerometers and magnetometers that allow the integration of angular measurement, acceleration and acceleration functions into very small electronic and electromechanical components And terrestrial magnetic field. Although it is complex to explain the functioning of these devices to know their characteristics in a global way is interesting. Solid state gyros have several possible configurations. They can use a cylindrical resonator made of piezoelectric elements (their deformation produces accumulation of electric charges) or of micro vibratory structures inserted in a silicon wafer. The combination of these devices allows to obtain integrated electronic devices capable of measuring angles of inclination, acceleration, and terrestrial magnetic field. Obtaining in this way all the necessary variables to determine the position, speed and course of a moving object. The flight systems for quadcopters of the platform free hardware Arduino, among others, that began its development in Italy in 2005, combine all these functions. The signals generated by the sensors are processed in a microprocessor which applies several cascading regulation loops, thus achieving that pilot control movements act in combination with the corrections of the flight control system. A piloting known as "fly by wire (fbw)" is developed where the pilot actions do not act directly on the control organs of the aircraft but on the control algorithm that introduces the necessary corrections and compensations.

Fbw systems have their maximum representation in modern fighters, whose aerodynamic design is deliberately unstable to allow evasive maneuvers impossible to perform with conventional piloting. Obviously, the absence of the control system precludes

the flight of the aircraft. We can therefore already consider that a quadcopter of any size or configuration is an aircraft of multiple rotating wings, governed by an fbw system that allows the pilot to act on it as it would on a conventional aircraft, adding at the same time multiple possibilities of self-stabilization and correction of flight path and attitude.

AERODYNAMIC PRINCIPLES OF FUNCTIONING OF A QUADCOPTER

Next, the physical principles that allow the movement of a quadcopter in the 3 spatial axes will be presented in a very simple way. To do this, the axes of rotation of any aircraft will be defined first and then the whole explanation will be developed on a quadcopter with frame in X configuration. The chassis in the form of H and + will be analyzed in other sections but only from the Structural or aerodynamic point of view, since the physical principles of

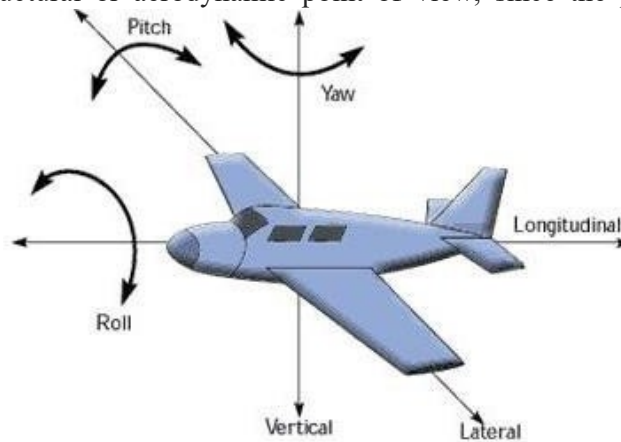


Fig. 2 Conventional aircraft with 3-axes of displacement

motion on the chassis in X are understood, the only difference appears for the chassis in + and is easily extrapolated. Figure 3 shows a conventional aircraft with its three axes of displacement. The movement on the lateral axis that corresponds to bites or ascents is denominated pitch (Pitch). The rotation around the longitudinal axis essential to abandon a rectilinear flight path is called Roll, and finally, the movement around the vertical axis, used in the planes in a coordinated way with the warping is called Yaw. In the case of a multirole aircraft, the names of the movements and the axes are defined identically, although it is necessary to clarify that a forward pitching will be accompanied by the displacement (forward) in the same direction and vice versa (retreat). Equivalently, right and left warping movements will cause the aircraft to move in those directions. Next, all four basic flight situations will be studied: level stationary flight, forward (forward) and backward, right and left (right and left) scrolling and yaw in a clockwise and counterclockwise steady flight. To understand the operation of a multirotor it is imperative to know clearly the concept of the reaction pair derived from Newton's third law. In a simple way it could be stated, applied to a motor that moves a propeller, in the following way: if a motor to turn a propeller clockwise at a certain speed of rotation n develops a torque of value p , on the bench Of the motor will appear an equal and opposite pair.

As indicated above in the case of a helicopter that pair is compensated in flight by the action of the tail rotor.

A second point to keep in mind is that a torque is the product of a force by the distance to the point where it is applied. From this fact very important conclusions are deduced on the behavior of the system:

1. The higher the torque, the higher the reaction torque.

The larger diameter of the propeller, for a same pitch (this concept will be defined later but can be assumed for the moment as the angle of inclination of the blades), greater reaction torque.

Having made these clarifications it suffices to indicate that all the movements of a multirole aircraft will be based on compensating or decompensating the reaction pairs of the different rotors to achieve a resultant in the desired direction. Therefore, the analysis with the simplest situation of level stationary flight will be started.

Level flight

It is assumed that the quadcopter is stationary (hovering) and level. That is, static at a certain height of the floor. In the following graphs the red arrows are perpendicular to the black plane and indicate the vertical thrust (sustencation) of each rotor, the orange arrows indicate the direction of the motor's reaction torque (opposite its direction of rotation) and the green arrow simply points Which would be the nose of the aircraft. The circles in yellow correspond to rotors with sense of clockwise rotation and blue circles to rotors with sense of counterclockwise rotation. As can be seen from the figure, the quadcopter with configuration in X uses two motors rotating in a clockwise direction and two in a counterclockwise direction. The propellers used have the blades designed anti-symmetrically and therefore, although the direction of rotation is opposite all of them produce push down (lift). Understanding the physical principle of the reaction pair is very easy to analyze how the aircraft maintains the flight Stationary: all motors rotate at the same speed, so the reaction pairs are the same on the 4 motors and, since the chassis places them symmetrically, they cancel each other out. There is, therefore, no resulting force that tends to spin the quadcopter around its vertical axis and equal being the thrust of the 4 motors will remain static and level. Obviously, the above analysis is purely theoretical since the multiple aerodynamic effects, residual asymmetries and atmospheric conditions do not allow stable stationary flight if the control and stabilization system does not make small corrections in real time.

Forward and backward pitch (forward and reverse)

Once the stationary flight is understood, the other movements made by the quadcopter will be very easy to analyze. The next situation corresponds to the aircraft passing from stationary flight to a forward pitch that makes the tail rotors up and down the nose rotors. This effect is achieved simply by increasing the thrust of the 2 tail rotors equally, or decreasing equally the two of the nose.

As can be seen from the graph, the red arrows that indicate the vertical thrust are larger in the back than in the previous one.

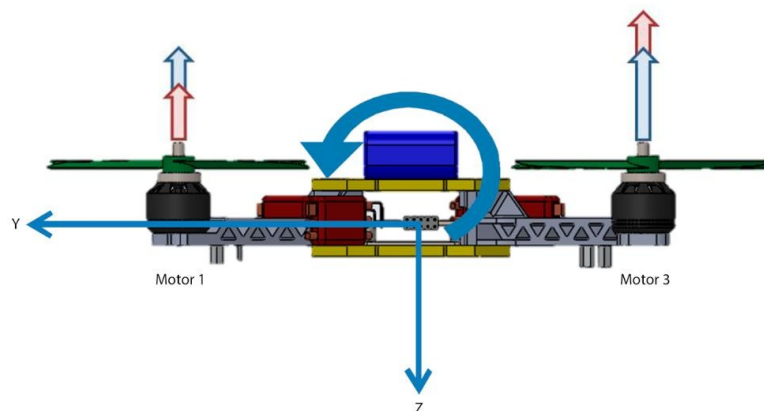


Fig. 3 Quad copter Axes of Motion

This change in the spin regimes will also modify the reaction pairs. The reaction pairs for this movement are insignificant since the ones corresponding to the rear engines compensate each other equally than the two of the forwards. It is very important to keep in mind that as soon as the quadcopter moves forward, the force vectors of the motors will not be perpendicular to the ground, decomposing into two forces: one vertical and the other in the direction of pitch. Thus, whenever there is a forward pitching, the aircraft begins to advance in that direction. The control system will ensure that there is no loss of height in this process.

The backward pitching movement opposite to that described above. It should be borne in mind that, as in the case of forward pitching, the backward pitching will be associated with the backward movement of the quadcopter.

According to the Theorem of the Quantity of Motion (TQM from now on) it is necessary that, on the z axis, the forces must compensate the weight, so that the drone is stable and at a certain height. On the y axis, in this state, there are no components of the motor forces.

Equation of equilibrium z-axis:

$$\sum_{i=1}^4 T_i = mg \quad (1)$$

This does not introduce any variation in the state of the drone if the differential that is added in the motor 3 is the same one that is extracted in the motor 1. In contrast, according to the Kinetic Moment Theorem applied to the mass center one has to Approximation, the mass center is considered to be at the intersection of the three axes previously defined.

$$\overline{GK} = \sum \overline{GP} \times \overline{F_{ext}(P)} \quad (2)$$

$$I_G \dot{\Omega} = \begin{bmatrix} 0 \\ d \\ 0 \end{bmatrix} \times \begin{bmatrix} 0 \\ 0 \\ -T_1 \end{bmatrix} + \begin{bmatrix} -d \\ 0 \\ 0 \end{bmatrix} \times \begin{bmatrix} 0 \\ 0 \\ -T_2 \end{bmatrix} + \begin{bmatrix} 0 \\ -d \\ 0 \end{bmatrix} \times \begin{bmatrix} 0 \\ 0 \\ -T_3 \end{bmatrix} + \begin{bmatrix} d \\ 0 \\ 0 \end{bmatrix} \times \begin{bmatrix} 0 \\ 0 \\ -T_4 \end{bmatrix} \quad (3)$$

$$\begin{bmatrix} I_{xx} & 0 & 0 \\ 0 & I_{yy} & 0 \\ 0 & 0 & I_{zz} \end{bmatrix} \begin{bmatrix} \ddot{\theta} \\ \ddot{\phi} \\ \ddot{\psi} \end{bmatrix} = \begin{bmatrix} -dT_1 \\ 0 \\ 0 \end{bmatrix} + \begin{bmatrix} 0 \\ -dT_2 \\ 0 \end{bmatrix} + \begin{bmatrix} dT_3 \\ 0 \\ 0 \end{bmatrix} + \begin{bmatrix} 0 \\ dT_4 \\ 0 \end{bmatrix} = \begin{bmatrix} d(T_3 - T_4) \\ d(T_4 - T_2) \\ 0 \end{bmatrix} \quad (4)$$

As can be seen in equation (4) the moments on the y-axis disappear as T4 is equal to T2. On the other hand, a differential of moments in the x-axis is created, which causes the appearance of an angular acceleration in that axis, giving rise to the movement previously explained. The expression for the angular acceleration that appears is as follows.

$$\ddot{\theta} = \frac{d(T_3 - T_1)}{I_{xx}}$$

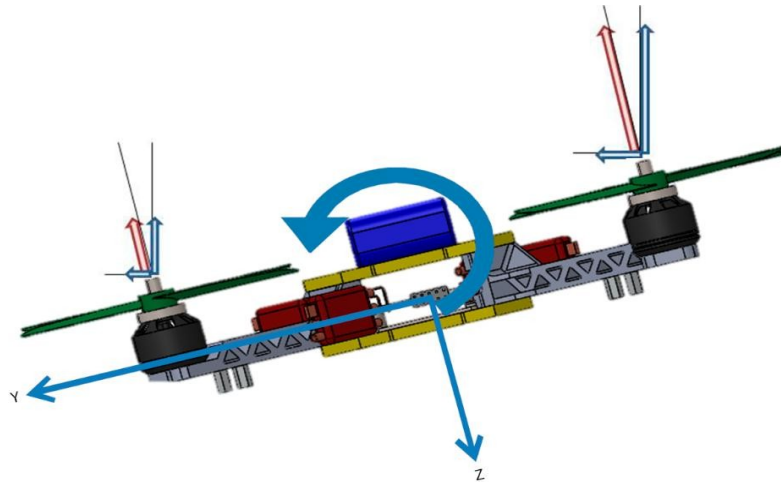


Fig. 4 Angular motion of a quadcopter

From this simple study we can derive design parameters since it is verified how a longer arm and / or minor inertia we obtain greater accelerations.

Right and left warping (lateral displacement)

The mechanism for the warping is identical to that described for pitch movements. The only difference in this case is that the pair of motors that increase their speed are the two located on the sides of the quadcopter (seen in its normal direction of advance). Thus, when the right pair of rotors is to be warped, the pair of rotors on the left side will increase their lift, their reaction pairs will compensate each other, and a rotation will occur on the longitudinal axis towards the right side. The warping towards the left side takes place in opposite way.

Just as in the pitching motion the vector resulting from the vertical thrust was decomposed into two forces: one to compensate for the weight of the aircraft and the other forward that produced its advance, in this case the decomposition of forces will give rise to a component which will cause, in an analogous way, the lateral displacement of the quadcopter.

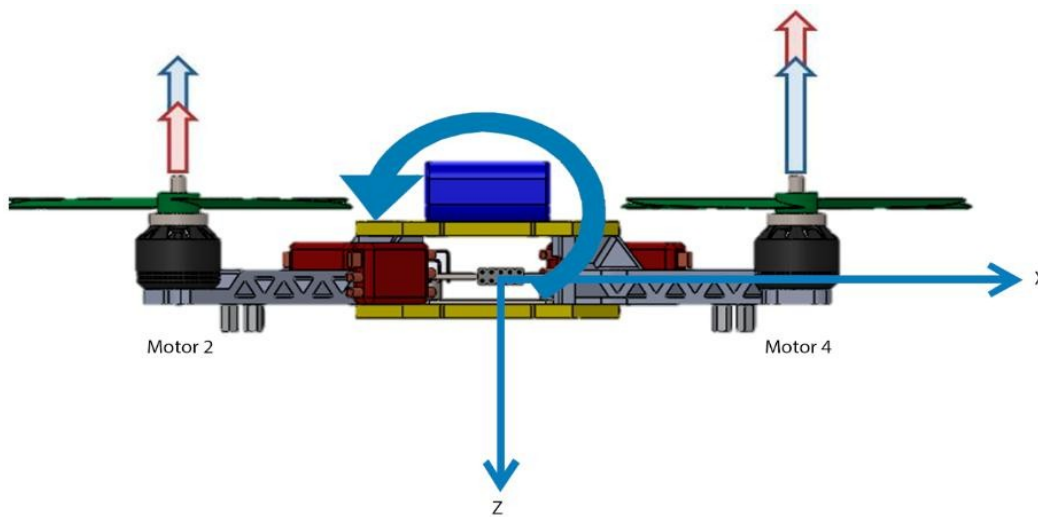


Fig. 5 Right & Left wrapping

In this case, the equilibrium equation 1 of the TQM is also fulfilled, and when the TMC is applied, equation number 4 is reached. This time, the forces that cancel out to create momentum are T1 and T3, whereas when a difference Between T2 and T4 a moment is generated on the positive y-axis whose angular acceleration is defined by equation 6:

$$\ddot{\varphi} = \frac{d(T_4 - T_2)}{I_{yy}}$$

In the same way, a horizontal component appears that generates the translation movement in the direction in which the drone has been inclined.

Stag flight in level stationary flight (turn on itself)

Just as in a helicopter, a tail rotor is necessary to counteract the torque exerted by the blades, the same problem occurs in a multicopter and, therefore, there are several ways to deal with this problem.

The most common thing in a multicopter is to have a pair of helices, so the most common thing to control the yaw is to spin half the motors in the opposite direction to the other half, thus the reaction pairs produced by the Helices counteract each other. The disadvantage of this method is the need to have two types of propellers. Because the propellers have a concrete aerodynamic profile, it is not enough simply to put the propellers upside down because, although thrust would be generated, it would not be enough.

Another method is to turn all the motors in the same direction and generate counterparts with some design feature. The main method is to tilt all the rotors from the vertical to counteract the torque produced by the propellers (Figure). In this way, as in the previous case, we can control the variable yaw the speed of two of the four rotors (in the case of the quadcopter).

The alternative, keeping the four propellers rotating in the same direction is to apply a method similar to the one introduced above, where one of the rotors is given a degree of freedom of rotation perpendicular to the arm. This degree of freedom is controlled by a servomotor attached to the flight control and, depending on the rotation of the engine, a yaw is achieved in one direction or another. It should be noted that the rest position of the motor is not parallel with the rest of the motors, but is rotated to avoid an unwanted yaw. This form of control of the yaw is used especially in tri-rotors, where something more of mechanical complexity is necessary to be able to control the yaw.

The last alternative is to place control surfaces at the outlet that redirect the air flow out of the propeller and provide a counterpart. The variation of the angle of these surfaces will achieve the yaw movement.

In our case, the first method will be used since the aim is to simplify both mechanical and aerodynamic design.

The analysis of the movement to be presented below consists of assuming the quadcopter in stationary flight leveled and cause a yaw or twist motion around its vertical axis.

The physical phenomenon on which this movement is based is different from the previous ones. In the cases studied, the reaction pairs of the motors were compensated in pairs so that no force capable of causing their rotation around the vertical axis was induced in the quadcopter. However, for the yaw movement the exact opposite is required: that the resulting pairs of the 4 motors are decompensated and a resultant is obtained in the desired direction of rotation. For this, will also act on the engines in pairs, but this time in pairs located transversely. The following figure (7) shows the distribution of thrust and reaction pairs corresponding to a yaw movement counterclockwise. As shown in the drawing, in order to obtain the reaction torque or resultant rotational force the rotors marked in blue will reduce their rotation speed and with it their lift (vector in red) and their reaction torque

(vector in orange). Simultaneously, the rotors marked in yellow will increase their speed of rotation increasing their lift and with it the reaction pairs.

Obviously, if the quadcopter is not to lose height, the total lift (vertical thrust) must be kept constant. It could be said roughly that the reduction of blue rotor lift is compensated by the increase of that produced by the yellow rotors, keeping the aircraft stable and level.

Consequently, counterclockwise rotation occurs as a result of the fact that the reaction pairs of the 4 rotors are not now compensated and a resulting torque / force is obtained which causes rotation about the vertical axis. The yaw clockwise takes place with the same principle but acting on the pairs of motors in reverse.

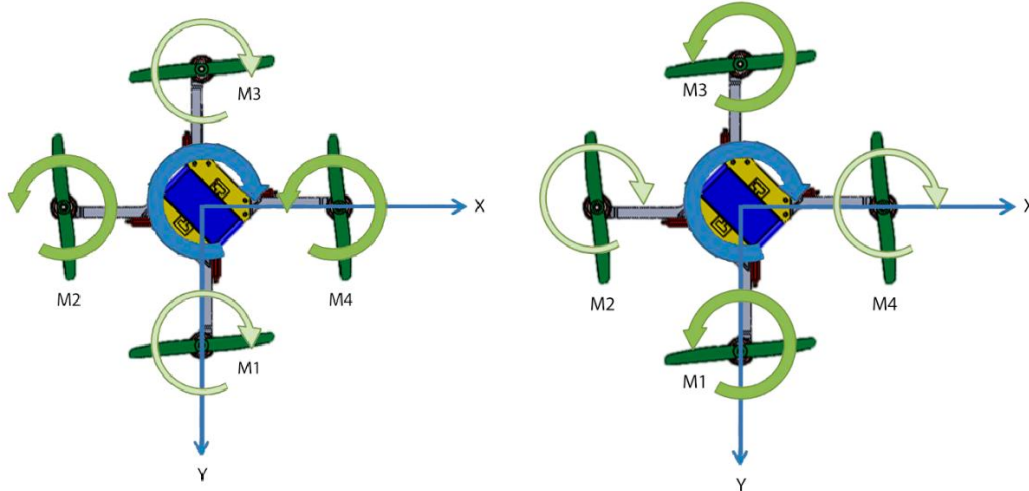


Fig. 6 Motor Rotation Directions

Regarding the yaw movement of quadcopters, it is important to note that, in general terms, it is less efficient than that of a helicopter. That is, its rotation about the vertical axis tends to be slower. The explanation for this phenomenon is clear: whereas in a helicopter the tail rotor is responsible exclusively for the movement of a quadrant in a quadcopter cannot obtain a torque of the same magnitude since the decompensation of the thrust of the engines has Which remain within the limits necessary to keep the aircraft level.

The moment that induces this movement can be expressed according to the following equation:

$$M_{\psi} = \sum_{i=1}^4 \tau_{mi} = \sum_{i=1}^4 (I_{zm} \cdot \dot{\omega}_i - \tau_{dragi}) \quad (9)$$

The moment of yaw occurs, as discussed above, by adding up the four rotational moments of the four motors. When rotating two in one direction and the other two in another direction, in steady state they balance and keep the drone stable in the movement of yaw.

On the other hand, by increasing the rotational speed of even motors and decreasing that of odd motors in the same way, that moment is created in the same direction as motors whose speed of rotation is decreased. This happens to preserve the amount of movement. In this case, the drone would be oriented anti-clockwise if the positive z-axis is considered when it points towards the ground or schedule if the images are observed. There are some special configurations of multirotor equipment where odd numbers of rotors are used to

obtain greater agility for this movement. In any case, a high yaw rate is not required for industrial applications, and that type of configuration is usually designed for aerobatics of an acrobatic nature, including variable pitch propellers governed by servos.

The maximum speed of the apparatus will be determined by two factors; the support of Apparatus, and air resistance. Due to the complexity of the aerodynamic analysis of the apparatus, the aerodynamic resistance of the apparatus will not be determined by analytical form. We can also determine the maximum slope that can maintain the apparatus maintaining the altitude and therefore its maximum linear acceleration.

$$\theta_{max} = \cos^{-1} \left(\frac{M_{tot} \cdot g}{F_{max}} \right) \quad (10)$$

Where $F_{max} = F_1 + F_2 + F_3 + F_4$

TYPES OF CHASSIS OR FRAMES

The frames of the quadcopters are usually classified into three categories: X, H and + and correspond to the structures in the following figure:

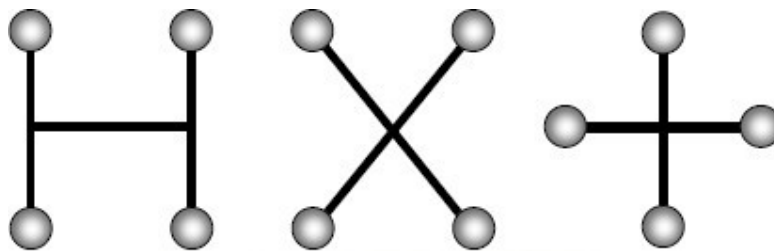


Fig. 7 Types of frame

Regarding the behavior and mode of operation of the quadcopter according to the type of chassis used, it is not necessary to perform a too deep analysis. In terms of operation the configurations H and X are identical. Its only difference lies in the ease and arrangement of space for the location of the elements to be carried by the quadcopter and its structural resistance. In general, the H-structure is more practical if it is intended to locate equipment of a certain size and weight. In fact, it is adopted in a good number of commercial quadcopters.

Commercial frames built in carbon fiber usually adopt configurations in X as the following equipment:

The configuration in + is probably the least used. In this case, the frame coincides structurally with the frame in X. That is, with a frame in X you can choose a configuration in X or in + but the control and the maneuvering procedure is modified.

It is enough to observe figure 9 to realize that the pitching movements will be realized by decompensating the lift produced by the front and rear engines only and that the roll movements will take place when the decompensation takes place on the lateral motors.

Without entering into complex aerodynamic considerations, it suffices to consider only that the forward, backward and lateral displacement movements will occur because of the lift differences only produced by 2 rotors, whereas in an X or H configuration they will occur by the difference of Thrust of the four rotors. It can be said, therefore, without more complex analyzes, that this configuration is less efficient.

PROPELLERS

The analysis of the components of the quadcopter will be started by the propeller since, in fact, it is the most important element since for a multirotor team each propeller is a rotating wing. In this document, the rotary wing is called because with the invention of the auto gyro flight theory was developed with rotating wings.

The propeller is responsible for converting the power supplied by the engine into useful power for the flight

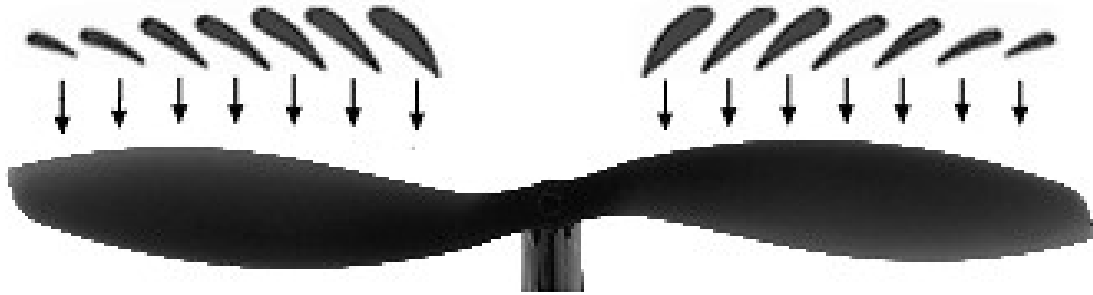


Fig. 8 Sections of Propeller

A propeller is formed by a set of aerodynamic profiles similar to those presented by the wing of an airplane and with a variable angle from the center of the propeller to the tips. In each section of propeller (each profile) the thrust effect is produced that is no more than the lift.

Given the characteristics of this document, it is meaningless to analyze the variables that influence the lift or analyze the fluid dynamics that generate it. It suffices to understand that the movement of the profile of the propeller, in our horizontal case, generates a greater pressure in the back than in the previous one giving rise to the vertical thrust (lift). The following figure shows the aerodynamic profile of the cross section of a propeller at 75% of its diameter. The highest edge is called the leading edge and the lowest trailing edge. The angle forming the line connecting the leading edge to the air (relative wind) is called the angle of attack.

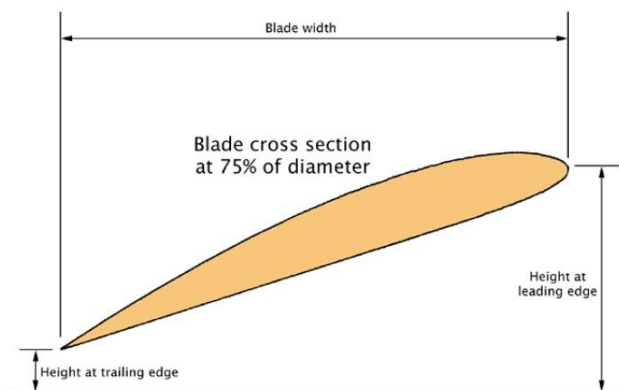


Fig. 9 Profile of a propeller

If you look at a propeller like the one in the following figure you can see that the torsion angle of each blade varies from the tips towards the center. It is smaller at the ends and more pronounced at the center. This shape adopted by the blades is due to the fact that the lift produced by an airfoil is proportional to its relative velocity of movement with respect to the air. Therefore, if it is considered that at the ends of the propeller where the radius is greater the linear velocity of the profiles located in that region is higher, it is evident the need to reduce the torsion (angle of attack) of the propeller. This fact in modeling sometimes becomes really extreme. When calculating the linear velocity at the propeller tips of small models where small diameter propellers are used that rotate at speeds in excess of 20,000 rpm, it will be seen that it is at the limit of the speed of sound. When that happens, it passes to the so-called supersonic regime where air can no longer be considered an incompressible fluid. For these cases, the ends of the propellers are designed with negative angles of attack.

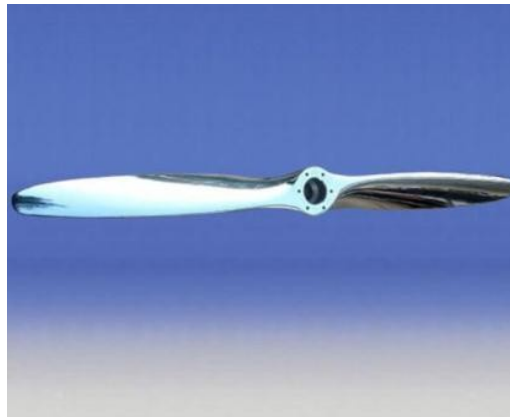


Fig. 10 General Propeller

In a quadrotor type helicopter a pair of propellers type puller and other pusher type are required. The names refer to the direction of rotation that the propeller must perform to generate a pushing force in favor of the flight of the vehicle.

A series of forces acting on any propeller are shown in figure 11 and must be known. The torque that turns it A, the thrust produced by it C (thrust) and the resultant of composing A, B.

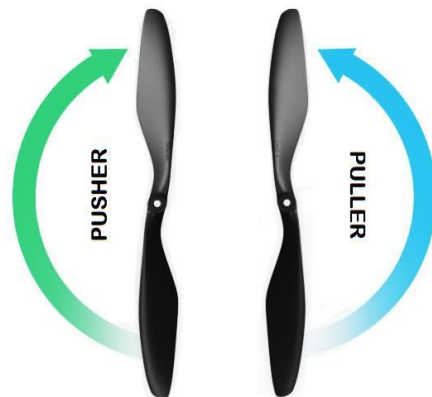


Fig. 11 Pusher Propeller

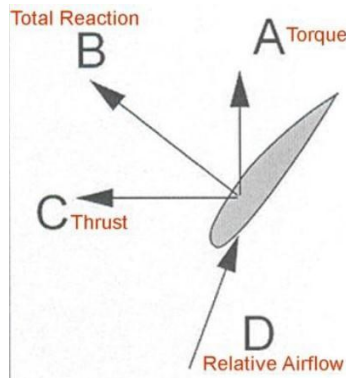


Fig. 12 Aerodynamic forces acting of a airfoil section

The torque is the one that develops the engine in its turn. It is very important to know that the pair of a moving propeller is a quadratic pair. That is, it is of the form $K \cdot V^2$ where K is a value that depends on the characteristics of the propeller and V is its speed of rotation.

The fact that the propeller resistor is quadratic has important implications for the operation of a multi-rotor aircraft. Just take the following example into account. It has designed a p-weight quadcopter that is powered by a 2000mAh battery. It is considered that the autonomy is very reduced and the battery pack is replaced by a 4000mAh battery whose weight is 3 times higher. In a first approximation one might expect autonomy to double. However, in order to keep the equipment in flight it will be necessary to lift the extra weight of the battery, for which it will be necessary to increase the speed of rotation of the motors. Since the resistant torque offered by the propeller is quadratic, if we assume, exaggeratedly, that it is necessary to double the speed of rotation, the torque that will develop the motor will be 4 times greater. Under these conditions, Brushless DC engines would consume approximately 4 times more current than in the initial conditions. Therefore, the autonomy would have been reduced to half that available with the light battery.

Although the example is extreme since it is based on the necessity of doubling the speed of rotation, what it pretends is to show that the fact that pairs are quadratic has as serious implications as reasonable increases in the speed of rotation, as a consequence of the increase Of weight, cause consumptions much more pronounced than those would be in case of being a linear pair.

A propeller is defined by two numerical parameters: its diameter in inches and its pitch. For example, 9x5, 10x4.7, 11x3.3 are actual propeller configurations. The diameter does not raise any doubt as to definition. Next, the concept of step will be defined.

The passage of a propeller can be defined as what would advance an aircraft in horizontal flight when a complete revolution occurs. That is, a 9x5 propeller indicates with its 5 "pitch that the airplane flying propelled by it advances 5" forward in each revolution. This step given as the definition of the helix is the geometric step. The actual advance of the aircraft will be inferior due to an aerodynamic phenomenon that in Spanish could be defined as sliding. Without going into complex details of fluid mechanics the slip could be explained intuitively by comparing the propeller with a screw that is screwed into a material. When dealing with the material of a fluid "the screw" does not advance in each turn of the screwdriver the distance that it would in a solid material since it "slips". The following figure shows the previous concept.

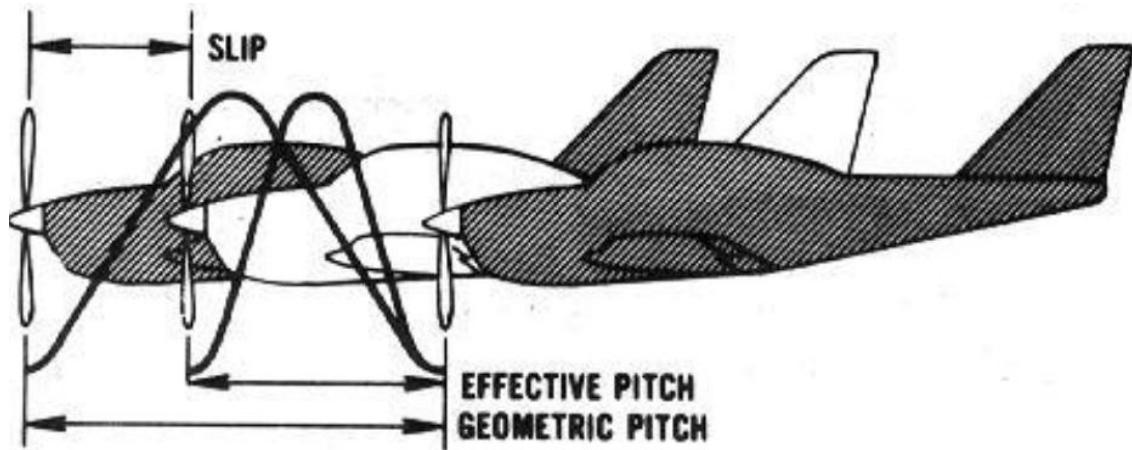


Fig. 13 Effective & Geometric Pitching

Selecting a propeller

When selecting a propeller for a quadcopter design the first consideration that must be made is relative to its quality of manufacture and rigidity. It is important not to forget that a quadcopter is an aircraft of rotating wings and that, therefore, the 4 propellers are the wings that have to support the weight in static conditions and still more in maneuver where the load factor increases due to the centrifugal force.

Therefore, propellers should be selected as rigid as possible, preferably carbon fiber or wood. Any flexible propeller of low cost will deform in the form of cone degrading the flight and the stability of the equipment.

With regard to diameter and pitch, the choice must be made along with that of the motor, although there is a parameter from which can be split: the diameter. As indicated by the performance of a propeller, the greater the diameter, the better the first approximation is (except in the case of serious constraints of space) to try to adapt the diameter of the propeller to that of the frame occupying During the turn as large as possible without obviously interfering between the rotors. It is necessary to know that the highest aerodynamic performance is obtained by using a 2-blade propeller of the largest possible diameter. This fact has been known since the beginnings of aviation, although that said it might be surprising to see classic airplanes with multi-blade propellers. However, it is sufficient to take into account the space restrictions that a conventional aircraft has for takeoff and landing to understand the need to reduce the diameter by increasing the number of blades. With regard to the design of multi-rotors, the diameter of the propeller should be chosen to encompass the largest possible area of the chassis provided that no tandem aerodynamic interference is achieved, where the vortices of the rotors interact between yes. The following figure shows this phenomenon:

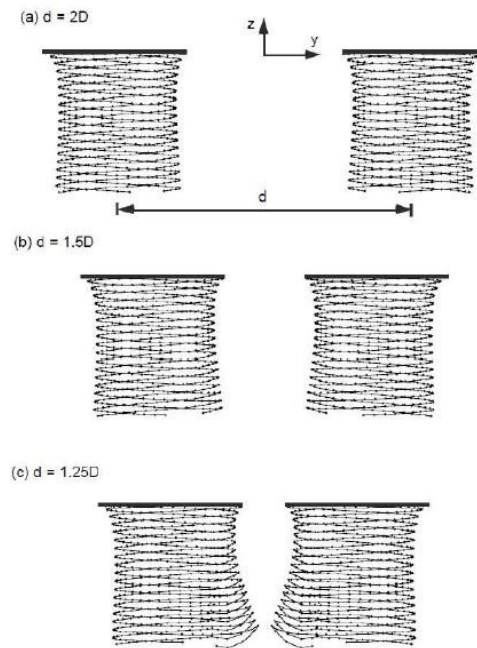


Fig. 14 Vertices of airflow

In it the vortices of the rotors have been represented for different distances between axes of the motors. In the figure to the axes of the motors are separated a distance D equal to 2 times the diameter of the propellers. In figure b, 1.5 times the diameter and in figure C to 1, 25 times the diameter.

The third figure already shows the effect of tandem vortex interference. Therefore, separations lower than those given by this value should not be used. Performing a review of the most popular quadcopters: Quantum Nova, Phantom, etc. It is possible to see how the manufacturers have respected both criteria: on the one hand, they have tried to occupy the maximum available area and, on the other, the recommended propellers establish a criteria of distances slightly superior to 1.25.

BRUSHLESS DC MOTORS (BLDC) OR ELECTRONIC SWITCHING ENGINES

Despite the extra complexity in its electronic switching circuit, the BLDCM presents several advantages over its counterpart, to name a few: higher torque / weight ratio, less operational noise, longer lifetime, less generation of electromagnetic interference and much more power per volume, practically limited only by its inherent heat generation, whose transfer to the outer environment usually occurs by conduction.

In spite of their performance differentials, the BLDCM's dynamic model can be roughly approximated by the well-known BDCM's. Fig. shows the basic electrical circuit of such motor, where u is the voltage applied to its armature, R_a is the armature's resistance, L_a is the inductance, $v_b = kv!$ Is the back-electromotive force induced in the armature, kv is the speed constant and ω is the angular speed.

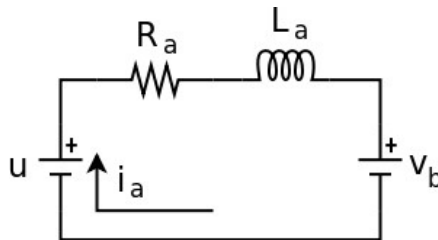


Fig. 15 Electrical circuit of a BLDC motor

A BLDC can be considered for functional purposes as a conventional DC motor in which the brushes and the manifold have been replaced by electronic equipment which injects the current into the appropriate windings, depending on the position of the rotor, to obtain a torque. However, in terms of electrical engineering, the BLDC is a synchronous machine since its rotation speed coincides with the frequency of the electronic equipment that feeds it. In fact, the control and variation of its speed takes place by controlling the switching frequency of the transistors that are part of the variable speed drive.

To understand this explanation, it is necessary to begin by describing the parts and operating principle of a BLDC.

A BLDC motor consists of two parts, the rotor and the stator. Obviously, the first is the one that moves and the second the one that stays static. Generally, the electric motors have a cylindrical rotor rotating inside a larger hollow cylinder which is acting as a stator. However, in this type of machine are possible 2 topologies: engines "Inrunner and Outrunner". These names that do not have a direct translation into Spanish simply indicate if the rotor is located inside the stator (inrunner) or if the rotor is the outrunner and the stator remains fixed therein.

The following figure shows the structure of a BLDC inrunner, i.e. the rotor rotates inside the envelope. As can be seen in the graph, the rotor is a cylinder inside which are usually permanent rare earth magnets: SmCo or NdFeBo. The second are the employees currently in modeling applications. The stator is formed by coils wound around polar cores of ferromagnetic material. When current is circulated through the coils, new magnetic poles are created that interact with the permanent magnetic poles of the rotor causing the rotation of the machine. The motor of the graph has 4 poles in the rotor and 6 poles in the stator. As the poles will have opposite signs this configuration is usually designated as 5N5S, i.e. 5 poles north and 5 poles south. It is not uncommon to find engines with asymmetric configurations where the number of north and south poles is different, especially in outrunner engines that develop greater torque. If you analyze the stator of the machine you can see that the coils of 3 different colors have been colored. This graphic reference

indicates, for example, that the green winding of the upper pole is connected in series with the green winding of the lower pole thus forming one of the 3 stator phases. The same happens with the other pairs of coils so that internally they can be connected to a common point: winding in star or forming a triangle whose vertices will be the outlets.

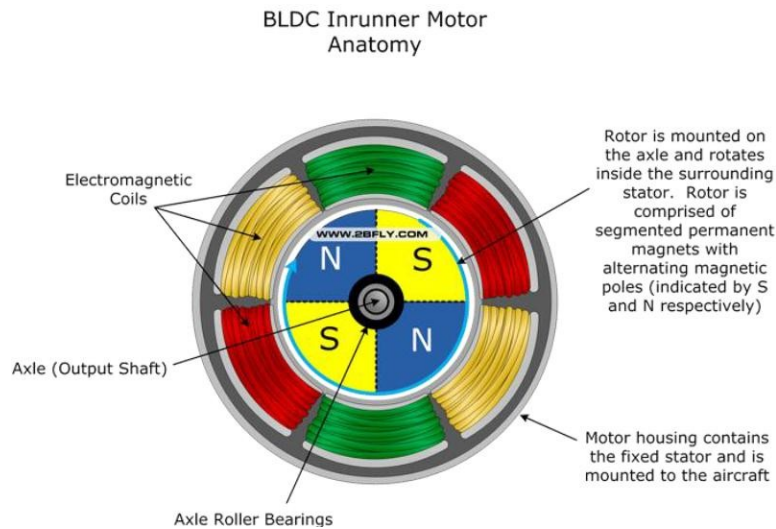


Fig. 17 In runner BLDC Motor - inner view

Figure shows a side view of the in runner motor, in which it can be seen how the rotor is housed inside the envelope in which are the polar masses on which the windings of the three phases of the machine have been wound.

In the configuration of Figure is an outrunner motor is shown. In this case, the poles formed by permanent magnets have adhered to the inner part of the outer shell which is movable and rotates mounted on bearings. Therefore, this envelope with magnets is the rotor of the machine, in the form of drum, that when turning by the outside receives the name of outrunner. The stator winding is mounted on this occasion in the center on the polar masses that are fixed to the back support of anchorage.

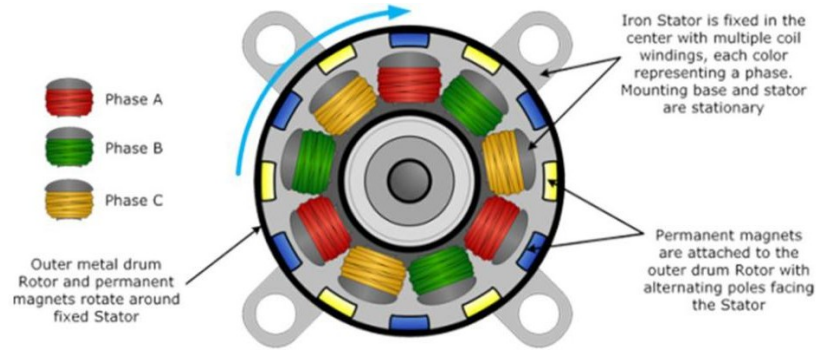


Fig. 18 Out runner BLDC Motor

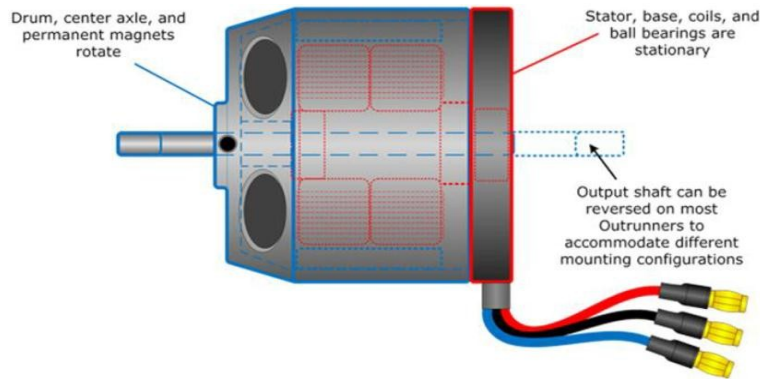


Fig. 19 Out runner BLDC Motor schematic

BLDC Inrunner Motor Anatomy

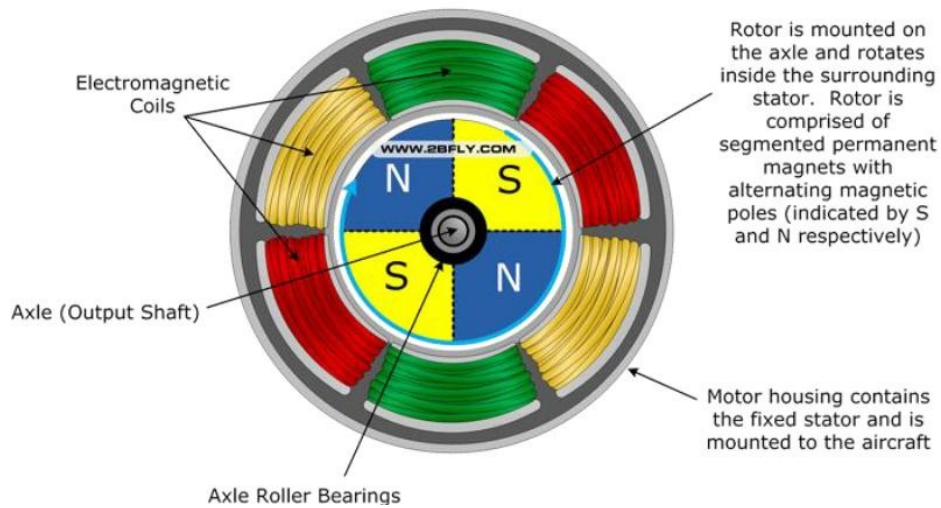


Fig. 20 BLDC Inrunner Motor Anatomy

Figure 20 shows the external appearance of the motor. In it you can clearly see the anchoring bench located on the right side and how the spin is performed by the outer drum inside which the permanent magnets are installed.

In motors designed with this structure for modeling applications it is very common to find shaft outputs on both sides and mounting accessories that allow them to be anchored to the model in different positions.

Although the two types of motor are conceptually identical and equations and operating principle the same, as with industrial synchronous machines their physical topology significantly modifies their characteristics and applications. Without going into more complex details it can be said that the main difference between an external rotor motor and an internal rotor motor is its speed of rotation and its ability to produce torque.

The inner rotor motor is slimmer and longer, so its design allows for much higher turning speeds without significant centrifugal forces. In fact, it is not uncommon to find models where the engine speed exceeds 20,000 rpm. We could say, therefore, that this type of motor is more apt to move small diameter propellers that need to rotate at a high speed of rotation as they happen in the systems called ducted fans for airplanes.

On the other hand, the outer rotor or rotating housing motors are flatter and have a larger diameter. This structure already makes it clear that its speed of rotation will be lower and its torque much higher. In fact, the design of a BLDC disc or rotary drum motor precisely seeks to generate a high torque. One of the most surprising applications of this type of machine, designed in the form of a flat and narrow disc, is its use to perform taxiing tasks (taxiing before arriving at head of track and return to the point of parking) displacing a plane of Line by electric traction. In this way, fuel economy, reduction of emissions and less wear of the turbines are achieved.

In their modeling application they may be considered suitable for moving larger diameter propellers and not very high passages at intermediate speed regimes. In general, it can be said that they are the most suitable type of motor for the design of multicopters.

Principle of operation: electronic switching

So far, the main properties of the BLDC motors have been described but their operational principle has not been indicated. The rotation of the rotor in a BLDC motor is based on what in Electrical Engineering is known as electronic switching. To understand it in a simple way will be used the diagram of figure 18, which will be repeated here for convenience.

If, in the motor shown in the previous figure, no current is introduced into any of the coils, the rotor remains obviously at rest. Imagine now on the said figure that an external system introduces current in the yellow phase in such a way that two magnetic poles are created, this winding with north polarity. If that happens the north (blue) poles of the rotor will suffer a force of repulsion and the south poles (yellow) one of attraction towards the winding of the same color. It will have been achieved so that the rotor rotates a fraction of a turn.

If the previous situation is maintained the motor would not continue its rotation keeping stable in the previous position. However, as soon as the rotor comes out of the influence of a pair of stator poles the current is nullified in them and introduced into the next the process of attraction and repulsion of the magnets will again take place. Therefore, if the current is injected periodically in the proper angular position, the rotation of the motor will be achieved.

These injections and shutdowns of the current are made by electronic switches inside the variable speed drive and is what is called electronic switching. The motor speed is varied

by increasing the frequency of activation and deactivation of the circulating currents by the stator winding. This involves changing the frequency of opening and closing the electronic switches of the inverter.

The previous switching process starts from a hypothesis that in practice is not theoretically feasible. It has been assumed that the injection or extinction of the current in each phase is achieved just when the magnetic poles of the rotor are in the correct angular position. In principle, this is not possible unless the motor incorporates a mechanism which informs the variator of the angular position of the rotor. In BLDC motors of industrial applications, for example the car addresses with electric assistance, the motor incorporates on the shaft an encoder (rotary encoder) that supplies the position of the rotor to the variator of speed. The variants existing in the market for these devices are multiple and, since the modeling engines do not use them, it makes no sense to raise more than their existence and the need to inform the variator of the position of the rotor. If a BLDC modeling engine does not incorporate any external systems that report the position of the rotor how it can function properly? The explanation for this question comes from the use of a control algorithm for the inverter called sensor less control. Explaining a control algorithm of these characteristics is not the subject of this document but a brief indication of its operating principle can be given.

The laws of Lenz and Faraday established at the end of the 19th century that if a magnetic field moves in the surroundings of a set of coils an electromotive force (tension) is induced in them. This law is the basis of the operation of the sensor less control that the variadores of modelismo use to avoid to add systems of measurement of the angular position of the rotor.

The control system operates in a simplified way as follows: The motor starts by injecting the currents for a given direction regardless of the rotor position. This injection of current causes the movement, still uncontrolled, of the motor that can even try to start in the opposite direction to the desired one. During the movement electromotive forces are induced due to the Law of Lenz in the phases that are not injecting current. The measurement of these electromotive forces by the variator allows to estimate the position of the rotor and to ensure that the electronic switching is synchronized with the rotor position. This transitorily unstable situation can be observed if gas is applied very slowly to the motors of a quadcopter in the form of a slight hesitation in the beginning of the rotation of the propellers.

Parameters defining a BLDC motor and characteristic curves

Before indicating the parameters usually obtained from BL = DC motors it is necessary to refer very closely to the two equations that govern their operation. In a BLDC motor it can be affirmed that torque and speed fulfill the following two relations:

$$V = K_1 \cdot N \quad (12)$$

$$T = K_2 \cdot I \quad (13)$$

Where V is the supply voltage, N is the speed of rotation, T is the motor torque and I is the current consumed. K₁ and K₂ are two own constants of each motor that depend on its constructive form, flux density of the magnets, etc.

The constant of the first equation is the one that supplies the most known parameter of the BLDC, usually called kV and indicated in terms of rpm / V (in fact it would be the inverse of the constant indicated in the equation). The constant kV of a BLDC motor, also in a simplified way, indicates the RPMs expected for a given supply voltage. Thus, a 1200 kV motor if fed at 1 V should rotate at 1200 rpm.

The second equation is not related to any data normally supplied by the manufacturer but is very important to understand the operation of the machine. The reading of equation (13) indicates that the current to be consumed is proportional to the constant of proportionality K₂ and that the current consumed is directly fixed by the torque that the

motor has to develop. This data is very important, as discussed above, because the resistant torque of a helix is quadratic and as indicated in an earlier example if it is intended to double the speed of rotation the torque will be multiplied by 4 and with it the current Consumed.

The other parameters that characterize this type of motor are:

1. The vacuum current (no load current) normally supplied for a certain supply voltage.
2. The resistance of the conductors of the windings.
3. The maximum permissible current (supplied normally along with the maximum time that can develop it).
4. The electrical power absorbed (sometimes in different conditions or for a set of propellers)
5. The number of poles. Normally expressed in the form 15N15S, 14N16S, etc.

For the use of simulation programs, if the motor is not among those selected it is relatively easy to obtain the vacuum current and the resistance of the windings, which together with the number of poles already allows to define the motor completely. The following graph shows all the characteristic curves of a BLDC motor, and it will comment on the operating point to be chosen for any model.

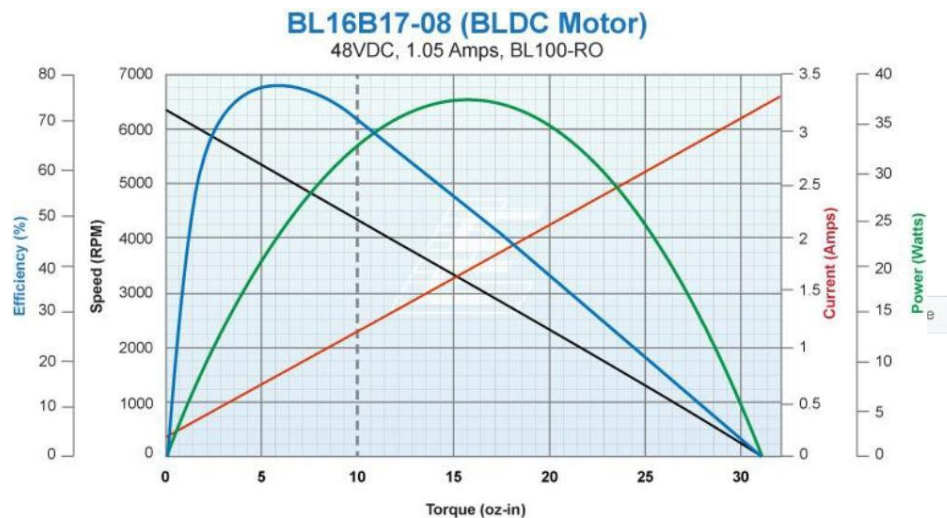


Fig. 21 Characteristic curve of a BLDC Motor

In these graphs you can see all the concepts shown above. If the velocity curve is analyzed in black, it is observed that with the stalled rotor the torque delivered by the motor is slightly more than 30 oz-in and that when rotated in vacuum the speed of rotation is higher than 6000 rpm.

If we analyze the red curve (torque-current) it is clear that equation 13 is satisfied and that the current grows linearly with the pair. The torque zero point corresponds to a current of about 0.2 A. This is the no load current which indicates the motor's consumption to magnetize and overcome the friction losses when it rotates with nothing attached to the shaft.

Finally, the curve of greater interest is the blue one, since in it the performance is represented in function of the pair developed. Performance is an indicator of how much input electrical power is being consumed to produce mechanical power in the shaft. A low

yield point indicates that a good part of the electrical power consumed is being used to heat the engine and not to produce mechanical work. Therefore, the operating point at which the propeller is driven to the engine must be as close as possible to the point of maximum performance. Otherwise, it would not only be wasting the battery power but would be overheating the motor.

Normally, the peak performance point of the motor is given with low pairs. For this reason, it is materially impossible to select a propeller which brings the engine to the point of maximum performance. However, selections should be made as close as possible to this value and any combination should be discarded after a simulation yields yields of less than about 70%. The graph shows a line of points corresponding to the selected work point for the motor. It is also possible to observe that a shift to the right produces an increase in the power absorbed and in the circulating current by the motor.

Before finishing with the section dedicated to the engines it is essential to make a comment about its operating temperature. Permanent magnets reduce their flux density as the temperature increases. If the temperature increase suffered by the motor is not very high once the cooling takes place the magnet recovers its magnetism. However, there is a temperature known as the Curie temperature above which a permanent magnet loses its magnetism.

Therefore, it is necessary to consider 2 aspects of the operation of a permanent magnet motor:

1. Even if the Curie temperature that causes definitive engine damage does not reach, the increase in temperature of the magnets reduces its flux density and causes the motor to degrade its operating characteristics.
2. Once the Curie temperature or values close to it have been reached, the motor will be irreparably damaged.

Therefore, the design should avoid heating the engine as much as possible. An ideal operating temperature would be around 40 ° C and 60 ° C should never be exceeded.

SPEED VARIABLES or ESCs (Electronic Speed Controllers)

Next, the structure of an ESC, its operating principle and some considerations on its choice will be discussed. The following figure shows an excellent diagram of the components of an electronic variator. Analyzing the diagram from right to left the following components can be observed:

1. Output filter capacitor: it is a capacitor used as a filter to eliminate oscillations in the voltage wave that is applied to the motor.
2. Set of 3 vertical branches of legs labeled as FET. These 6 switches are low-resistance channel MOSFET-JFET transistors (the ones they present when they are in saturation, i.e., closed). The three phases of the motor connected to the central point of each of the branches. Thus, by performing different combinations with the switches that are closed and those that are left open it is possible to apply positive, negative or zero voltage to each of the phases of the motor.
3. FET Driver Circuitry: this component is simply an element that adapts the logic outputs of the microcontroller to the voltage and current levels required to enter the gate of the transistors and produce their cutting and saturation (Opening and closing).

4. Microcontroller: in it is the program of governing the transistors. It receives as input the gas signal (throttle) and also the measurement of the electromotive forces induced in each phase, as it was described when referring to the sensor less control of the BLDCs. Their power comes from the component called BEC present in most inverters.
5. BEC = Battery Elimination Circuit: The BEC is a linear voltage regulator, i.e. an electronic circuit that reduces the voltage of the batteries and stabilizes it to feed the microcontroller and other components that need a voltage of logical levels, Usually 5 V in our system. The name BEC comes from the fact that in older models it was necessary to have a small additional battery of 4.8V to power the servos, receivers and other electronic circuits. closed and those that are left open it is possible to apply positive, negative or zero voltage to each of the phases of the motor.

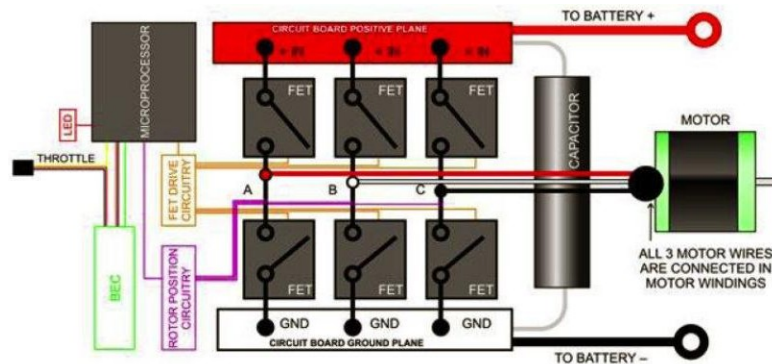


Fig. 22 Battery Elimination Circuit

Known its components the operation of the system can be summarized as follows:

1. The inverter is connected to the receiving equipment and an adjustment is made to tell the microcontroller the range of variation of the gas channel input signal. This procedure varies from manufacturer to manufacturer. Some more advanced operating parameters can also be selected, motor braking, motor cut-off when reaching a certain level of battery discharge, etc.
2. Once the calibration process has been done when the transmitter is activated by raising the gas control, the signal enters the microcontroller using its

Sensorless control algorithms vary by raising the opening and closing frequency of the transistors until the desired speed of rotation is reached.

The current market offers an infinite number of variators with very varied characteristics. In the following figure you can see 2 of the most popular.



Fig. 23 Electronic Speed Controllers

When selecting it, the following variables must be taken into account:

1. Maximum current you can handle
2. Number of cells for which it is designed (battery voltage)
3. Inclusion or not of BEC
4. Form of programming: from the transmitter by beeps or leds or by passive card.
5. Existence of optocoupling: galvanic separation of the drivers from the transistor doors.
6. Weight.

The electronic speed controller (ESC) is the interface between the control and power stage of brushless electric motors. It receives a signal from a low-power microprocessor and converts it into a three-phase high-power alternating signal.

The signal normally corresponds to a pulse width modulation signal PWM, whose frequency and duty cycle are determined by the factory. The duty cycle is usually in the range of 1 to 2ms and the frequency can take values of 50hz and 490hz.

The following figure shows a PWM signal, where T corresponds to the period and t to the pulse width, both quantities expressed in units of time.

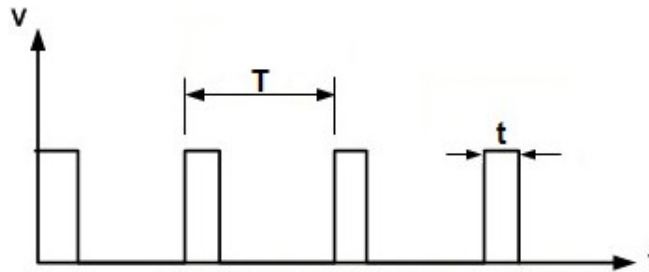


Fig. 24 General PWM Signal

$$D = \frac{t}{T} \quad (14)$$

BEC AND UBEC POWER SUPPLY SYSTEMS (Battery Elimination Circuits)

The BEC system and its functions have already been commented on in the previous point. Next, the difference between a BEC and a UBEC will be explained. In the first generation of electric models the linear regulator that incorporated the ESC was more than enough to feed all the electronic circuitry of the model. The BECs incorporated into the inverter in the form of linear regulators provided currents of the order of 1 A. The disadvantage of the BEC based on a linear regulator appears when the battery to be used is of a high number of cells. For example, a combination of Lithium-Polymer 4S uses 4 3.7V cells that are freshly charged at 4.2V. Therefore, linear regulator must reduce almost 17V to 5V of the logic power supply of electronic circuits. This reduction in voltage is done at the cost of dissipating the necessary power in the regulator, which is, in the first place, inefficient and secondly causes a high heating especially if it is intended to extract a considerable current from the regulator.

As a solution to this problem appeared the UBECs that are not linear regulators but DC-CC reducing converters. In this case, there is no problem of power dissipation because they are switched sources and the capacity to supply current of the UBEC is much higher and much more in line with the consumptions of the systems that a multi- rotor system incorporates.

The UBECs can be part of the variable speed drive or can be purchased separately as a simple DC converter that reduces the voltage of the batteries and adapts it to power all system circuitry. Its practical use is extremely simple. Its input is the battery and its output the power connector for all electronic components. In the following figure it is possible to observe a UBEC of 10gr of weight with an output of 5V and 5A.



Fig. 25 UBEC (Universal Battery Eliminator Circuit)

SELECTING BATTERIES

In the early days of electric modeling, the only available batteries were NiCad, currently banned for domestic use because of the presence of heavy metals. Its weight was high, its energy density low and its capacity of limited discharge. The advantage they presented was enormous strength and durability. Subsequently, NimH batteries with considerably higher capacities were used, but the intensive charging and discharging processes in this type of battery are strongly exothermic and the number of life cycles remained low without having improved the weight problem.

Towards the end of the 90 arrived the first batteries of Lithium Polymer (LiPo) of the mark Kokam arrived in Spain the batteries came in individual cells and the assembly had to be done manually. Its energy capacity was much lower than the current capacity and its discharge capacity about 15 times lower.

From that date until now the development of LiPo batteries and some variants such as LiFePo has been unstoppable. In fact, at this time it is unthinkable to use another compound both for its incredible price drop and for the higher daily benefits.

Therefore, a brief review on this type of battery will be made, later the most characteristic parameters that define them will be indicated and finally some advice will be given on the criteria to be applied in their choice.

A Lithium Polymer battery is actually a Lithium Ion Polymer battery. That is, there are no functional differences between Li-ion batteries and LiPo batteries. The differences between the first and the second lie in that the latter the liquid electrolyte is replaced by a solid polymer: polyethylene oxide, poly methyl methacrylate and a number of other compounds. The principle of operation of the battery is based on the circulation of lithium ions between two metal plates that act as anode and cathode. Although this type of battery is the one with the highest energy density and discharge capacity, it is not without its problems: if they are overloaded they tend to expand to the point of bursting and burning. If they are discharged below a certain threshold, secondary chemical reactions, oxidation of anodes and cathodes occur and the possibility of expansion and fire again appears. In fact, in the early days of its use, many cases of fire caused by failures during the loading process, or the use of batteries that had suffered impacts or deformations, were collected on the Internet. LiPo battery packs that are used in both modeling and industrial applications are made up of sets of cells connected in series or even in parallel series combinations of series. Each of the cells has a nominal voltage of 3.7V although at full load they reach 4.2V. Their discharge depth (minimum value of the voltage they can reach during use) should not fall below 2.8V. Next, the parameters that define the commercial LiPo battery packs will be indicated.

Parameters that define a "pack" of Lipo batteries

1. Number of cells: the batteries are designated as nSmP, for example 3S2P. This indicates that the battery in question consists of 2 branches of 3.7V cells connected in series, then connected in parallel. Series-Parallel combinations are used to obtain large capacities, although the most common configurations with all the cells in series are: 1S, 2S, 3S, 4S, etc. The overall voltage of the battery is obtained by multiplying the number of cells by 3.7.
2. Capacity: The capacity of the battery pack is designated by the letter C and indicated in mAh. That is, the data that is given is the amount of energy that the battery is able to deliver. Thus, for example a battery of $C = 4000\text{mAh}$ would theoretically be able to provide a current of 4A for one hour reducing its voltage slightly (up to the result of multiplying its number of cells by 2.8V, minimum permissible voltage).
3. Discharge capacity: This data is given in multiples of C, so a battery can be 25C - 50C, 40C - 60C, etc. This indicates what indicates is the maximum current that can be drawn continuously from the battery and that which can be removed for a short time. For example, if the previous packet of $C = 4000\text{mAh}$ is labeled as 40C-60C, it means that it is suitable for work by continuously discharging $40 * 40000\text{mA}$, i.e. 160 A and briefly 60 * 4000mA or what is 240 A. Obviously, the battery life under these conditions would be divided by at least 40 in the first and by 60 in the second. In actual practice, the reduction is even greater since the behavior is not linear and as the number of discharge C increases its capacity decreases.

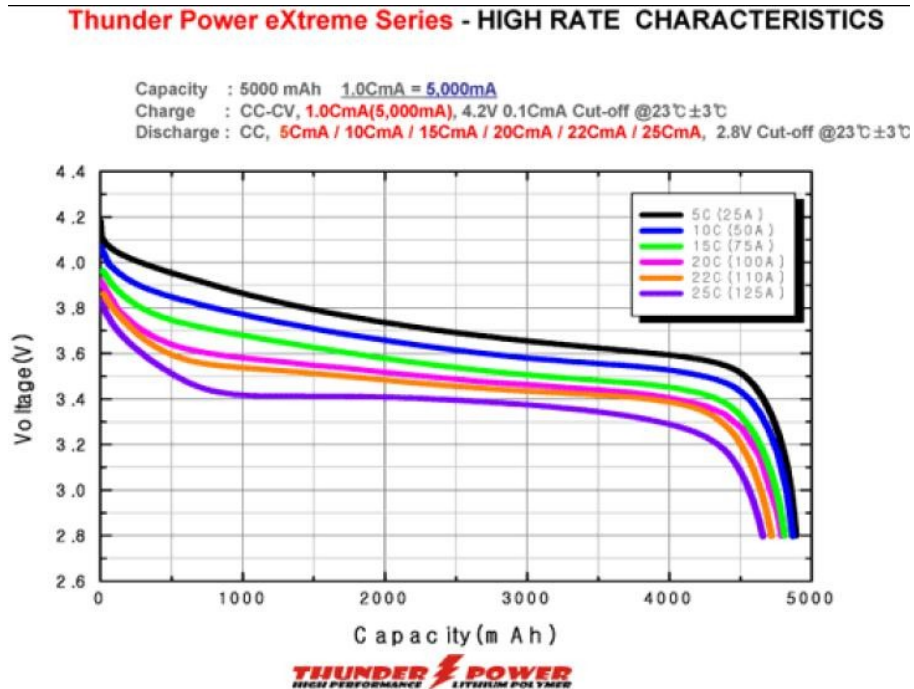


Fig. 26 V vs mAh curves

All of the above concepts are readily understood in view of a family of curves supplied by a manufacturer of battery packs for modeling:

In the family of curves it is possible to observe how as the discharge increases in multiples of C, there is a greater internal voltage drop in the battery and its capacity is reduced.

The correct charging of a battery based on lithium polymers is essential for the durability of the same as to avoid any type of accident or failure that could put at risk the safety of the person who handles it. The voltage of a cell of this type of batteries, as mentioned above, is 3.7 Volts, this voltage is not constant and it varies according to the percentage of charge when the battery is at 100% in 4.2 Volts. So in the process of charging should not exceed this limit as it could damage the battery. Due to this limitation it is necessary to use a suitable charger for LiPo batteries and to select the number of cells that are connected properly, if the value is wrong, there is a risk of overcharging the battery. The vast majority of chargers on the market have built-in a system that auto detects the number of cells connected to avoid risks.

The charger uses a known method of charging constant current / constant voltage (cc / cv), means that during the first phase of charging the battery a fixed current is applied, as the voltage of the battery is close to the limit of 100%, The charger automatically starts to reduce the current level and applies a constant voltage during the remaining stage. The charger interrupts the charge phase once the voltage of 4.2 Volts is reached for each cell. It is also important to select the current level that the charger will deliver to the battery during charging. It follows a rule in most cases that says that you never have to charge the battery above its capacity, i.e. above 1C. It means that, for example, if a battery with 2000 mAh capacity is available, a current of more than 2 Amps must never be supplied during the charging phase.

However, as the technology specializes, there are commercially available Batteries that support 2C, 3C, even up to 5C of charging current. So we can reduce the loading times. If we charge the battery to 1C, it will be completely full in 1 hour, however, if we charge it at 5C the duration of the charge is reduced to 1/5 Hours, 12 minutes.

Also important is the balance of the battery, which allows you to charge all the cells for Equal reaching the level of 4.2 Volts in each of them without exceeding this limit. Occurs if we have more than one cell, for example, a 3S battery, the charger will reach 12.6 Volts when the charging cycle is completed, however, if the cells have different voltage at the beginning of the operation there is a risk that these differ their level at the end of it. One could exceed 4.2 Volts while the others would not be fully charged. To avoid this and to avoid risks, it is used the balance that loads all the cells alike, with an error of 0.001-0.03 Volts, by reading the voltage of each cell separately thanks to a connection that have all LiPo batteries, the cable Of rolling. A built-in circuit in the charger allows you to charge the cells using the main power cable of the battery.

Criteria for the correct selection of a battery pack

Exposing all the factors that determine the choice of one or the other battery pack is extremely long and tedious, although a brief indication of the procedure can be given.

1. Choice of number of cells: the most common in these cases is to make the choice of the entire traction system, propeller, motor, variator and battery by means of a simulation program. Or, determine the proper supply voltage that the propeller motor assembly is in the zone of suitable performance and thrust and from there determine the number of cells. The most common is to use 2S, 3S, 4S configurations.
2. Choice of capacity: capacity must be chosen depending on the desired flight time and the weight of the package. As already indicated above, a reasonable increase in autonomy is not always achieved by increasing the capacity enormously if a large increase in weight is produced.
3. Choice of discharge capacity: the discharge capacity must be sufficient for the maximum current consumed by the battery to be in the range that the manufacturer estimates as suitable for continuous discharge. For example, if my system consumes 100 A, and the capacity of my battery is 5000mAh, its permanent discharge capacity must be at least 20C. In this sense it is very important to note that it is not always a good idea to select batteries with very high discharge capacities. For example, if our capacity requirements in mAh are 2000mAh, and my consumption is 40 A maximum, it is possible to select any battery that has discharge capacity 20C, or a higher value, 25C, 30C, 40C, etc. Although a priori it would seem most logical to choose the battery capacity 40C would be making a mistake. The higher the discharge capacity of the battery the greater its weight and also the greater an internal resistance and therefore its voltage drop. Therefore, by choosing a battery of continuous discharge capacity of 40C we would increase the weight and would have less voltage than selecting a discharge capacity 25C, lighter and with a lower voltage drop. Therefore, this criterion could be summarized by saying that batteries with very high discharge capacities should not be selected if they are not really going to use that property. For this reason in this case the choice of 25C that allows a continuous download of 60 A for an application that will consume a maximum of 40 A is perfectly valid and allows a margin of safety in case any modification of the design increases subsequently the consumption.

GLOBAL TRACTION AND CONTROL SYSTEM: ELECTRICAL DIAGRAM

Finally, the complete connection of a quadcopter with all the elements described will be shown. In them it is observed the connection of all the components to the control system and they do not need more explanation than to clarify that the motors have to turn in opposite directions in pairs.

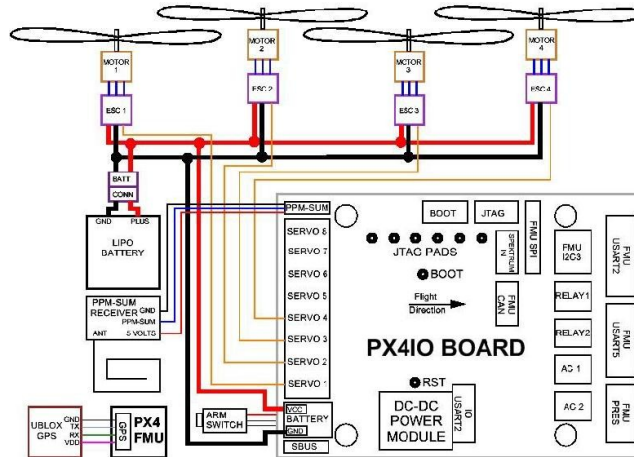


Fig. 27 Quadcopter Control System

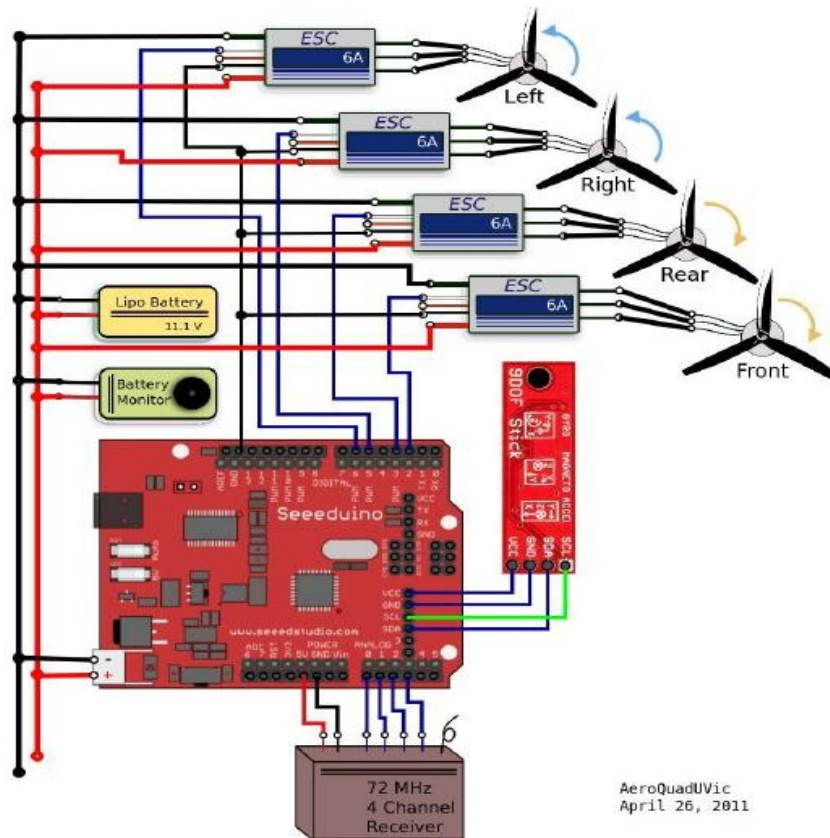


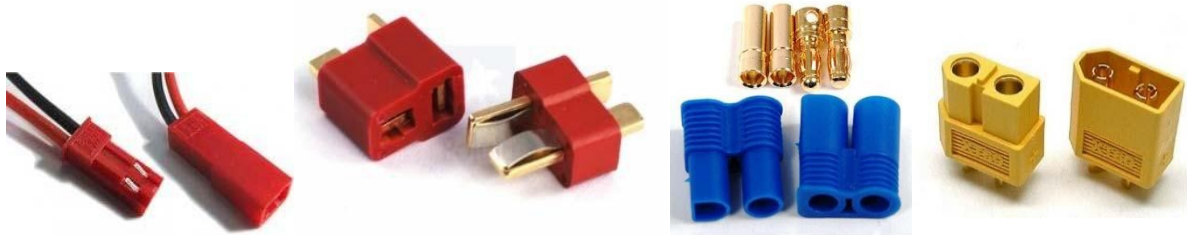
Fig. 28 Aero Quad architecture

AeroQuadUVic
April 26, 2011

Connections

The batteries usually have two types of connectors already mentioned, the main power cable and the roll wire. The first is responsible for delivering and receiving energy

Which has the battery, the second is responsible for performing a correct balance of the battery cells as explained above



For each of these cables there are many connectors, whose choice will depend on the use of the battery and the power requirements of the selected design, all of them have safety mechanisms that avoid inverting the polarity when connecting them.

The power cable connectors are as follows:

JST Connector: A small connector used for requirements up to 5 amps nominal. Used in batteries of reduced capacity, below 1500 mAh, to power the motors of very small UAVs and the onboard electronics of the models of a higher range.

Dean Ultra connector: A widely used type of connector whose price is relatively high compared to its competitors, can withstand a rated current level of up to 50 Amperes. EC3 connector: Bullet type connectors capable of withstand a continuous current of 60 Amps. The "bullet" type, seen in the picture, is very popular in high power applications thanks to the fact that they have a larger contact surface.

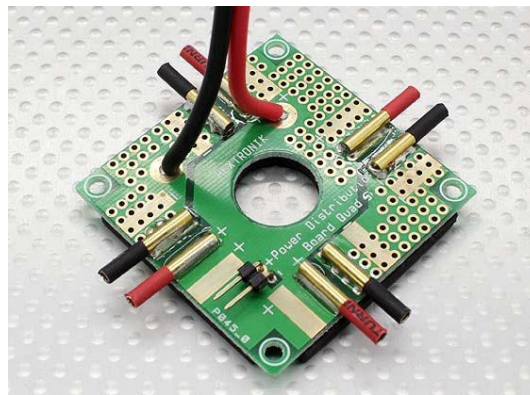
EC5 Connector: Larger version of the EC3, with 5 millimeter pins, increases the contact surface thereby increasing its rated current capacity as it can reach up to 120 amperes.

Connector XT-60: One of the most popular connectors in the market for model aircraft thanks to its good value for money. Just as the EC3 connectors use "bullet" technology when making the connection and are capable of supporting currents of 65 Amperes. The protective case is made of nylon that does not melt when welding, and its shape makes them easy to connect and disconnect. There is a higher version able to withstand an intensity of up to 90 Amps at rated speed. In turn the connectors of the cables to perform the rolling are also of many types and will depend on the manufacturer brand, being the type JST-XH the most used. There are other models such as Thunder Power, Polyquest and JST-EH.



When designing the feeding and loading system, it is necessary to take into account the uniformity of the connections made before proceeding to purchase and choose the most suitable option, most specialized manufacturers offer versatility when it comes to the manufacture of the battery to incorporate the connector that best meets the needs of the project.

Power Distribution Board



Another of the main elements of unmanned aerial vehicles of the multi-rotor type is the power distribution plate, which is responsible for distributing the power of the power system between the different motors. This board is a printed circuit capable of withstanding high levels of current that has a series of ports in which the different elements are connected, there will be a port in which the terminals of the battery (or alternative power system) will go through Of the internal circuit of the plate will be connected to the power outputs of the same whose number will depend on the amount of rotors that own the aircraft. The most conventional only have this distribution circuit power, in the market can find others that also include a circuit that provides power or transmission of signals of a voltage lower than the electronics of the aircraft, as long as a system Additional power supply.

The plate, as its name indicates, is responsible for distributing the power but does not have any element to know how to do it, it is the drive associated with each motor that is responsible for requiring adequate supply of the battery in each Moment in line with the orders received from the flight controller. If a motor has to rotate faster, to perform whatever the movement, the inverter connected to the distribution board will be in charge of letting the necessary power to the winding of the motors so that it turns at the desired speed. When choosing the right plate, you have to take into account the maximum current flow you can have, this occurs when all motors rotate at maximum revolutions.

The distribution plate must be able to withstand the nominal current flow rate when all motors require maximum supply, leaving a safety margin to avoid possible breakdowns, this value is given in Amperes and must be provided by the manufacturer. The distributor plate is generally placed in the body of the aircraft as centered as possible for a better reach with all the variators and associated motors, because the amount of energy that circulates through it is an element prone to heat so it should Be provided with the maximum possible ventilation.

Flight Controller

The flight controller is the brains of the aircraft, capable of rotating the engines in the right way to achieve the desired movement by the ground controller or following the program guidelines in automatic flight.

It is a circuit of variable complexity that has a series of inputs and outputs, as well as a series of built-in sensors that determine in real time the position of the aircraft. The controller is in charge of processing both the information received by the sensors and the address data to send, through a series of algorithms, the appropriate commands to the motors using PWM signal for the correct flight.

The number and quality of sensors incorporated by the controller varies by model. Some carry a simple gyroscope that indicates the orientation in the space of the aircraft, however, most of the drivers currently used incorporate an Inertial Measurement Unit (IMU). The IMU is an electronic device capable of measuring and reporting both the speed of the aircraft, its orientation and the gravitational forces acting on it. To obtain this data is provided with accelerometers, gyroscopes and magnetometers

The controller can also receive another series of status data through other types of sensors such as a sonar or laser that indicates the distance of the vehicle to a point. Another device that usually includes the flight controllers of this class of vehicles is a GPS unit, capable of giving real-time information of the geographical coordinates of the aircraft. In addition to tracking the position of the UAV, the inclusion of GPS allows to perform waypoint flights, three-dimensional reference coordinates, which allows the aircraft to follow a route established by the user automatically between a numbers of locations.

Thanks to the information obtained by the controller, it is able to perform many tasks, depending on the ability of each will be able to develop more complex or less flight capabilities.

Depending on the task to be performed the aircraft will choose one type of controller or another, as we increase the degree of complexity and the capabilities of the same, will also increase its price.

It is also important to take into account when choosing the flight control system the ability to modify the programming thereof. Most systems

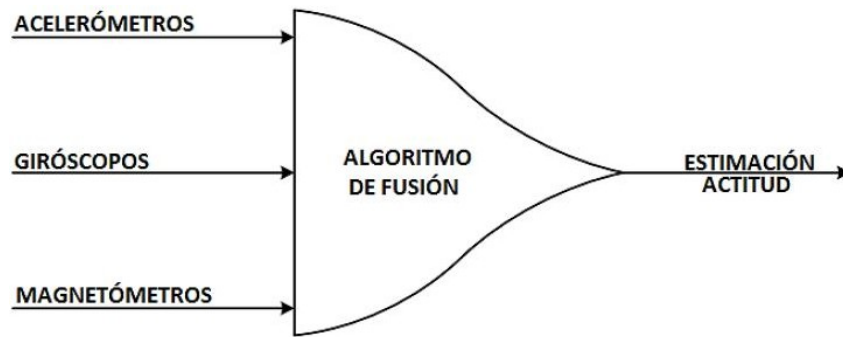
Available are closed systems that provide the services described by the manufacturer, however, if the user wants to modify the behavior or include new features, there are open source devices on the market. A microcontroller board can also be programmed to carry out the tasks performed by the controller.

Inertial measurement unit

The inertial measurement unit, known as the IMU (Inertial measurement unit), is an electronic sensor that measures the velocity, orientation and gravitational forces of a mobile system. This sensor owes its development to the evolution in MEMS microelectromechanical systems, which in the 1990s saw the emergence of the first commercial products; Among them are the inertial sensors that were developed by the company Analog Devices Inc. for automotive applications. (MEMS Microelectromechanical Systems)

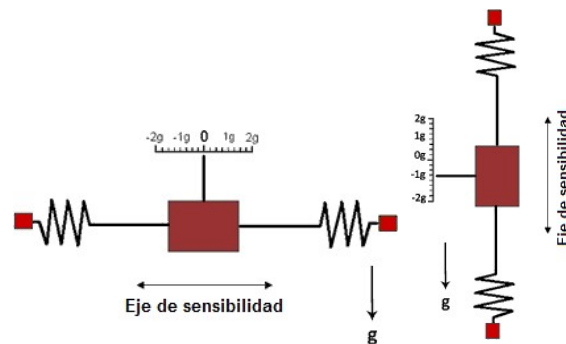


A system for determining the attitude of a mobile device is composed of gyroscopes, accelerometers and magnetometers which together represent an inertial unit of nine degrees of freedom (9DOF). The gyroscopes alone cannot provide a perfect measure of the rotational movements of a UAV, as they are commonly affected by external noise and tend to drift continuously. Therefore, it is necessary to incorporate magnetometers and accelerometers (the latter are very sensitive to vibrations but in the company of a gyroscope it is possible to differentiate between vibration and rotation) by means of a sensorial fusion algorithm. (Fux, 2008)



Accelerometer

An accelerometer is a sensor that measures your own acceleration or specific force. This can be thought of as a suspended mass which is attached to two springs on its sides, as shown in Figure.

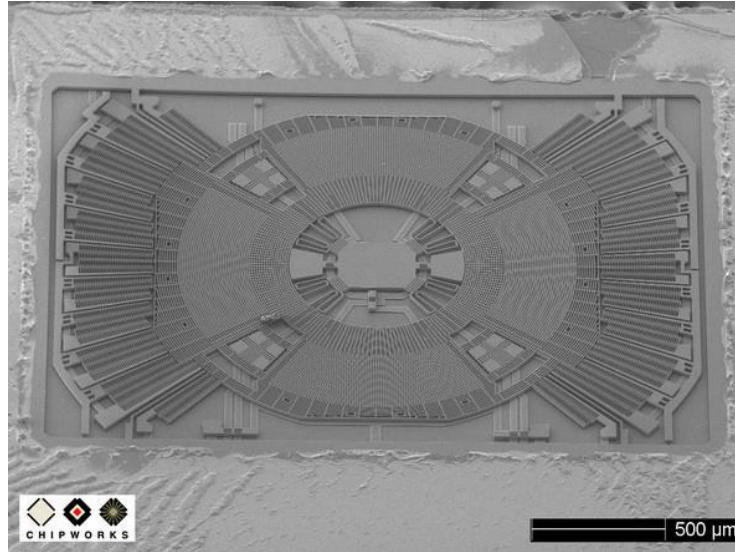


This mass is known as the test mass, and the direction in which it can be displaced is known as the axis of sensitivity.

Due to the gravitational force, it is necessary to analyze the spring mass system vertically, so that gravity acts parallel to the axis of mass sensitivity, as shown in Figure 40-b. It will be assumed that the accelerometer will measure both the linear acceleration due to motion, and the pseudo-acceleration caused by gravity. It receives this name because the acceleration of gravity does not necessarily result in a change of speed. This offset caused by gravity must be removed from the accelerometer measurement. (VectorNav Technologies)

Gyroscope

Typically used is the vibrating structure MEMS gyroscope, which detects the variation of the speed of rotation on an axis. It is called a vibrating structure because when rotating the gyroscope on an axis, by Coriolis effect, a vibration is produced that is measured by capacitive plates. The signal generated by the plates is treated to be proportional to the angular velocity.

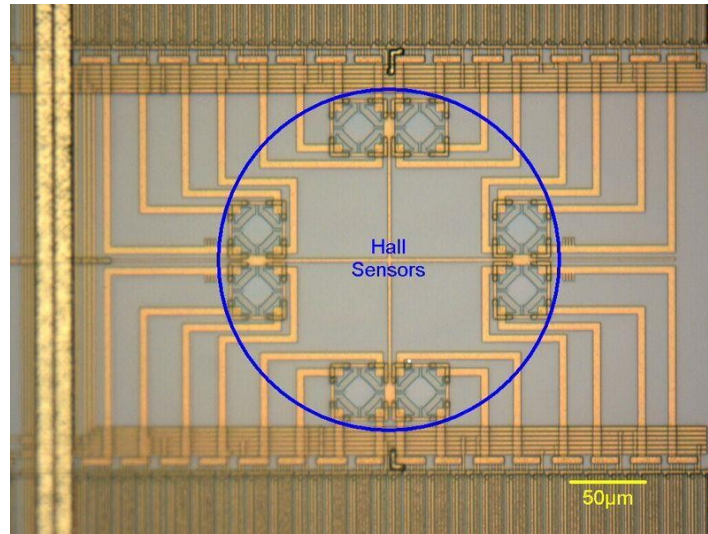


MEMS-type gyroscopes are commonly affected by various sources of error; The most common one appears when the gyro presents a measurement different from zero even though it is immobile. This error influences during the calculation of the angles of inclination, through methods of numerical integration. This factor can be corrected by determining the offset present in the measurement over an extended period of time in still state. (VectorNav Technologies)

Magnetometer

This sensor is based on the Hall effect, although it is not the only one. The Hall effect on these sensors can be described as the situation in which a current carrying semiconductor is placed in a magnetic field, the semiconductor load carriers will experience a force perpendicular to the magnetic field and current. At equilibrium a voltage will be created between the corners of the semiconductor.

The processing of this voltage will allow to know the value of the applied magnetic field. The measurement delivered by the sensor is the result of the addition of the earth's magnetic field to the fields generated by the objects near the sensor (VectorNav Technologies). The latter is considered as a disturbance, which is divided into two categories; The first is known as hard iron, which are all objects that have a permanent magnet, such as motors. The second category is called soft iron which are all those ferromagnetic objects that deflect the magnetic field perceived by the sensor. (Bouabdallah S., Design and control of framers with application to autonomous flying, 2007). The placement of several sensors of this type in a strategic way, also allows knowing the direction of the field lines.



Wireless Communication Modules

In the field of microcontrollable mobile devices, the two most widely used technologies are communication via infrared signals and communication via radiofrequency signals. (Ferrer Ferrer, 2012)

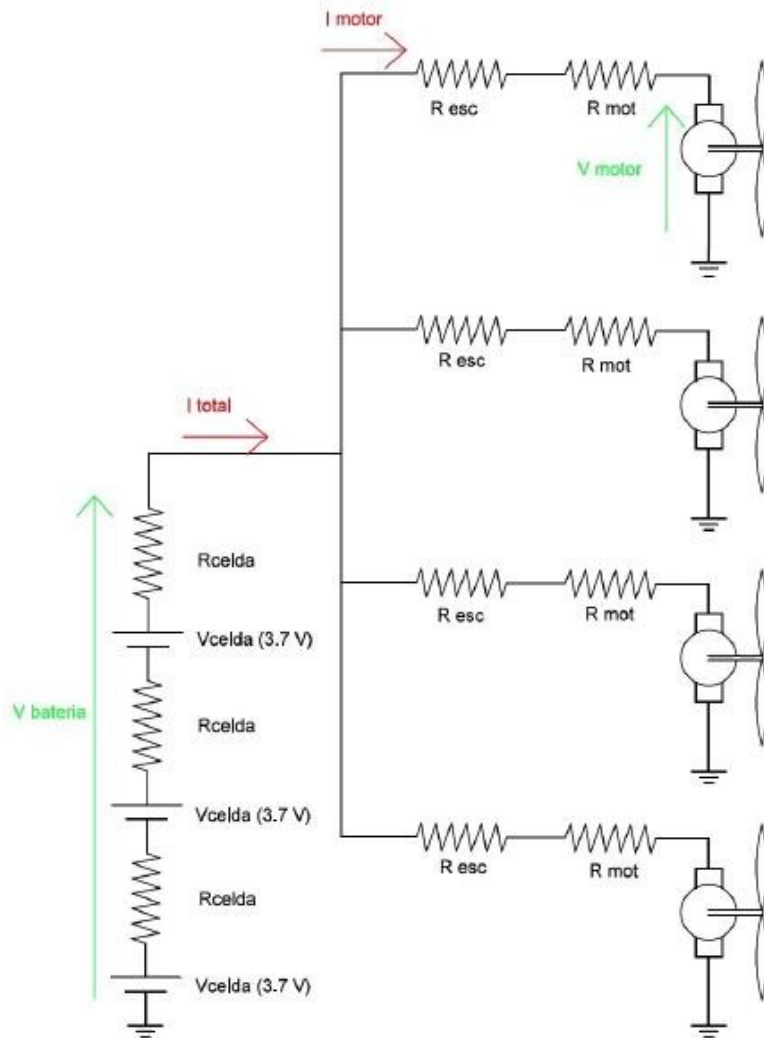
O Infrared communications systems offer significant advantages over radiofrequency systems. When using light as a medium, these systems have a channel whose bandwidth is very large and is not regulated anywhere in the world. Infrared systems are immune to interference and radio noise, but suffer from degradations caused by infrared noise in indoor and outdoor environments, mainly from the sun and fluorescent and incandescent light sources. (Zamorano Flores & Serrano Moya, 2002)

An example of infrared systems for outdoor environments is the Earth link AstroTerra Corporation, which in optimal weather conditions can reach distances of 3.5km and transmission speeds of 622Mbps. The main application of this product is the interconnection of high-speed networks, such as fast Ethernet, FDDI and ATM. For indoor environments, an example is the use of IrDA standard transceivers whose price is less than \$ 5. (Zamorano Flores & Serrano Moya, 2002)

O Unlike infrared communication, in radiofrequency systems, the use of the frequency spectrum is regulated by the International Telecommunication Union (ITU), which defines the spectrum range where it is necessary to acquire a license to operate. Within the radiofrequency communications we can find a wide range of protocols: ZigBee (IEEE 802.15.4), Wireless HART, Bluetooth, WiFi, WiMax, among others. (Ferrer Ferrer, 2012).

Electrical Parameters

The electrical diagram of the device is as follows:



Currently BLDC (Direct Brushless Direct Current) motors are classified mainly according to the parameter K_v , where:

We know that:

$$K_v = \frac{RPM}{Voltios} \quad (15)$$

$$K_t = \frac{30}{K_v \cdot \pi} \quad (16)$$

In this way we obtain the parameter:

$$K_t = \frac{Par}{Amperios} \quad (17)$$

Knowing the angular velocities and the necessary force we can now relate them to the voltage and current of each motor:

$$\frac{RPM}{K_v} = V_e \quad (18)$$

$$\frac{J}{K_t} = I_e \quad (19)$$

Where V_e is the input tension and I_e is the current. However, we must consider the resistance of the connectors and cables to the input as well as the resistance of the connectors, so that the equations remain as follows, where R_c is the resistance of connectors and cables:

$$\frac{RPM}{K_v} = (V_e - R_c \cdot I) \quad (20)$$

The term R_c also includes the internal resistance of the battery. In general, lithium batteries, see their maximum discharge capacity determined due to internal resistance. However, it is not typically provided by manufacturers. There is no standard by which to classify the quality of aeromodelling batteries and the differences between batteries of different prices are not clear.

We must take into account the current that consumes the motor without load, which represents the current of Vacuum I_0 , so the above equation is:

Then:

$$J = K_t I_e - K_t I_0 \quad (21)$$

$$\frac{J + K_t I_0}{K_t} = I_e \quad (22)$$

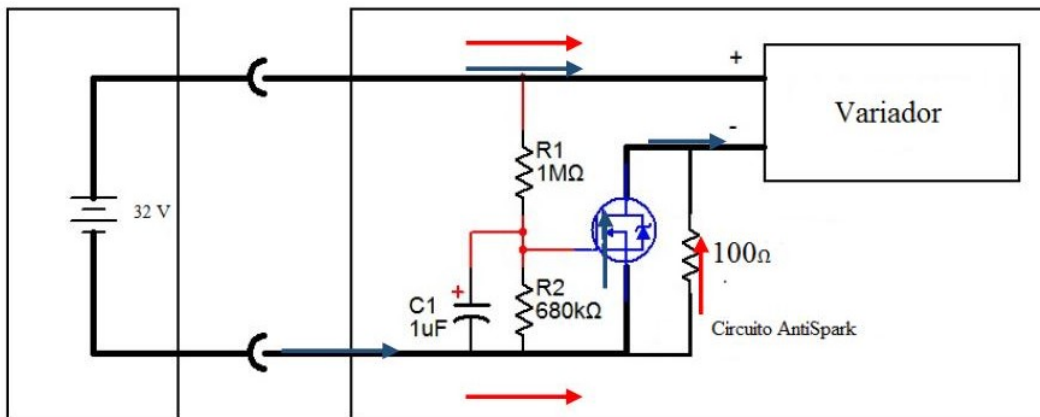
We can calculate the input electrical power as:

$$P_{e,entrada} = I_e \cdot V_e \quad (23)$$

Anti-Spark System

Next, the design of a system in charge of avoiding the undesirable ones is detailed Sparks when connecting the battery system. Due to the high level of voltage and charge of the, Batteries, when these are connected to give power to the engines a spark occurs that can end up damaging the connectors and be dangerous for the user of the aircraft. The spark occurs because the battery voltage exceeds the breakdown voltage of the air gap between the two connectors. The way to avoid this unwanted phenomenon is to perform a preload of the input capacitors of the electronic circuit to be fed, the inverters in the case studied. This will increase the breakdown voltage and eliminate the problem.

Therefore, a system must be designed to allow the capacitors to be precharged of the inverters, before making the total power connection. The solution is decided to circulate a small current through a resistor for a short time to charge the capacitors and then divert the current flow through another circuit that offers less impedance to power the circuit. This is achieved by including a more capacitive transistor system. In The following figure shows the proposed circuit.



At first the transistor is open so the current flows as indicated by the red arrows, through the resistance of 100Ω that will provide a limited current to charge the capacitors of the inverter. The transistor closes after the charge time of the capacitor of the circuit Will depend both on the capacity of the unit and on the resistances involved in the Scheme, according to the following formula:

$$V(t) = V_f \left(1 - e^{-\frac{t}{RC}} \right) \quad (24)$$

Being:

$V(t)$: The voltage in the capacitor

V_f : The voltage between the capacitor plates T : The charge time of the capacitor

A : Circuit resistance in Ohmios C : Condenser Capacitance

The chosen values of the circuit components are obtained in such a way that The charge time of the capacitor thereof, is sufficient for the capacitors

Of the inverters are charged through the resistor. To know this time value Just solve the equations of the capacitor.

The voltage between the capacitor plates is obtained by solving the mesh so that:

$$I_f = \frac{V_{bat}}{R_1 - R_2} = \frac{32 V}{680 K\Omega + 1M\Omega} = 1.9048 \cdot 10^{-5}$$

$$V_f = I_f \cdot R_2 = 1.9048 \cdot 10^{-5} \cdot 1M\Omega = 19.05 V$$

The value of V (t) is given by the circuit voltage at that point, i.e., the voltage Necessary to the input of the transistor to close the circuit. In the case of the transistor used, which will be detailed later, this value corresponds to 3 Volts.

$$t = -(R_1 + R_2) \cdot C \cdot \ln\left(1 - \frac{V(t)}{V_f}\right) = -1.68M\Omega \cdot 1\mu F \cdot \ln\left(1 - \frac{3V}{19.04V}\right) = 0.28s$$

So that time value more than enough to cause the load of the drives before the main power circuit closes. Once the transistor operates as a closed circuit the current will flow where the blue arrows in the diagram of Figure 44 indicate. In this case it is observed that the energy will circulate through the transistor whose impedance must be the smallest possible to avoid losses by dissipation and Maximize the efficiency of the batteries.

Other parameters:

Engine Efficiency:

$$\eta_{mot} = \frac{P_{mec}}{P_{ele}} \quad (25)$$

Battery duration:

$$Duración = \frac{I_e}{\frac{Capacidad}{10000}} \quad (26)$$

Calculation of parameters at maximum power

In this case, when simplifying BLDCs as traditional DC motors, we will assume that the maximum is given by applying the full voltage of the batteries to motor terminals. In this case we will need to solve the following system of equations where cp represents an empirical constant that is determined by the density of the air and by the aerodynamic profile of the propeller

$$\left\{ \begin{array}{l} RPM = K_v \cdot V_{mot} \end{array} \right. \quad (27)$$

$$\left\{ \begin{array}{l} P_e = C_p \cdot Pitch \cdot D^4 \cdot RPM^3 \end{array} \right. \quad (28)$$

$$\left\{ \begin{array}{l} I = I_0 + \frac{J}{K_t} \end{array} \right. \quad (29)$$

$$\left\{ \begin{array}{l} V_{mot} = V_{bat} - I \cdot R_{tot} \end{array} \right. \quad (30)$$

Calculation of parameters at maximum efficiency

The intensity of an engine at the point of maximum efficiency is determined by finding the maximum of equation 25 replacing the mechanical powers by the product of equation 21 and 20 and the electric by equation 23. For this we assume conditions of flight of 80 % Of engine speed, represented by parameter FP. In this way, the apparatus may have sufficient power to deal with disturbances.

$$I_{\eta max} = \sqrt{\frac{V_{bat} \cdot FP \cdot I_0}{(R_c + R_{bat})}} \quad (31)$$

Starting from the above equation, multiplying by Kt, we find the available torque to move the propeller:

$$J = (I_{\eta max} - I_0) \cdot K_t \quad (32)$$

Therefore, we must now find the effective voltage that is available at motor terminals

$$V_{mot} = V_{bat} - (I_{\eta max} \cdot (R_m + R_{bat})) \quad (33)$$

$$RPM = V_{mot} \cdot R_v \quad (34)$$

$$P_{mec} = RPM \cdot 2 \cdot \frac{\pi}{60} \cdot J \quad (35)$$

$$P_{ele} = V_{bat} \cdot I_{\eta max} \quad (36)$$

$$\eta_{max} = \frac{P_{mec}}{P_{ele}} \quad (37)$$

ORIENTATION OF A BODY IN THE SPACE

The orientation of a body in three-dimensional space is defined by three degrees of freedom or three linearly independent components. In order to be able to easily describe the orientation of an object relative to a reference system, it is customary to assign a new system to it, and then to analyze the spatial relationship between the two systems.

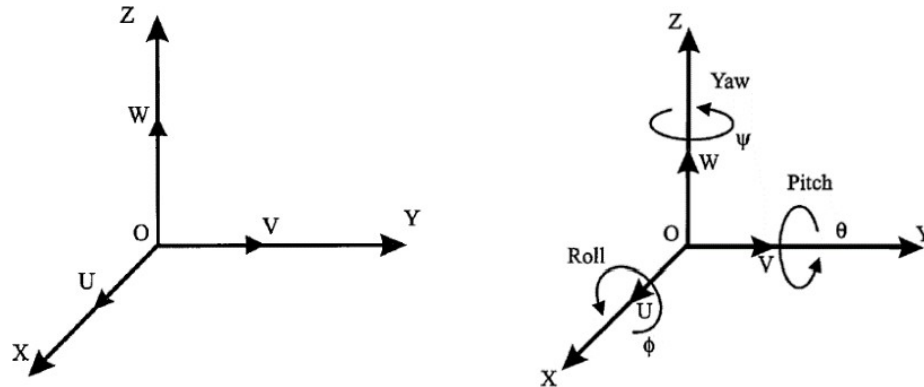
The spatial representation of the orientation of an object is defined by a global rotation matrix, which is composed of the continuous application of several successive rotations of the body.

Any reference system attached to a body whose orientation is to be described can be defined with respect to a fixed system by three angles: φ , θ , ψ , called Euler angles.

Euler's rotation theorem requires successive rotations about three axes of the fixed system, without performing two consecutive rotations on the same axis. There are altogether 12 different rotational representations.

In aeronautics the most used one is the representation of Tait-Bryan for the angles of Euler RPY (Roll: Rolling, Pitch: Inclination, Yaw: Orientation). The OUVW system (figure 46) can be oriented with respect to the OXYZ system following the following steps:

- I. Turn the OUVW system at an angle ψ to the axis OZ. This action corresponds to the so-called yaw angle.
- II. Turn the OUVW system an angle θ with respect to the axis OY. This action corresponds to the so-called pitch angle.
- III. Turn the OUVW system at an angle ϕ to the axis OX. This action corresponds to the so-called roll angle.

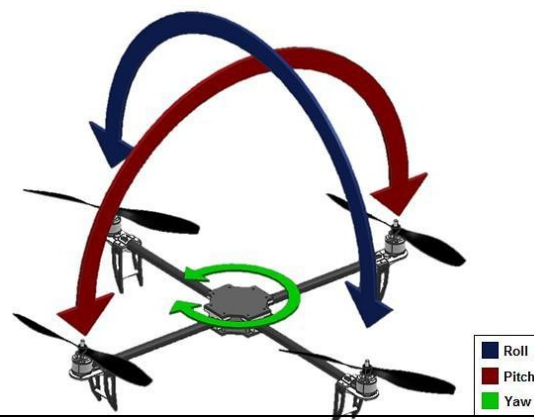


The global rotation matrix of the RPY representation is given by:

$$R = R_{Z\psi} R_{Y\theta} R_{X\phi} = \begin{bmatrix} C\phi & -S\phi & 0 \\ S\phi & C\phi & 0 \\ 0 & 0 & 1 \end{bmatrix} \begin{bmatrix} C\theta & 0 & S\theta \\ 0 & 1 & 0 \\ -S\theta & 0 & C\theta \end{bmatrix} \begin{bmatrix} 1 & 0 & 0 \\ 0 & C\psi & -S\psi \\ 0 & S\psi & C\psi \end{bmatrix}$$

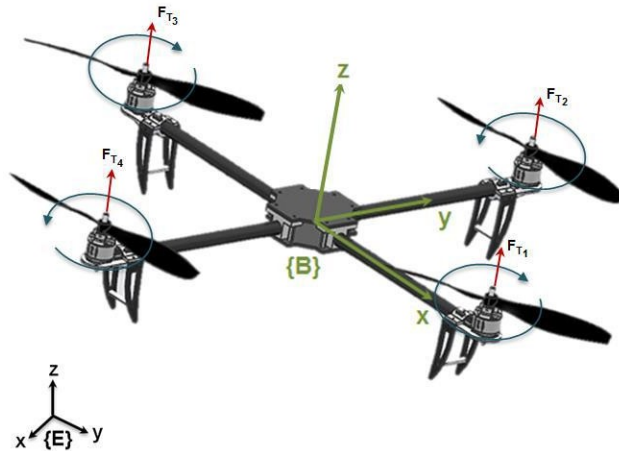
$$R = \begin{bmatrix} C\phi C\theta & C\phi S\theta S\psi - S\phi C\psi & C\phi S\theta C\psi + S\phi S\psi \\ S\phi C\theta & S\phi S\theta S\psi - C\theta C\psi & S\phi S\theta C\psi - S\phi S\psi \\ -S\theta & C\theta S\psi & C\theta S\psi \end{bmatrix}$$

In Figure, the RPY angles of a frame are specified:



THEORETICAL MODEL

For the development of the theoretical model the following notation should be considered:



Where,

{E}: Fixed reference frame (ground).

{B}: Body reference frame.

F_{T_i} : Propeller thrust force i .

Aerodynamics of the quadrotor

The thrust forces and drag torques produced by the propellers are calculated by considering the blade element theory (BEM), where the thrust force and the pulling torque are expressed from the Following way:

$$F_T = C_t \rho D^4 \omega^2$$

$$Q = \frac{C_p D^5 \omega^2}{2\pi}$$

Where,

F_T : Thrust force. [lbf]

Q : Drag torque. [ft.ft]

C_t : Thrust coefficient.

C_p : Power coefficient.

ρ : Density of air. [slugft³]

D : Propeller diameter. [ft]

ω : Rotation speed of the propeller. [rps]

Rotational cinematic kinematics

The angular velocity of a body with reference system {B} is given by the following relation:

$$\omega = \begin{bmatrix} 1 & 0 & -\sin\theta \\ 0 & \cos\varphi & \cos\theta\sin\varphi \\ 0 & -\sin\varphi & \cos\theta\cos\varphi \end{bmatrix} \dot{\theta}$$

Where the angular velocity vector $\omega = [\omega_x, \omega_y, \omega_z]^T$ is related to vector $\theta = [\phi, \theta, \psi]^T$ in terms of the matrix of the rotating rates of the Euler angles (Jacobian matrix).

$$\begin{bmatrix} \phi \\ \theta \\ \psi \end{bmatrix} = \begin{bmatrix} 1 & 0 & -\sin\theta \\ 0 & \cos\phi & \cos\theta\sin\phi \\ 0 & -\sin\phi & \cos\theta\cos\phi \end{bmatrix}^{-1} \begin{bmatrix} \omega_x \\ \omega_y \\ \omega_z \end{bmatrix}$$

$$\begin{bmatrix} \phi \\ \theta \\ \psi \end{bmatrix} = \begin{bmatrix} 1 & \sin\phi\tan\theta & \cos\phi\tan\theta \\ 0 & \cos\phi & -\sin\phi \\ 0 & \frac{\sin\phi}{\cos\theta} & \frac{\cos\phi}{\cos\theta} \end{bmatrix} \begin{bmatrix} \omega_x \\ \omega_y \\ \omega_z \end{bmatrix}$$

The above matrix equation represents the model of the rotational kinematics of the quadrotor with respect to the fixed reference system {E}.

Dynamics of the quadrotor

The model of the rotational dynamics of the quadrotor is expressed by the use of Euler's equation:

$$\sum T = I \cdot \dot{\omega} + \omega \times (I \cdot \omega)$$

Where,

T: Vector of external torques.

I: Inertia matrix.

ω : Vector of angular velocities of {B}.

To apply (63), the following considerations are assumed:

1. The structure of the quadrotor behaves like a rigid body (isotropic, homogeneous and continuous structure).
2. The structure is symmetric, therefore, the inertia matrix **I** is diagonal.
3. The center of mass coincides with the origin of the body reference system {B}. O Propellers behave like a rigid body.
4. The thrust force and the pulling torque are proportional to the square of the angular velocity of the propellers, therefore, (59) and (60) can be rewritten as follows:

$$F_T = b\omega^2$$

$$Q = k\omega^2$$

Equation (63) can be written as:

$$\dot{\omega} = I^{-1}(\omega \times (I \cdot \omega) + T)$$

The Torque Vector $\mathbf{T} = [\tau_\phi, \tau_\theta, \tau_\psi]^T$ Is composed of the moments generated by the thrust forces and the moments of drag of the propellers in each axis of rotation of the frame of reference $\{B\}$:

The torque τ_ϕ , is the moment generated around the x-axis by the thrust forces FT_4 and FT_2 .

The torque τ_θ , is the momentum generated around the y-axis by the thrust forces FT_1 and FT_3 .

The torque τ_ψ is the momentum generated around the z axis by the drag torques Q_1 , Q_2 , Q_3 and Q_4 .

Thus, the expression for the vector of torques T is written as:

$$T = \begin{bmatrix} \tau_\phi \\ \tau_\theta \\ \tau_\psi \end{bmatrix} = \begin{bmatrix} l(F_{T_4} - F_{T_2}) \\ l(F_{T_1} - F_{T_3}) \\ Q_1 - Q_2 + Q_3 - Q_4 \end{bmatrix}$$

Applying the equations (64) and (65) in (67), we have:

$$T = \begin{bmatrix} \tau_\phi \\ \tau_\theta \\ \tau_\psi \end{bmatrix} = \begin{bmatrix} lb(\omega_4^2 - \omega_2^2) \\ lb(\omega_1^2 - \omega_3^2) \\ k(\omega_1^2 - \omega_2^2 + \omega_3^2 - \omega_4^2) \end{bmatrix}$$

Where l is the distance from the center of mass of the quadrotor to the axis of the propeller.

Solving Eq. (66):

$$\begin{bmatrix} \omega_x \\ \omega_y \\ \omega_z \end{bmatrix} = \begin{bmatrix} I_{xx} & 0 & 0 \\ 0 & I_{yy} & 0 \\ 0 & 0 & I_{zz} \end{bmatrix}^{-1} \left(- \begin{bmatrix} \omega_x \\ \omega_y \\ \omega_z \end{bmatrix} \times \left(\begin{bmatrix} I_{xx} & 0 & 0 \\ 0 & I_{yy} & 0 \\ 0 & 0 & I_{zz} \end{bmatrix} \begin{bmatrix} \omega_x \\ \omega_y \\ \omega_z \end{bmatrix} \right) + \begin{bmatrix} \tau_\phi \\ \tau_\theta \\ \tau_\psi \end{bmatrix} \right)$$

$$\begin{bmatrix} \omega_x \\ \omega_y \\ \omega_z \end{bmatrix} = - \begin{bmatrix} \omega_y \omega_z (I_{yy} - I_{zz}) I_{xx}^{-1} \\ \omega_x \omega_z (I_{zz} - I_{xx}) I_{yy}^{-1} \\ \omega_x \omega_y (I_{yy} - I_{xx}) I_{zz}^{-1} \end{bmatrix} + \begin{bmatrix} \tau_\phi I_{xx}^{-1} \\ \tau_\theta I_{yy}^{-1} \\ \tau_\psi I_{zz}^{-1} \end{bmatrix}$$

(70) represents the model of the rotational dynamics of the quadrotor.

Simplification of the model

The state vector $\mathbf{x}(t)$ takes the following form:

$$x(t) = \begin{bmatrix} \theta \\ \omega \end{bmatrix} = \begin{bmatrix} \varphi \\ \theta \\ \psi \\ \omega_x \\ \omega_y \\ \omega_z \end{bmatrix}$$

The first order differential equations are:

$$\dot{x}(t) = \begin{bmatrix} \dot{\theta} \\ \dot{\omega} \end{bmatrix}$$

Where \mathbf{x} is formed by equations (62) and (70).

$$\dot{x} = \begin{cases} \dot{\varphi} = \omega_x + (\sin\varphi \tan\theta)\omega_y + (\cos\theta \tan\theta)\omega_z \\ \dot{\theta} = (\cos\varphi)\omega_y + (-\sin\varphi)\omega_z \\ \dot{\psi} = \frac{\sin\varphi}{\cos\theta}\omega_y + \frac{\cos\varphi}{\sin\theta}\omega_z \\ \dot{\omega}_x = -\omega_y\omega_z(I_{yy} - I_{zz})I_{xx}^{-1} + \tau_\varphi I_{xx}^{-1} \\ \dot{\omega}_y = -\omega_x\omega_z(I_{zz} - I_{xx})I_{yy}^{-1} + \tau_\theta I_{yy}^{-1} \\ \dot{\omega}_z = \omega_x\omega_y(I_{yy} - I_{xx})I_{zz}^{-1} + \tau_\psi I_{zz}^{-1} \end{cases}$$

The model (73) can be complex for the design of controllers, so a simplified model should be obtained that describes the behavior of the aircraft in an approximate way. In this way, they will take into account considerations (Bouabdallah, Noth, & Siegwart, PID vs. LQ Control Techniques Applied to an Indoor Micro Quadrotor, 2004) and (Bresciani, 2008) to simplify the model obtained in (73).

The dynamic model of equation (70) considers the gyroscopic effect of the structure. The influence of this effect is negligible with respect to the action of the rotors, especially when considering a situation close to the stationary flight.

In stationary flight condition, the matrix of the Euler angles of rotation can be approximated to the identity matrix 3x3. Thus, equation 20 can be rewritten as:

$$w \approx \begin{bmatrix} 1 & 0 & 0 \\ 0 & 1 & 0 \\ 0 & 0 & 1 \end{bmatrix} \dot{\theta}$$

$$\begin{bmatrix} \omega_x \\ \omega_y \\ \omega_z \end{bmatrix} \approx \begin{bmatrix} \dot{\varphi} \\ \dot{\theta} \\ \dot{\psi} \end{bmatrix}$$

THE CONTROL SYSTEM OF A CUADRICOPTER

Conventional, line or sports aircraft are designed to have a self-stabilizing balance. That is, if an external disturbance tends to remove them from their level flight the natural tendency of the aircraft is to return by itself to the neutral position. This is not applicable to acrobatic aircraft or fighters where design is subtracted to increase maneuverability.

In the case of aircraft with rotating wings the situation is complicated since already the helicopter, with a single rotor, is by its own unstable topology and accurate correction systems. It is sufficient to understand that control of the tail rotor is necessary to compensate for the reaction torque produced by the main rotor if an uncontrolled yaw movement is not desired.

In the case of multirotor systems the situation is much more complex still. A multicopter presents structural advantages but its level of instability is such that its flight and handling would be impossible of not existing a stabilization system that acted automatically on the rotating regimes of the rotors. It is what with certain aircraft is called "Fly by Wire".

This section will show, in a general way, what the control structure of a quadcopter is and what elements compose it. Since it will be necessary to use some equation, we will start by defining some of the variables that will appear later.

If the rotor angular speeds, numbered from left to right and from front to back, are designated as: $\omega_1 \omega_2 \omega_3 \omega_4$

The displacement angles of the quadcopter will be:

1. *alabeo* = ϕ
2. *Cabeceo* = θ
3. *Guiñada* = γ
4. Vertical thrust = L

And, therefore, the speed of movement according to these angles will be the derivative of the same with respect to time:

5. *alabeo* velocity = $d\phi dt = \dot{\phi}$
6. *cabeceo* velocity = $d\theta dt = \dot{\theta}$
7. *guiñada* velocity = $d\gamma dt = \dot{\gamma}$
8. Lift velocity = $dL dt = \dot{L}$

One of the movements will now be considered and the result will be extrapolated to all others. Taking into account that the yaw is produced by the difference between the rotational speeds of the rotors located at the diagonal ends of the quadcopter (a configuration in X or H is considered) it will be assumed that the yaw rate can be calculated as:

$\dot{\gamma} = ((\omega_1 + \omega_3) - (\omega_2 + \omega_4))$ where k is simply a constant of proportionality. If the set of equations is presented in matrix form, and for simplicity it is assumed that all constants of proportionality are the same, the movement of the quadcopter can be expressed as:

$$\begin{bmatrix} \dot{\phi} \\ \dot{\theta} \\ \dot{\psi} \\ \dot{L} \end{bmatrix} = \begin{bmatrix} k & -k & -k & k \\ k & k & -k & -k \\ k & -k & k & -k \\ k & k & k & k \end{bmatrix} \begin{bmatrix} \omega_1 \\ \omega_2 \\ \omega_3 \\ \omega_4 \end{bmatrix} = [K] \begin{bmatrix} \omega_1 \\ \omega_2 \\ \omega_3 \\ \omega_4 \end{bmatrix}$$

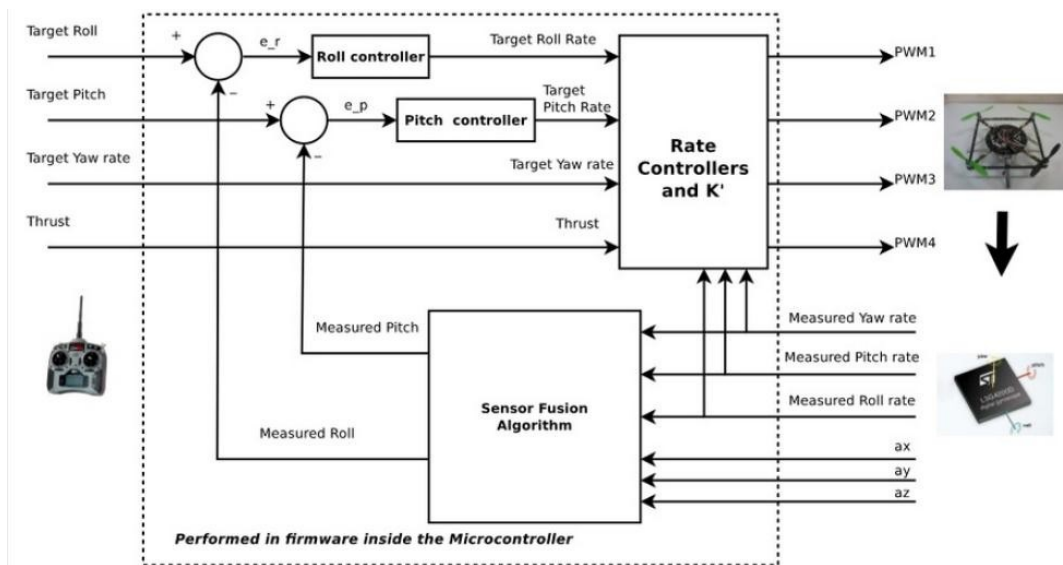
The solution to this problem is to use a closed-loop system. To do this, the signal obtained from the gyroscopes and solid state accelerometers present in the flight control system is obtained by obtaining the matrix of ratios of speed of movement according to the 3 axes and is compared with the desired value, indicated by the Pilot by acting on the station's controls. The difference (error) between the measured variable and the desired variable is the input to a PID controller, well known to all engineering students, and its output is the one that provides the PWM signal that is actually applied to each inverter to set the speed of desired rotation in each rotor

One would think that these control loops completely solve the problem, and therefore there is no need to further complicate the flight system algorithm. However, it is not so.

The gyroscopes measure angular velocities that, once integrated, allow to know the angle of roll, pitch, etc. Of the quadcopter. The integration made for this process is numerical and, therefore, already contains errors inherent to the mathematical calculation. In addition, all gyros have a certain "offset" with temperature. This is nothing more than a measurement error that causes them to indicate zero when they should not, and also presents the variability associated with the temperature at which the sensor is located.

On the other hand, the accelerometers measure the acceleration on the 3 axes of the object to which they are fixed. This measurement can be considered accurate when performed on a body at rest. If the object is in motion, especially if it is subjected to vibration, its measurement is not quite accurate either. Thus, if the control system is simplified to the point of Figure 50, complete stabilization will not be achieved.

The solution to solve this problem could be called "measurement fusion of the sensors" and consists in fusing the angular and acceleration measurements by introducing a predictive mathematical algorithm: usually a Kalman filter, an extended Kalman filter (EFK) or the use Of DCM (Direct Cosine Matrix) and a calculation based on quaternions, all complex mathematical processes but that can be understood intuitively from the following diagram:



Chapter 2

Literature Review

Aerial vehicles have proved their capability in both military field such as patrolling, surveillance as well as reconnaissance, and civil areas including transport, rescue and agriculture of various applications over a hundred years, while enhancing their capabilities over time, and fulfilling ever-changing mission requirements. By means of smaller, safer and lighter platforms, UAVs propose an exclusive set of advantages compared to piloted aircrafts. Military and civil operations are the main areas where these advantages are effectively utilized.

In addition, future UAVs are expected to perform much more extended missions with higher aerodynamic performance and higher degrees of automatic flight. There are two prominent categories of mini UAVs; fixed-wing UAVs and multi-rotors. Fixed-wing UAVs are mini UAVs with propelled electrical batteries with longer ranges than UAVs with similar sizes of multi-rotor systems that require a runway or launcher for landing and knockout.

On the other hand, the multi-rotor UAVs have rotor systems generally carrying three or four propellers that are capable of vertical take-off and landing (VTOL) and hovering over an area while carrying sufficient payload. In addition, they are more manoeuvrable than fixed wing UAVs with the ability of quickly transition from hover to cruise flight.

However, the horizontally mounted rotor system is placed at the wings or the body that results in an enormous increase in drag force opposing the cruise flight. As a result of this decrement in the aerodynamic performance, fixed wing UAVs are more logical to be used to fulfil the missions needed high speed, long range and endurance flight. The fixed-wing UAVs has longer flight time and duration, but it is not simple to secure a safe landing space, especially in the city and rugged train areas.

VTOL systems make more sense in operations such as mountainous and rural areas where there is no landing and take-off runway. In addition, VTOL systems must be used to operate like a helicopter in the required tasks such as hovering. However, if endurance is of first priority then a fixed wing type will most likely be preferred due to the efficiency of the cruise flight. If both of these features are demanded in a single operation then a fixed wing vertical and take-off landing (VTOL-FW) with level flight capability becomes the best option.

- Going to unmanned small scale VTOL vehicles also termed as Micro Unmanned Aerial Vehicle (UAV).
- They have more than one rotor hence named as multirotor systems.
- They have fixed pitch propellers in compare to variable pitch propellers in helicopters.
- Presently more research is done in this field owing to the advantages of it to its size.

Selection of Airframe Configuration



Lockheed XFV-1 1951,
Lockheed - American Aerospace manufacturer.⁽¹⁾



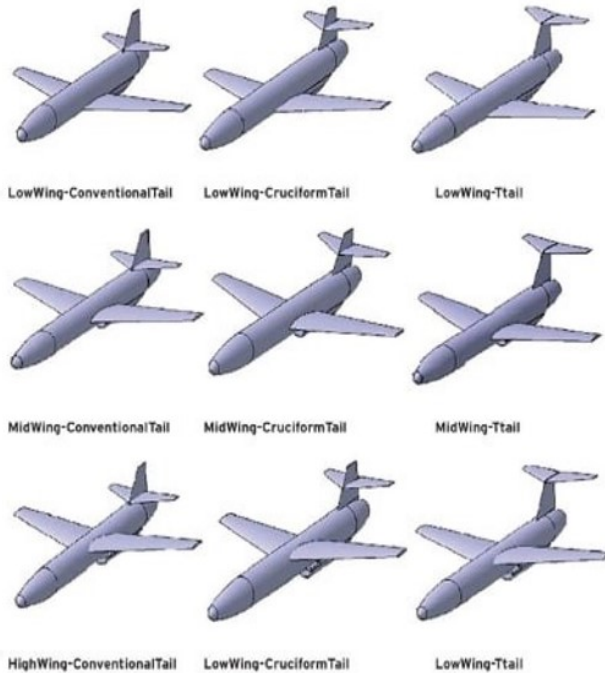
Harrier Jump Jet - 1957
Hawker Aircraft Company⁽¹⁾



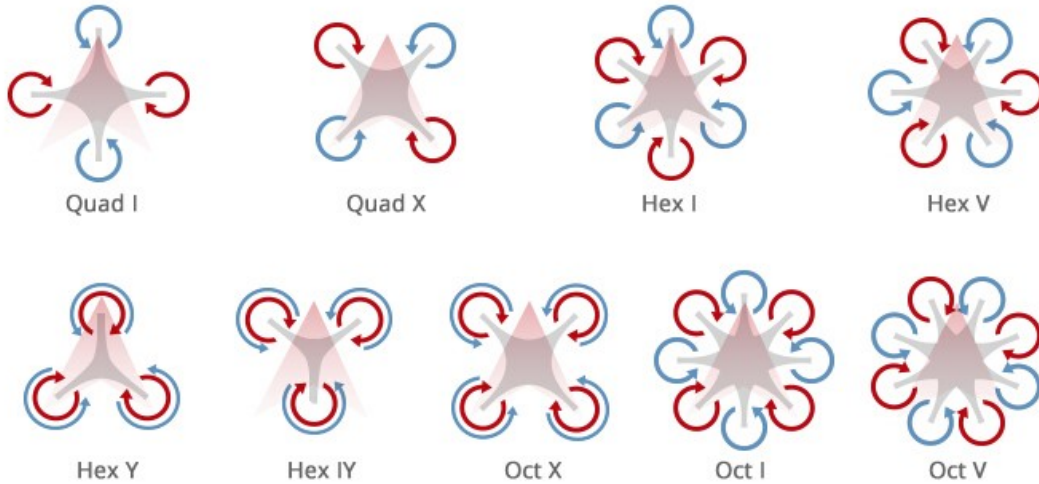
Yak-38 1970, Soviet National Aviation,



Bell Boeing V-22, USA Department of
Defence -1981⁽¹⁾



Fixed-wing configurations



Multirotor configurations

Comparison of Multi Rotor & Fixed Wing Configurations



Multirotor

- + Easy to control and maneuver
- + Have the ability to hover
- + Can fly vertically and horizontally
- + Takeoff and land vertically
- + More compact in size
- + Often lower priced
- + Can land in designated spot
- Limited flying time
- Small payload capabilities
- Less stability in the wind
- Lower flight speeds



Fixed Wing

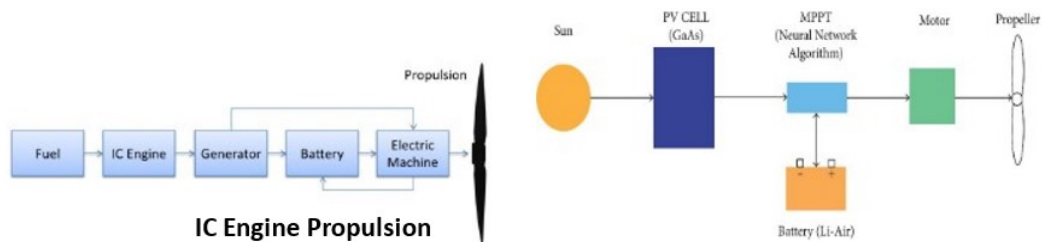
- Training is usually needed to fly one
- Unable to maintain fixed position
- Can only fly horizontally (forward)
- Require hand or mechanical launch
- Less compact in size
- Can be expensive
- Difficult to land, more space needed
- + Longer average flight times
- + Can carry a heavier payload
- + Greater stability in the wind
- + Generally higher flight speeds



Key impact factors for choosing Fixed wing multi rotor UAV (1)

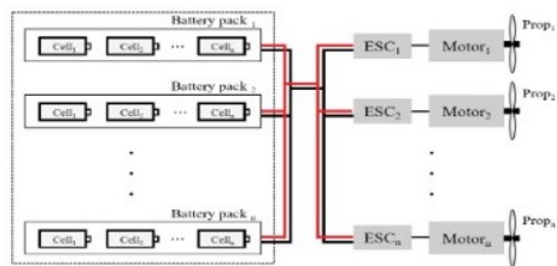
- Longer Endurance
- Increases Payload Capacity
- Can be operated in sever wind conditions.
- Longer Battery life

Propulsion Systems



IC Engine Propulsion

Solar-Battery Propulsion

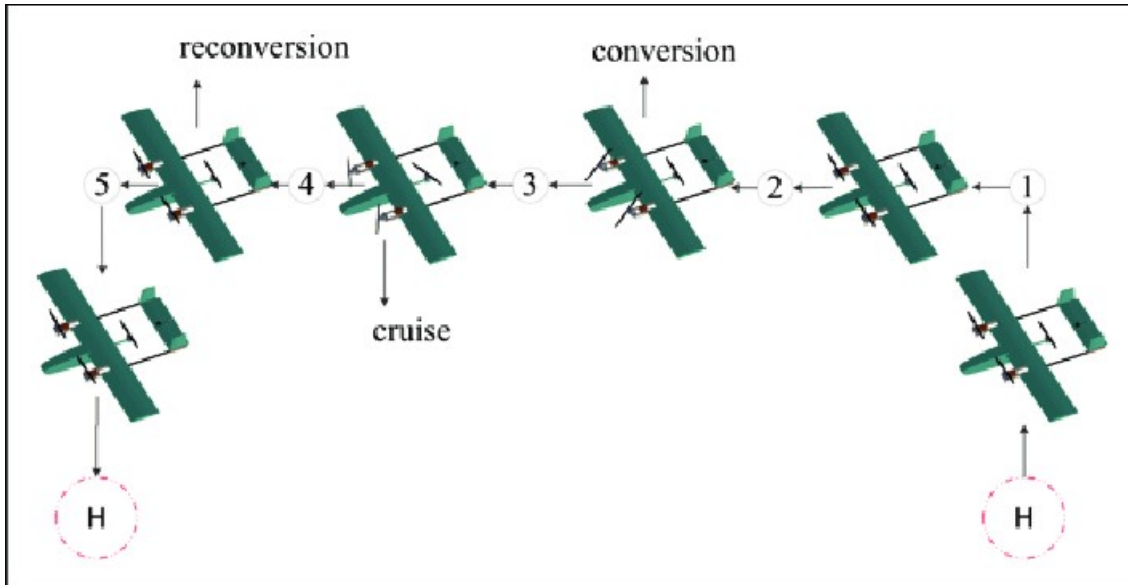


Electric Propulsion

Chapter 3

Requirements Specifications

Mission Profile



Objectives

- Design & development a fixed wing multirotor UAV with the payload capacity of 1 Kg (Medical kit or Vaccines).
- To achieve the max. Flight endurance of 30 min. with the range of 2 Km.
- Development of designed prototype using 3D printing additive manufacturing process.

Methodology

1. Literature review on UAV systems and Mission profiles and requirements

- Performing through investigation on UAV airframe configurations and their performance characteristics.
- Performing market tradeoff study on UAV system components.
- Selection of suitable airframe configuration and mission profiles.

2. Initial sizing, thrust to weight ratio and wing loading estimation

- Developing design constraint diagrams.
- Iterative sizing and takeoff weight estimation.
- Performing preliminary CFD analysis and determining the performance characteristics.

3. Development of UAV mathematical model & System components tradeoff Study

- Selection of UAV system components (Motor, ESC, Flight controller, Landing gear & Propellers) with the tradeoff study.

- Development of mathematical model for Rigid body flight equations of motion using MATLAB.

4. Design of UAV Components

- Design of Wing & Control surfaces based on the required lift conditions.
- Design of Fuselage, based on the required payload and weight distribution.
- Design of Landing gears and performing structural analysis.

5. Design Optimization and development of final drawings

- Optimization of UAV structures using Topology optimization and lattice structure study using Ansys.
- Post processing of resulted components.
- Validation of optimized components for required load conditions.
- Development of final assembly and drawings.

6. Fabrication on UAV components

- Performing manufacturability assessment on UAV components.
- Preparation of CAD models for 3D-Printing process.
- Post processing of 3D printed components.
- Creating of Assembly of UAV components.

7. Testing of developed UAV as per mission requirements

- Developed UAV will be tested with the payload of 1Kg under various flight modes.
- Monitoring Performance and efficiency during the flight.

Scope for Future Work

1. Improving the design for transition-based flight modes.
2. Developing the airframe for tilt-rotor systems.
3. Developing Image processing algorithms for better flight operations & disaster management activities.

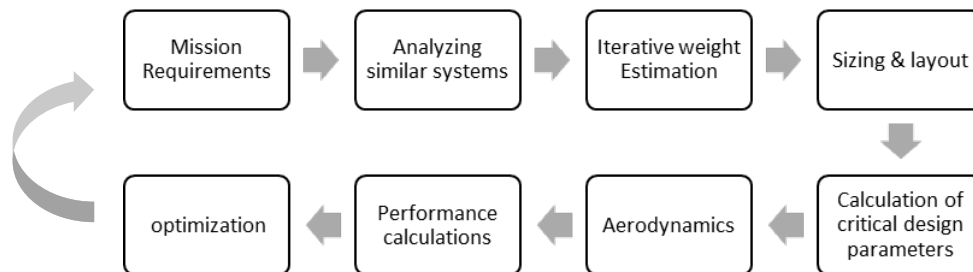
Chapter 4

DESIGN

Design Statement

Sl. No	Requirements
1	Minimum Endurance – 30 min.
2	Maximum Payload – 0.3 KG
3	Maximum Speed – 30 Km/Hr
4	Maximum Altitude – 600 m
5	Operational Temperature - 60° C

Design Methodology



As per the mission and operational requirements, the possible take-off weight of the UAV is estimated based on the historical data for general aircraft conceptual design i.e. ($W_e / W_{T0} = 0.85$). Knowing the minimum aerodynamic characteristics for the given operational range helps us to predict the preliminary sizing of major aircraft components and lifting devices required to sufficiently satisfy the mission requirements. Analysing these initial sizing parameters at give operational conditions will help us to know more aerodynamic parameters to check for optimization and iterative calculations were considered to optimize the performance of the UAV.

Assumptions for the design

1. $T/W = 1.5$ (thrust to weight ratio)
2. Considered UAV as a light aircraft.
3. UAV will be powered with a hybrid power system. i.e. (Li-ion battery + Solar PV arrangement to increase the endurance)

1. Sizing of the UAV

- a. Weight Estimation
- b. Wing loading
- c. Initial sizing of wing

- i. Determining the lift-coefficient of wing
- ii. Determining the lift-coefficient of airfoil
- iii. Calculation of possible max. wing loading
- iv. Selection of airfoil for the wing
- v. Thickness ratio selection criteria
- vi. Airfoil generation and analysis at different ranges of Reynolds numbers
- vii. Aspect ratio selection, verifying with the possible wing loading & determining the new wing span required.
- viii. Taper ratio
- ix. Root chord
- x. Tip chord
- xi. Mean Aerodynamic Chord
- xii. Sweep angle selection
- xiii. Twist angle
- xiv. Dihedral angle
- xv. Selection of high lifting devices & wing tip
- xvi. Sizing of Horizontal & Vertical Stabilizer
- d. Aerodynamic forces
- e. Landing Gear
 - i. Positioning
 - ii. Tire sizing & Forks
 - iii. Static Analysis
- f. Material Selection
- g. Weight Breakdown & C.G

2. Power system selection

- a. Battery Capacity
- b. Solar charge Controller

3. Performance of B-1800

- a. Flight Envelope

4. Summary

5. Future Scope of Work

- a. Development of Bladeless Propulsion system based on coanda effect
- b. Landing gear development to land & take-off from both land & water.

A. Weight Estimation

$$\frac{W_{To} - 15}{W_{To}} = 0.85 \quad \text{Eq.1}$$

Considering estimating the possible take-off and empty weight of an aircraft is the very first step in sizing of the UAV. The ratio of W_e / W_{To} can be obtained from the historical data for conceptual aircraft design. It can be stated as W_e / W_{To} is about 0.85. One of the design requirements of the UAV is to carry a payload of 15 Kg weight. As $W_e = W_{To}$ ratio is about 0.85 at Eq. (1), then W_{To} can be found as **100 Kg**.^[1]

In order to continue further, knowing the dimensions of the wing is very much important as wing plays major role to lift the aircraft in to the air. In order to know the dimensions of the wing a market study is been carried out considering the payload capacity and endurance that is relevant to our design statement. And we found that the average wing span for a UAV of carrying max. Payload of 15 Kg. with an endurance of 2 hrs in the range of 4.5 m to 5m. As the larger aspect ratio reduces the power consumption to keep the given weight in the air and results in less induced drag wing span of 4.8 m is for preliminary sizing of the UAV.

B. Wing loading

With the wing span of 5 m and max. Take-off weight of the UAV i.e. 100 Kg got the wing loading as 40 Kg/m².

C. Initial sizing of the wing

a. Calculating the required lift co-efficient of the UAV at cruise velocity

With the basic understanding of aerodynamic forces, for steady state flight we know that

$$\begin{aligned} \text{Lift} &= \text{Weight} \\ L &= \frac{1}{2} \times V^2 \times \rho \times S \times C_L \end{aligned}$$

As per one of the design requirement, the maximum flight speed as 150 Km/hr (i.e. velocity of 41.66 m/s) and flying altitude as 6000 m ASL. We found that the density of air is 0.661Kg/m³ @ 6000 m.

We know that the basic lift co-efficient formula as,

$$C_{Lc} = \frac{2 \times \left[\frac{W}{S} \right]}{V_c^2 \times \rho} \quad \text{Eq.2}$$

Where;

- a. C_L = Lift Co-efficient
- b. W/S = Wing Loading in, Kg/m²
- c. V_c = Cruise Speed of the UAV, in m/s
- d. ρ = Density of air at flying altitude, in m
- e. W = Max. Take-off weight of the UAV in Kg
- f. S = Wing span in m

We found that the lift co-efficient required for the B-14H1800 as =0.861
 In order to find the lift coefficient for the wing & airfoil alone at cruise velocity;

$$C_{L@Wing} = \frac{C_{Lc}}{0.95} \quad Eq.3$$

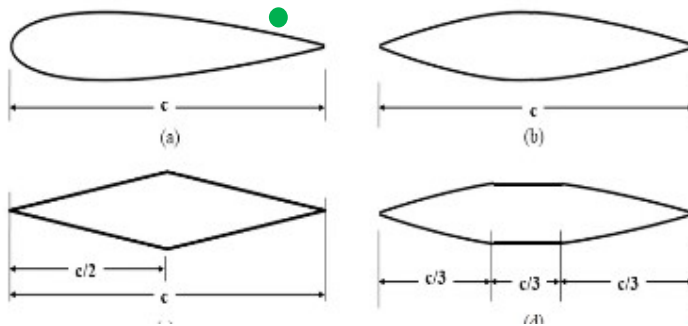
$$C_{L@airfoil} = \frac{C_{L@wing}}{0.9} \quad Eq.4$$

We found that;

Based on the $C_{L@airfoil}$ the selection of airfoil is made, considering the ability of the airfoil to produce sufficient lift with lesser angle of attack and larger stalling angle makes the airfoil suitable to use in the aircraft or UAV.

b. Selection of airfoil

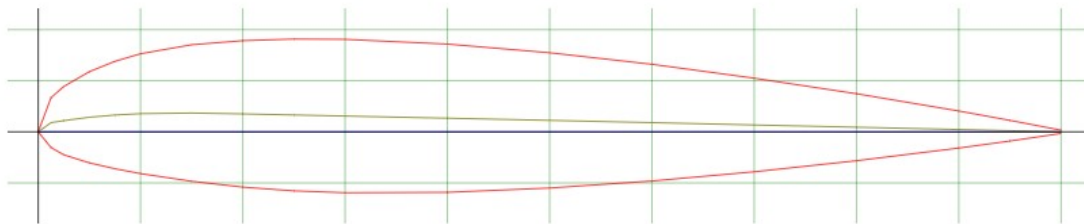
As selection of an airfoil for any aircraft is always depends on the operational flight regime.



And as our flight regime is subsonic a general use airfoil is selected. For low speed general light aircraft max. t/c of 15% to 18% is recommended.

Selected t/c as 15%

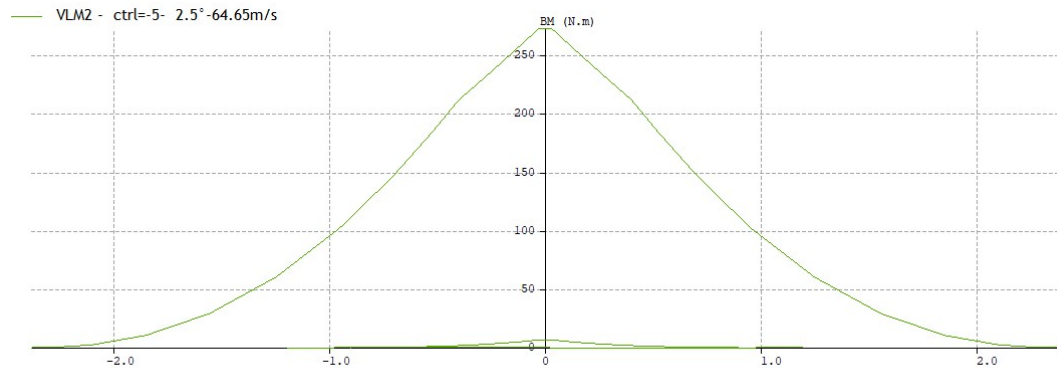
Airfoil selected: NACA 23015



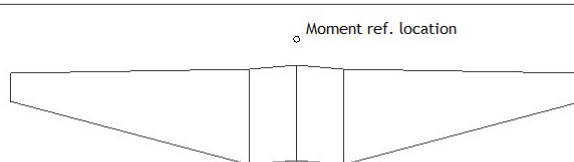
Preliminary wing analysis

Parameters	Values	units
Maximum cruise speed	41.6	m/s
Max. Wing loading	40	Kg/m ²
Airfoil	NACA23015	
Aspect ratio	8.46	
Wing area	2.72	m ²
Wing span	4.8	m
Taper ratio	0.3	
Root chord, C _r	.6	m
Tip chord, C _t	.2	m
Sweep angle	0 °	
Twist angle	2 °	
Dihedral angle	1 °	

Bending Moment

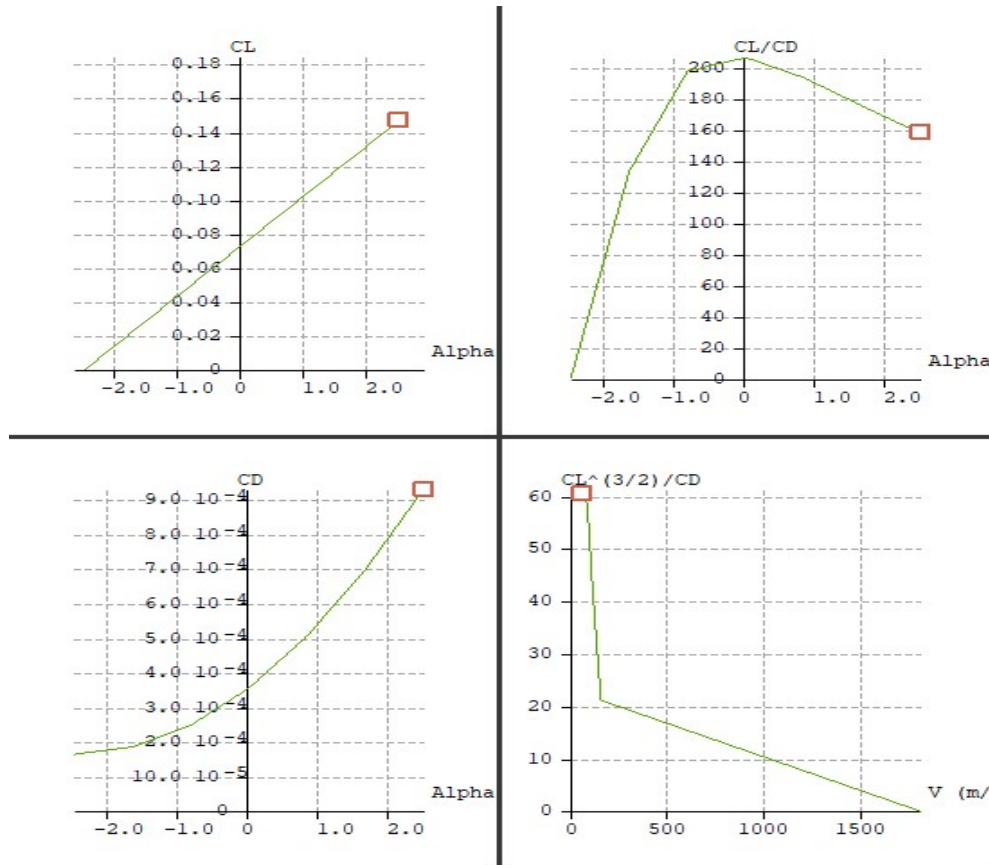


Wing Load = 20.202 kg/m²
 Tail Volume = 0.507
 Root Chord = 0.801 m
 MAC = 0.625 m
 TipTwist = 2.000 °
 Aspect Ratio = 8.462
 Taper Ratio = 3.338
 Root-Tip Sweep = -1.677 °
 XNP = d(XCp.Cl)/dCl = 0.000 m
 Mesh elements = 2076



X_CP = -0.220 m
 X_CG = -0.218 m
 Wing Flap 1 Moment = 1.3354 N.m
 Wing Flap 2 Moment = 0.3275 N.m
 Wing Flap 3 Moment = 0.3275 N.m
 Wing Flap 4 Moment = 1.3354 N.m
 Elev Flap 1 Moment = 0.1751 N.m
 Elev Flap 2 Moment = 0.1751 N.m
 Fin Flap 1 Moment = 0.0600 N.m
 Fin Flap 2 Moment = 0.0600 N.m

Aerodynamic characteristics of 5 m Span wing.



With the basic understanding of, in order to get maximum endurance, the UAV must fly in a condition such that it is experiencing least drag and should produce maximum lift in order to keep the UAV in air. At the same time flying in $C_l^{(3/2)} / C_d$ maximum condition reduces the power consumption in order to produce thrust in cruise condition. After the iterative performance analysis over the market available UAV wing characteristics, it's been observed that going for larger aspect ratio and increasing wing area for the given operating condition, will substantially makes the UAV statically and dynamically stable and aerodynamically safe design.

Wing Sizing (Main wing)

i. Span & Wing area

$$AR = \frac{b^2}{S}$$

Since, higher aspect ratio results in reduced wing loading and produces more lift, the aspect ratio of 10 is chosen for initial calculations. and by iterating for the better performance we found that the aspect ratio of 10.75 gives a better performance & span of 6 m is suitable for the wing loading of 40 kg/m² with the wing area of 3.347 m².

ii. Taper ratio

$$\lambda = \frac{C_t}{C_r} \quad (0 \text{ to } 1)$$

Taper ratio plays a very important role to reduce induce drag, with the reference below found that the taper ratio of 0.3 can be used for most practical & good performative results.

iii. Mean aerodynamic Chord, Root & Tip Chord

Root Chord:

$$C_{root} = \frac{2S}{b(1+\lambda)}$$

Up on substituting the span of 6m, wing area of 3.47 m² & taper ratio λ of 0.3, found that the suitable root chord length as 0.88 m.

Tip Chord:

$$C_{tip} = \lambda \times C_{root}$$

And with the root chord length of 0.88 m got the wing tip chord as 0.266 m.

Mean aerodynamic chord:

$$\bar{c} = \frac{2}{3} \times C_r \times \left[\frac{(1+\lambda+\lambda^2)}{1+\lambda} \right]$$

With the C_r & C_t of 0.88 m & 0.26 m found the mean aerodynamic chord length as 0.571 m.

iv. Sweep angle

Initially we considered the wing as a rectangular box with 0° sweep angle wing, due to the lift force produced by the wing it is assumed that the wing is experiencing a bending and shear load. And in reality addition to the normal load, the wing experiences a tangential forward force which equals the leading edge suction force minus the wing drag.

Typically sweep angle has a major contribution and corresponding effects on maximum lift produced, Drag co-efficient, critical MACH no. , Structural weight & Stability.

Selection of sweep angle can be made on the flight regime, as our flight regime is subsonic and with the MACH no. of 0.12 the sweep angle is chosen as 0°.

v. Twist angle

As we all know Wing twist or Twist angle is an aerodynamic feature added to aircraft wings to adjust lift distribution along the wing. And with the two categories of wing twist (i.e. geometrical twist and aerodynamic twist) aerodynamic twists are most commonly used in most of the monoplanes and light aircrafts to avoid the tip stalling.

Considering our UAV as a light aircraft the aerodynamic twist is assumed as 2°

vi. Dihedral angle

As our selective wing type is a high wing type, and 2° of dihedral angle is been used to as it affects the roll movement of the UAV proportional to the amount of sideslip. The effect produced by the above condition is also known as Dihedral effect. Dihedral effect is also a critical factor in the stability of an aircraft about the roll axis (the spiral mode). It is also pertinent to the nature of an aircraft's dutch roll oscillation and to manoeuvrability about the roll axis.

D. Selection of high lifting devices

High lift devices are movable surfaces or, in some cases, stationary components that are designed to increase lift during some phases or conditions of the flight. The most common high lift devices are flaps, slats and Krueger flaps, but the category also includes less common installations such as lead-edge root extensions.

The main purpose of using the high lifting devices are:

- To allow a steeper approach without increasing the speed of the aircraft
- Reduces the distance required to take-off and land
- Reduces the speed at which the aircraft will stall
- They increase the pilot’s visibility of the runway

Effects of using Flaps

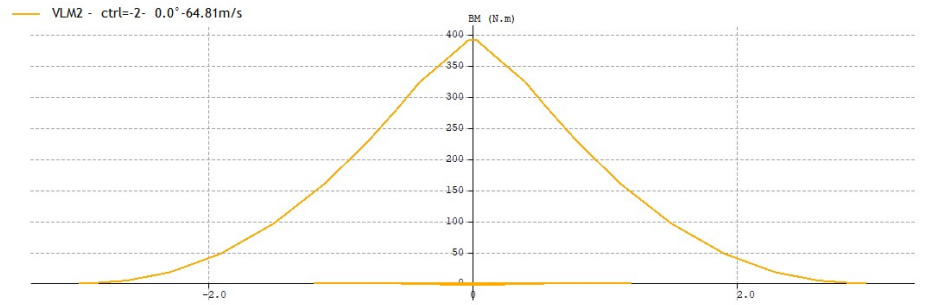
- **Relation with Centre of pressure:**
 - Flap movement, up or down, will cause a change of pitching moment. This is due to Centre of Pressure (CP) movement.
 - Centre of pressure is a point where all the lift of the aircraft is considered to be concentrated.
- **Relation with lift and drag:**
 - Lowering flap increases both lift and drag, but not in the same proportion. Although the lift is a larger force, and proportional increase in the drag is greater, so the maximum lift/ drag ratio decreases.

In our case **fowler type flaps are used** as it is most widely used in all the military, modern aircrafts which allows our UAV will have a suitable and appropriate function to maintain the operational requirements.

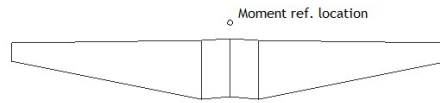
E. Final design Parameters of Wing for B-14H1800

Parameters	Values	units
Maximum cruise speed	41.6	m/s
Max. Wing loading	40	Kg/ m ²
Airfoil	NACA23015	
Aspect ratio	10.75	
Wing area	3.347	m ²
Wing span	6	m
Taper ratio	0.3	
Root chord, C _r	.88	m
Tip chord, C _t	.26	m
Sweep angle	0 °	
Twist angle	2 °	
Dihedral angle	1 °	
Material of the wing	Polyethylene terephthalate - PET	

Bending Moment Diagram



Wing Load = 16.433 kg/m²
 Tail Volume = 0.369
 Root Chord = 0.801 m
 MAC = 0.615 m
 TipTwist = 2.000°
 Aspect Ratio = 10.755
 Taper Ratio = 3.338
 Root-Tip Sweep = -1.341°
 XNP = d(XCp.Cl)/dCl = 0.000 m
 Mesh elements = 2076



X_CP = -0.221 m
 X_CG = -0.220 m
 Wing Flap 1 Moment = 0.8078 N.m
 Wing Flap 2 Moment = 0.1646 N.m
 Wing Flap 3 Moment = 0.1646 N.m
 Wing Flap 4 Moment = 0.8078 N.m
 Elev Flap 1 Moment = 0.0836 N.m
 Elev Flap 2 Moment = 0.0836 N.m
 Fin Flap 1 Moment = 0.0307 N.m
 Fin Flap 2 Moment = 0.0307 N.m

Achievements

IJERT International Journal of Engineering Research & Technology
ISSN : 2278 - 0181, www.ijert.org
(Published by : ESRSA Publications)

CERTIFICATE OF PUBLICATION

This is to certify that

Dr. Balaji B

Has published a research paper entitled

Design & Performance Evaluation of 3- Blade Propeller for Multi-Rotor UAV

In IJERT, Volume 10, Issue 10, October - 2021

Registration No: IJERTV10IS100158 Date: 08-11-2021 Chief Editor, IJERT

IJERT International Journal of Engineering Research & Technology
ISSN : 2278 - 0181, www.ijert.org
(Published by : ESRSA Publications)

CERTIFICATE OF PUBLICATION

This is to certify that

Arun V

Has published a research paper entitled

Design & Performance Evaluation of 3- Blade Propeller for Multi-Rotor UAV

In IJERT, Volume 10, Issue 10, October - 2021

Registration No: IJERTV10IS100158 Date: 08-11-2021 Chief Editor, IJERT

IJERT International Journal of Engineering Research & Technology
ISSN : 2278 - 0181, www.ijert.org
(Published by : ESRSA Publications)

CERTIFICATE OF PUBLICATION

This is to certify that

Kallapalli Chamukya R

Has published a research paper entitled

Design & Performance Evaluation of 3- Blade Propeller for Multi-Rotor UAV

In IJERT, Volume 10, Issue 10, October - 2021

Registration No: IJERTV10IS100158 Date: 08-11-2021 Chief Editor, IJERT

IJERT International Journal of Engineering Research & Technology
ISSN : 2278 - 0181, www.ijert.org
(Published by : ESRSA Publications)

CERTIFICATE OF PUBLICATION

This is to certify that

Yasfwanth B S

Has published a research paper entitled

Design & Performance Evaluation of 3- Blade Propeller for Multi-Rotor UAV

In IJERT, Volume 10, Issue 10, October - 2021

Registration No: IJERTV10IS100158 Date: 08-11-2021 Chief Editor, IJERT

Design & Performance Evaluation of 3- Blade Propeller for Multi-rotor UAV

Arun V
Department of Mechanical Engineering
K.S School of Engineering & Management
Bangalore-India
mec invento@gmail.com

Rallapalli Chanukya R
Department of Mechanical Engineering
K.S School of Engineering & Management
Bangalore-India

Yashwanth B S
Department of Mechanical Engineering
K.S School of Engineering & Management
Bangalore-India
mec invento@gmail.com

Prof. Dr. Balaji B
HOD, Department of Mechanical Engineering
K.S School of Engineering & Management
Bangalore - India
hod.mech@kssem.edu.in

Abstract— This work emphasis on research, designing and development of an 3-blade efficient propeller for an existing UAV to produce maximum thrust in an operating range of 2000 rpm to 3000 rpm. And CFD analysis will be performed to determine the performance characteristics of the propeller.

Keywords— UAV, Quadcopter, Propellers, Multicopters, VTOL

I. INTRODUCTION

A propeller is a device that converts mechanical energy into a force, which we call thrust, and is used to propel the vehicle to which it is attached. The propeller features one or more lifting surfaces called propeller blades that are rotated rapidly using an engine. The thrust is the aerodynamic lift force produced by the blades and is identical to the force produced by a wing. Propellers are, by far, the most common means of generating thrust for any general Aviation aircrafts or modern UAVs.

II. 3-BLADE PROPELLER GEOMETRY

A.

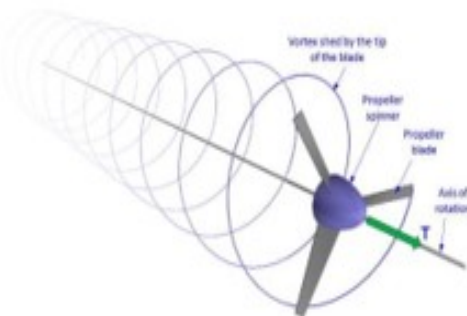


Figure 1 – Propeller Helix

A three-bladed propeller is shown in Figure 1, rotating about an axis. The spinner is an aerodynamically shaped cover, whose purpose is to reduce the drag of the hub of the propeller and to protect it from the elements. The propeller blades are

what generate the thrust of the device, denoted by T . The pressure differential between the front and aft face of the propeller blade results in a vortex that is shed from the tip of the blade and is carried back by the airflow going through the propeller. This forms the typical helical shape shown in the figure-1. A frontal projection of the three-bladed propeller is shown below.

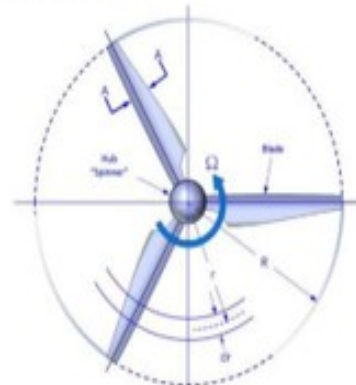


Figure-2 Frontal projection of the 3-blade propeller

Where R is the blade radius, r is the radius to an arbitrary blade station, and U is the rotation rate, typically in radians per second or minutes. The blade of a propeller is really a cantilevered wing that moves in a circular path rather than along a straight one. Just like an airplane's wing, the plan form of the propeller blade has a profound impact on the magnitude of the thrust force created, as well as at what "cost." What constitutes "cost" is the amount of power required to rotate it, as well as side effects such as noise.

III. GEOMETRIC PROPELLER PITCH

Consider the propeller in Figure - 3, whose diameter is D and radius is R . As the propeller rotates through a full circle, its tip rotates through an arc length (circumference) of $C = 3.14 \times D = 2 \times 3.14 \times R$. As the propeller rotates it "screws" itself forward a certain distance P for each full rotation. The

distance it would cover in one full revolution is called the geometric pitch or pitch distance, PD, of the propeller. It is commonly specified in terms of inches of pitch. Thus a propeller designated as a 42-inch pitch prop would move 42 inches forward in one revolution (using the metal screw through wood analogy). The angle the helix makes to the rotation plane is called the geometric pitch angle and is denoted by β .

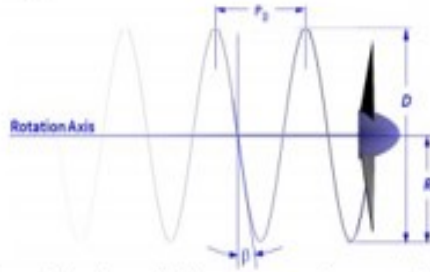


Figure-3 schematic showing propeller properties

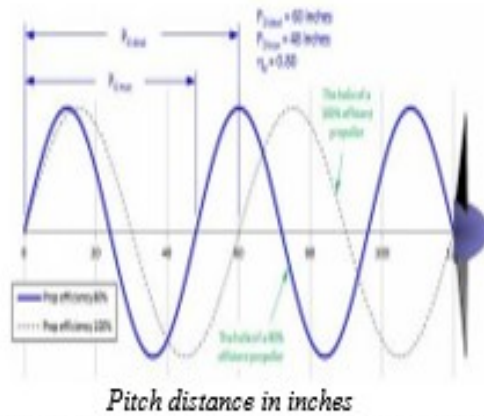


Figure-4 the propeller will advance a shorter distance (pitch distance) in a low-viscosity fluid than the geometric pitch indicates

IV. FUNDAMENTAL FORMULATION

Considering the geometry shown in figure-3 we can now define the following characteristics of the propeller:

$$\tan\beta = \frac{PD}{2\pi r_{ref}} \quad (\text{Eq. 1})$$

Where;

r_{ref} = reference radius, usually 75% of the propeller radius R.
 PD = Pitch distance of the propeller
 Generally, the value of PD ranges from 60% to 85% of the diameter of the propeller. The pitch-to-diameter ratio is also used to identify propellers

Pitch-to-diameter ratio

$$\frac{PD}{D} \quad (\text{Eq. 2})$$

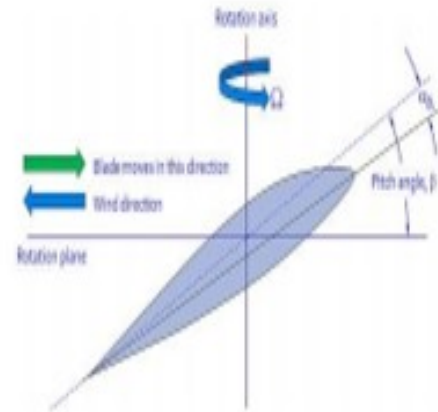


Figure-5 Definition of propeller pitch angle

A propeller moving through a low-viscosity fluid like air will cover less distance per revolution than the geometric pitch would indicate. Therefore, the angle formed between the rotation plane and a tangent to the blade tip helix at each blade station is less than the geometric pitch angle. This angle is called the helix angle and is denoted by ϕ . It can be estimated if the forward speed of the propeller is known using the following expression:

Helix angle:

$$\tan\phi = \frac{2\pi r n}{v_0} \quad (\text{Eq. 3})$$

V. DESIGN STATEMENT

Propellers for UAVs operate under various operating conditions, ranging from the sea level to stratosphere altitudes. Apparently, it is appropriate to adopt a variable pitch system to provide the optimal propulsive efficiency under the aforementioned conditions. However, its adoption imposes additional weight and complexity due to the addition of actuators and pitch links. Additionally, these pitch links and actuators will practically be exposed to external flows at low temperatures from -70 to -80°C at stratospheric altitudes. The extreme environment and mechanical complexity may lead to an increased possibility of malfunctions and uncertainty. Consequently, the demand for reliability and being ultra-lightweight, which are top-level constraints of UAVs, makes it difficult to adopt the variable pitch system. Therefore, fixed-pitch propellers are generally used. When the fixed-pitch propellers are optimized for aerodynamic performance at high-altitude operation, the required torque, approximately at sea level, becomes considerably large and exceeds the specification for electric motors. This can lead to low climbing performances or, sometimes, the inability to climb. On the other hand, as altitude increases, the rotational speed of the propeller gradually increments, which consequently results in an increase of the required power. Thus, the maximum required power occurs under high-altitude climbing conditions. In this respect, the design of UAV propellers must not only take into account the two conflicting constraints but also simultaneously maximize efficiency under the desired operating condition.

VI. DESIGN REQUIREMENTS

The ultralight weight aircraft, has a total length, total width and design total weight of approximately 1.2 m, .5 m, and 2.5 kg, resp

Details View	
[-] Details of Enclosure2	
Enclosure	Enclosure2
Shape	Cylinder
Cylinder Alignment	Y-Axis
Number of Planes	0
Cushion	Non-Uniform
<input type="checkbox"/> FD1, Cushion Radius (>0)	15 mm
<input type="checkbox"/> FD2, Cushion (>0), +ive Direction	30 mm
<input type="checkbox"/> FD3, Cushion (>0), -ive Direction	30 mm
Target Bodies	All Bodies
Merge Parts?	No
Export Enclosure	Yes

actively. It uses 4-propellers mounted on each arm. The maximum available torque should correspond to the climb condition at sea level, requiring the highest thrust. The maximum power condition should correspond to the climb operation where the highest rotational speed is required. Considering the motor diameter, the design propeller diameter was fixed at 0.25 m. as a geometry constraint. In conformance with the mission profile, which is mainly aimed at climbing to high altitudes, the climb condition of 4 km was set as the propeller design point.

VII. AIRFOIL SELECTION & POSITIONING^[2]

Airfoil	r/R	Chord length in inches C	R	Chord length in mm C	Pitch in inches	Pitch in mm	Alpha
NACA 4515	0.3	1.5915	38.1	40.4341	0.7968	20.23872	4.8
NACA 5513	0.4	1.875	50.8	47.625	1.1512	29.34048	5.199
NACA 5513	0.5	2.109	65.5	53.5886	1.5485	39.3319	5.59
NACA 4512	0.6	2.285	76.2	58.059	1.9557	49.67478	5.92
NACA 4510	0.7	2.391	88.9	60.7822	2.3338	59.27852	6.05
NACA 4410	0.8	2.351	101.6	59.7154	2.6948	68.44792	6.11
NACA 4309	0.9	2.0985	114.3	53.3019	3.00465	76.31811	6.05
NACA 4309	1	1.2565	127	31.9151	3.283	81.3582	5.82

VIII. CAD MODEL PREPARATION



Figure-7 10 inch Propeller cad model

IX. CFD ANALYSIS PREPARATION

Considerations

- Speed – 3000 rpm
- Inlet Velocity – 15m/s
- Angle of attack = 10°
- Propeller Dia = 250 mm
- Number of Blades = 3
- Propeller Material = Carbon fiber

Step-1

Creating Enclosures – Cylindrical Enclosures

Step – 2

Creating Enclosures – Box Enclosure

Details View	
[-] Details of Enclosure3	
Enclosure	Enclosure3
Shape	Box
Number of Planes	0
Cushion	Non-Uniform
<input type="checkbox"/> FD1, Cushion +X value (>0)	300 mm
<input type="checkbox"/> FD2, Cushion +Y value (>0)	400 mm
<input type="checkbox"/> FD3, Cushion +Z value (>0)	300 mm
<input type="checkbox"/> FD4, Cushion -X value (>0)	300 mm
<input type="checkbox"/> FD5, Cushion -Y value (>0)	400 mm
<input type="checkbox"/> FD6, Cushion -Z value (>0)	300 mm
Target Bodies	All Bodies
Merge Parts?	No
Export Enclosure	Yes

Step -3

Creating Boolean-1

Tool Body: Propeller

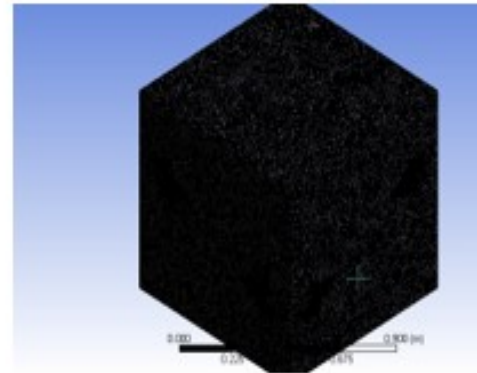
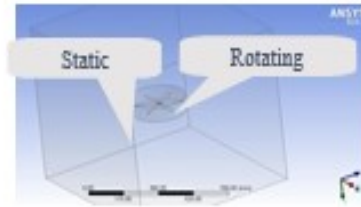
Target Body: Cylindrical Enclosure

Now we have only 2 Bodies i.e.

1. Rotating Domain
2. Static Domain

Creating Boolean-2

Tool Body: Rotating Domain
Target Body: Static Domain



Step-4

A. Meshing

1. Inseted Mesh sizing for rotating domain
Max- Element size – 8 mm

Details of "Face Sizing" - Sizing	
Scope	
Scoping Method	Geometry Selection
Geometry	74 Faces
Definition	
Suppressed	No
Type	Element Size
<input type="checkbox"/> Element Size	10.0 mm
Advanced	
<input type="checkbox"/> Defeature Size	Default (4.e-002 mm)
Behavior	Soft
<input type="checkbox"/> Growth Rate	Default (1.2)
Capture Curvature	No
Capture Proximity	No

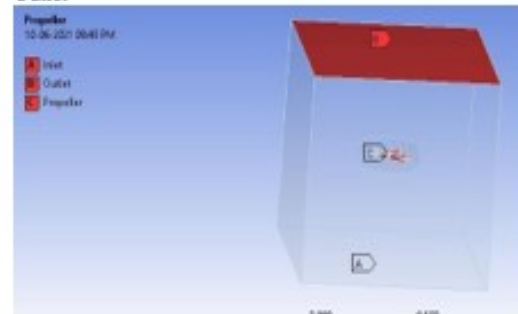
2. Mesh Settings – Static Domain
Max- Element Size – 15 mm

Details of "Mesh"	
Physics Preference	CFD
Solver Preference	Fluent
Element Order	Linear
<input type="checkbox"/> Element Size	15.0 mm
Export Format	Standard
Export Preview Surface Mesh	No
Sizing	
<input type="checkbox"/> Use Adaptive Sizing	No
<input type="checkbox"/> Growth Rate	Default (1.2)
<input type="checkbox"/> Max Size	15.0 mm
Mesh Defeaturing	
<input type="checkbox"/> Defeature Size	Default (7.5e-002 mm)
Capture Curvature	
<input type="checkbox"/> Curvature Min Size	Default (0.15 mm)
<input type="checkbox"/> Curvature Normal Angle	Default (18.0°)
Capture Proximity	No
Bounding Box Diagonal	1553.5 mm
Average Surface Area	66279 mm ²
Minimum Edge Length	0.16208 mm
Quality	
Check Mesh Quality	Yes, Errors
<input type="checkbox"/> Target Skewness	Default (0.900000)
Smoothing	Medium
Mesh Metric	None
Inflation	
Assembly Meshing	
Advanced	

Step-5

Creating named Selections

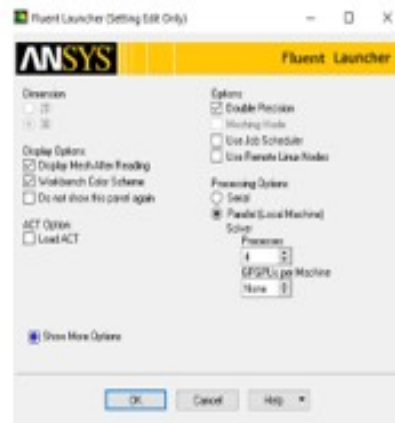
Propeller
Inlet
Outlet



Step-6

Updating the Mesh

Step-7



Step-8

Setup
Selecting Transient and Gravity



Step-9

Model – Viscous Laminar

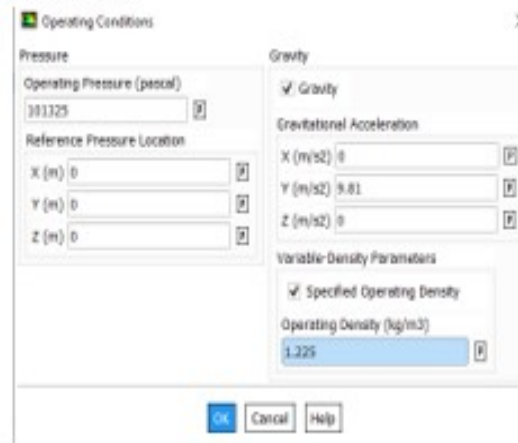


Step-10

**Cell Zone Conditions
Rotating Domain**



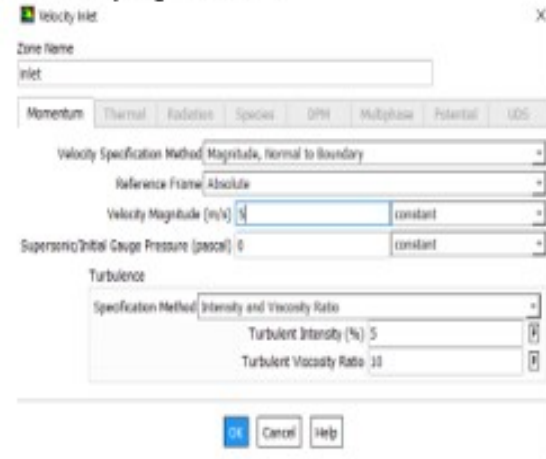
Static Domain



Step-11

Boundary Conditions

Inlet velocity magnitude = 5 m/s



Reference Values

Reference Values

Compute from:

Reference Values

Area (m2)

Density (kg/m3)

Enthalpy (J/kg)

Length (m)

Pressure (pascal)

Temperature (K)

Velocity (m/s)

Viscosity (kg/m-s)

Ratio of Specific Heats

Reference Zone:

Step-12

Report Definitions

Create new force report- Thrust Force

Force Report Definition

Name:

Options:

For Zone

Average Over (Time Steps):

Force Vector:

X	Y	Z
<input type="text" value="0"/>	<input type="text" value="1"/>	<input type="text" value="0"/>

Report Files (1/1):

- report-def-1.rpt

Report Plots (1/1):

- report-def-1.rpt

Create Output Parameter Highlight Zones

B.

C. Step-13

D. Calculation Activities

Create- Solution Data Export

Initialization

File Type:

Area:

Pressure (Pa):

Temperature (K):

Velocity (m/s):

Viscosity (kg/m-s):

Ratio of Specific Heats:

Step-14

Initialization – Initialization method – Hybrid

Initialization

Initialize

Initialization Method: **Hybrid** (Initialize with values from the Case, Duration = 1)

Standard

Step-15

Initialize

Step-16

Run Calculation

Time Steps – 0.00015

Number of Steps – 10

Max. Iterations / step – 1 (selected for less computing time)

Run Calculation

Check Case...

Time Stepping Method: Time Step Size (s):

Number of Time Steps:

Options:

Extrapolate Variables

Data Sampling for Time Statistics

Sampling Interval:

Time Sampled (s):

Solid Time Step

User Specified

Automatic

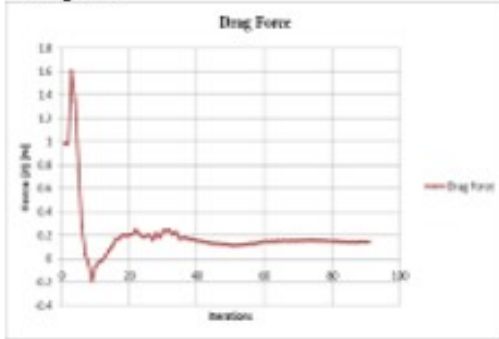
Max Iterations/Time Step: Reporting Interval:

Profile Update Interval:

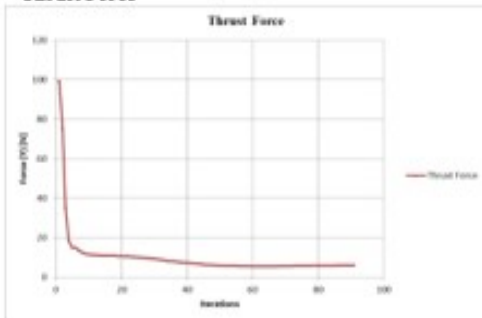
Step- 17
Run Calculation

X. RESULTS

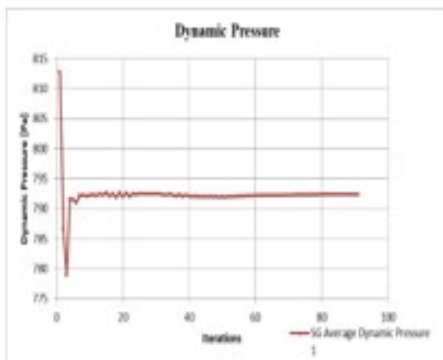
Drag Force



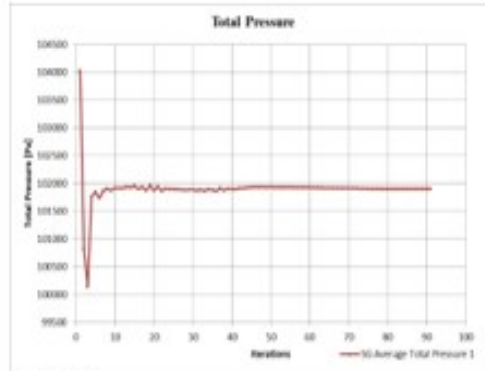
Thrust Force



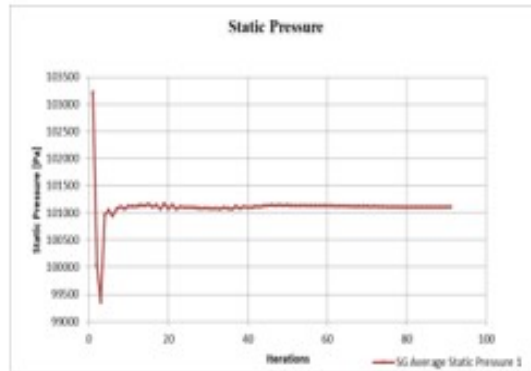
Dynamic Pressure



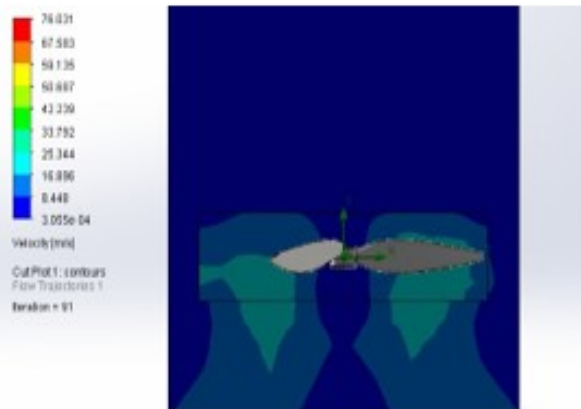
Total pressure

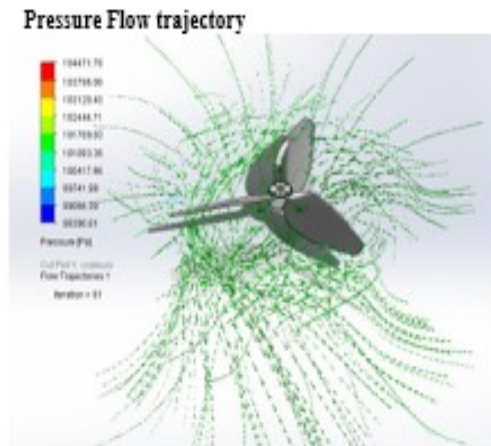


Static Pressure



Counter plots
Velocity contour





XI. CONCLUSION

A 3 blade propeller of diameter 254mm and a 3D CAD model is prepared with the combination of airfoils and radial distribution of NACA 4309, NACA 4410, NACA 4510, NACA 4512, NACA 5513 & NACA 5521 is prepared. The model is been analyzed through Ansys CFD following the steps as discussed above. It's been found that the developed propeller with carbon fiber material is capable of producing 5.7 N of thrust force at 3000 rpm. Hence we can use the developed propeller in any mini UAVs with the 1200 KV motor with an 11.1 v Lipo battery.

XII. REFERENCES

1. Design and Performance Evaluation of Propeller for Solar-Powered High-Altitude Long-Endurance Unmanned Aerial Vehicle. International Journal of Aerospace Engineering, Volume 2018, <https://doi.org/10.1155/2018/5782017>
2. Glasscock, R.R. Design, Modelling and Measurement of Hybrid Powerplant for Unmanned Aerial Vehicles (UAVs), Master's Thesis, 2012, Queensland University of Technology.
3. Ansys – 18 Fluent Tutorial Guide



International Journal of Scientific Research in Science, Engineering and Technology
Print ISSN: 2395-1990 | Online ISSN : 2394-4099 (www.ijsrset.com)
doi : <https://doi.org/10.32628/IJSRSET229249>

Design and Analysis of High Endurance Fixed Wing Multirotor UAV

Dr. Balaji B¹, Dr. Abhishek M R², Arun V³

¹Professor and Head, Department of Mechanical Engineering, K. S School of Engineering and Management, Bangalore, Karnataka, India

²Associate Professor, Department of Mechanical Engineering, K. S School of Engineering and Management, Bangalore, Karnataka, India

³Research Scholar, Department of Mechanical Engineering, K.S School of Engineering and Management, Bangalore, Karnataka, India

ABSTRACT

Article Info

Volume 9, Issue 2
Page Number : 277-287
Publication Issue :
March-April-2022
Article History
Accepted : 10 April 2022
Published: 21 April 2022

Current work emphasis on research, design and development of a fixed wing multirotor Unmanned Ariel Vehicle (UAV) which operate under V - TOL configuration. In this investigation an effort is made to develop a high endurance and high payload capacity UAV which can have a payload capacity of 15 Kg and which can serve with the endurance of 2 hrs per cycle.

Keywords : UAV, V-TOL, Fixed wing UAV, Solar Hybrid, High Endurance

I. INTRODUCTION

Aerial vehicles have proved their capability in both military field such as patrolling, surveillance as well as reconnaissance, and civil areas including transport, rescue and agriculture of various applications over a hundred years, while enhancing their capabilities over time, and fulfilling ever-changing mission requirements. By means of smaller, safer and lighter platforms, UAVs propose an exclusive set of advantages compared to piloted aircrafts [1]. Military and civil operations are the main areas where these advantages are effectively utilized. In addition, future UAVs are expected to perform much more extended missions with higher aerodynamic performance and higher degrees of automatic flight. There are two prominent

categories of mini UAVs; fixed-wing UAVs and multi-rotors. Fixed-wing UAVs are mini UAVs with propelled electrical batteries with longer ranges than UAVs with similar sizes of multi-rotor systems that require a runway or launcher for landing and knockout [2] [1].

The Fig.1 illustrates the mission profile chosen for the UAV. The multi-rotor UAVs have rotor systems generally carrying three or four propellers that are capable of vertical take-off and landing (VTOL) and hovering over an area while carrying sufficient payload. In addition, they are more maneuverable than fixed wing UAVs with the ability of quickly transition from hover to cruise flight. However, the horizontally mounted rotor system is placed at the wings or the

body that results in an enormous increase in drag force opposing the cruise flight. As a result of this decrement in the aerodynamic performance, fixed wing UAVs are more logical to be used to fulfil the missions needed high speed, long range and endurance flight. The fixed-wing UAVs has longer flight time and duration, but it is not simple to secure a safe landing space, especially in the city and rugged train areas. VTOL systems make more sense in operations such as mountainous and rural areas where there is no landing and take-off runway. In addition, VTOL systems must be used to operate like a helicopter in the required tasks such as hovering. However, if endurance is of first priority then a fixed wing type will most likely be preferred due to the efficiency of the cruise flight. If both of these features are demanded in a single operation then a fixed wing vertical and take-off landing (VTOL-FW) with level flight capability becomes the best option.

II. Mission Profile

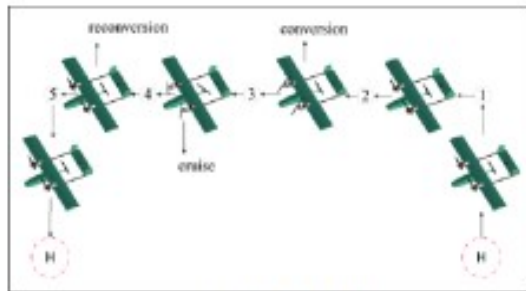


Fig.1 Mission Profile

III. Design Statement

Sl. No	Requirements
1	Minimum Endurance – 2Hrs
2	Maximum Payload – 15 KG
3	Maximum Speed – 150Km/Hr
4	Maximum Altitude – 6000m
5	Operational Temperature - 60° C

IV. Design Methodology

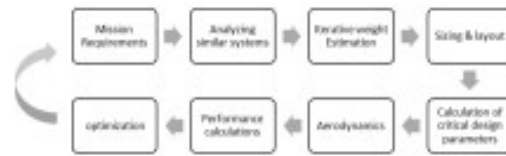


Fig. 2 Design Methodology

The design methodology illustrated in fig. 2 represents a iterative design process. As per the mission profile and operational requirements, the possible take-off weight of the UAV is estimated based on the historical data for general aircraft conceptual design i.e. ($W_e/W_{T0} = 0.85$). Knowing the minimum aerodynamic characteristics for the given operational range helps us to predict the preliminary sizing of major aircraft components and lifting devices required to sufficiently satisfy the mission requirements. Analyzing these initial sizing parameters at give operational conditions will help us to know more aerodynamic parameters to check for optimization and iterative calculations were considered to optimize the performance of the UAV [3].

V. Assumptions for the design

1. T/W = 1.5 (thrust to weight ratio)
2. Considered UAV as a light aircraft.
3. UAV will be powered with a hybrid power system. i.e. (Li-ion battery + Solar PV arrangement to increase the endurance)

VI. Design Process

A. Weight Estimation

$$\frac{W_{TO} - 15}{W_{TO}} = 0.85 \quad \text{Eq. 1}$$

Considering estimating the possible take-off and empty weight of an aircraft is the very first step in sizing of the UAV. The ratio of W_e / W_{T0} can be obtained from the historical data for conceptual aircraft design. It can be stated as W_e / W_{T0} is about

0.85. One of the design requirements of the UAV is to carry a payload of 15 Kg weight. As $W_e = W_{TO}$ ratio is about 0.85 at Eq. (1), then W_{TO} can be found as **100 Kg.**

In order to continue further, knowing the dimensions of the wing is very much important as wing plays major role to lift the aircraft in to the air. In order to know the dimensions of the wing a market study is been carried out considering the payload capacity and endurance that is relevant to our design statement. And we found that the average wing span for a UAV of carrying max. Payload of 15 Kg. with an endurance of 2 hrs in the range of 4.5 Km to 5 Km. As the larger aspect ratio reduces the power consumption to keep the given weight in the air and results in less induced drag wing span of 4.8 m is for preliminary sizing of the UAV.

B. Wing loading

With the wing span of 5 m and max. Take-off weight of the UAV i.e. 100 Kg got the wing loading as 40 Kg/m².

C. Initial sizing of the wing

Calculating the required lift co-efficient of the UAV at cruise velocity

With the basic understanding of aerodynamic forces, for steady state flight we know that

$$\text{Lift} = \text{Weight}$$

$$L = \frac{1}{2} \times V^2 \times \rho \times S \times C_L$$

As per one of the design requirement, the maximum flight speed as 150 Km/hr (i.e. velocity of 41.66 m/s) and flying altitude as 6000 m ASL. We found that the density of air is 0.661Kg/m³ @ 6000 m.

We know that the basic lift co-efficient formula as,

$$C_{Lc} = \frac{2 \times \left| \frac{W}{S} \right|}{V_c^2 \times \rho} \tag{Eq. 2}$$

Where;

- B. C_L = Lift Co-efficient
- C. W/S = Wing Loading in, Kg/m²
- a. V_c = Cruise Speed of the UAV, in m/s

- b. ρ = Density of air at flying altitude, in m
- c. W = Max. Take-off weight of the UAV in Kg
- d. S = Wing span in m

We found that the lift co-efficient required as =0.861 In order to find the lift coefficient for the wing & airfoil alone at cruise velocity;

$$C_{L@wing} = \frac{C_{Lc}}{0.95} \tag{Eq. 3}$$

$$C_{L@airfoil} = \frac{C_{L@wing}}{0.9} \tag{Eq. 4}$$

We found that;

$C_{L@wing}$	0.9071
$C_{L@airfoil}$	1.0779

Based on the $C_{L@airfoil}$ the selection of airfoil is made, considering the ability of the airfoil to produce sufficient lift with lesser angle of attack and larger stalling angle makes the airfoil suitable to use in the aircraft or UAV.

b. Selection of airfoil

As selection of an airfoil for any aircraft is always depends on the operational flight regime. Fig. 3 illustrates the various airfoil shapes for different flight regimes.

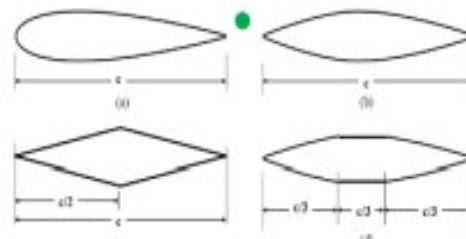


Fig. 3 Airfoil shapes for different flight regimes

And as our flight regime is subsonic a general use airfoil is selected. For low speed general light aircraft max. t/c of 15% to 18% is recommended. Selected t/c as 15%

Airfoil selected: NACA 23015

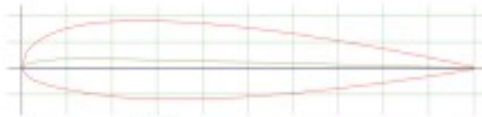


Fig. 4 NACA 23015 Airfoil

Performance characteristics of the airfoil are;

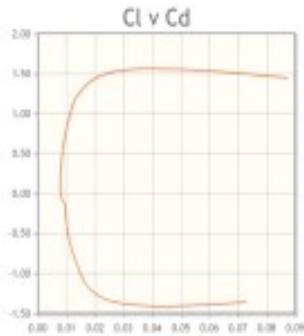


Fig. 5 C_l vs C_d

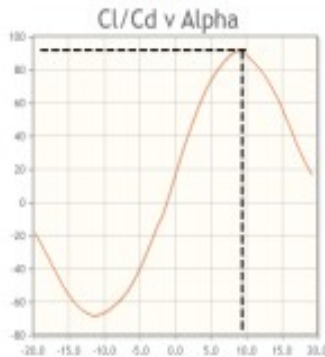


Fig 6 C_l/C_d vs Alpha

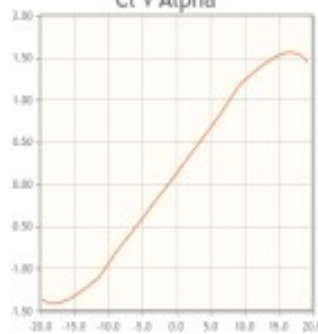


Fig.7 C_l vs Alpha

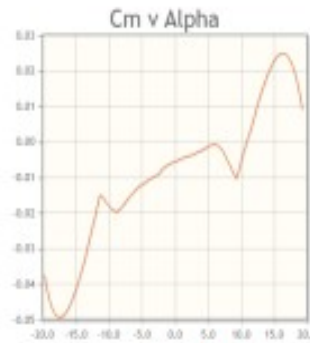


Fig. 8 C_m vs Alpha

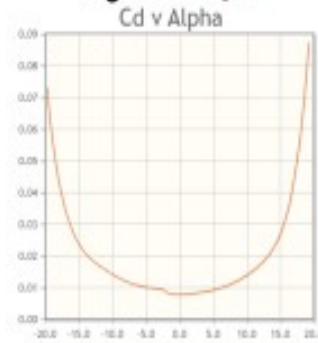


Fig.9 C_d vs Alpha

Analysis prerequisites;

Reynold's number = 10,00,000

Mach number = 0.12

Observations from Fig. 7;

- Max. C_l = approx. 1.7
- Stalling α = approx. 17°

Since the maximum C_l and stalling angle α is within the operating range.

NACA 23015 airfoil is selected. [9] [1]

Preliminary wing analysis

Parameter	Values	units
Maximum cruise speed	41.6	m/s
Max. Wing loading	40	Kg/m ²
Airfoil	NACA23015	
Aspect ratio	8.46	
Wing area	2.72	m ²
Wing span	4.8	m
Taper ratio	0.3	
Root chord, C _r	.6	m
Tip chord, C _t	.2	m
Sweep angle	0°	
Twist angle	2°	
Dihedral angle	1°	

With the basic understanding of aerodynamic principles, in order to get maximum endurance, the UAV must fly in a condition such that it is experiencing least drag and should produce maximum lift in order to keep the UAV in air. At the same time flying in C_L(3/2) / C_D maximum condition reduces the power consumption in order to produce thrust in cruise condition. After the iterative performance analysis over the market available UAV wing characteristics, from fig. 11 it's been observed that going for larger aspect ratio and increasing wing area for the given operating condition, will substantially makes the UAV statically and dynamically stable and aerodynamically safe design . [1]

Bending Moment

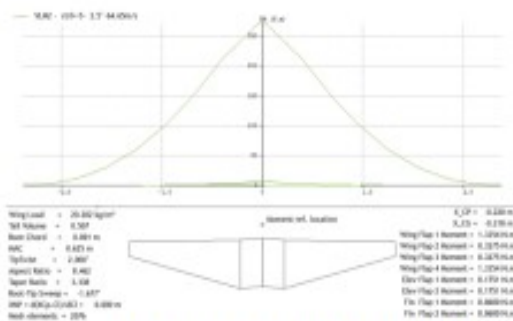


Fig. 10 Bending Moment of Preliminary wing

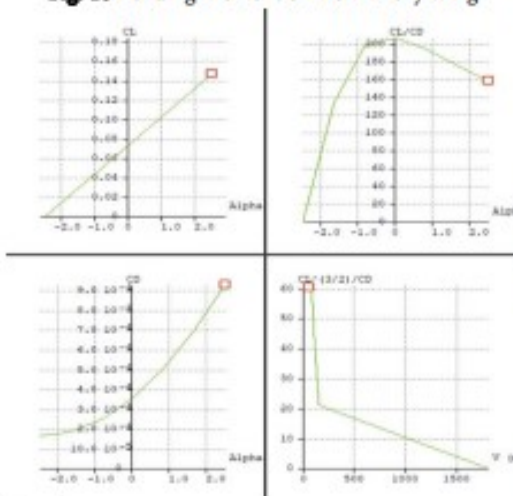


Fig. 11 Aerodynamic Performance of 4.8 m span wing

VII. Wing Sizing

Main wing

i. Span & Wing area

$$AR = \frac{b^2}{S}$$

Since, higher aspect ratio results in reduced wing loading and produces more lift, the aspect ratio of 10 is chosen for initial calculations. And by iterating for the better performance we found that the aspect ratio of 10.75 gives a better performance & span of 6 m is suitable for the wing loading of 40 kg/m² with the wing area of 3.347 m² [1].

ii. Taper ratio

$$\lambda = \frac{C_t}{C_r} \quad (0 \text{ to } 1)$$

Taper ratio plays a very important role to reduce induce drag, with the reference below found that the taper ratio of 0.3 can be used for most practical & good performative results [2].

iii. Mean aerodynamic Chord, Root & Tip Chord

Root Chord:

$$C_{root} = \frac{2S}{b(1 + \lambda)}$$

Up on substituting the span of 6m, wing area of 3.47 m² & taper ratio λ of 0.3, found that the suitable root chord length as 0.88 m.

Tip Chord:

$$C_{tip} = \lambda \times C_{root}$$

And with the root chord length of 0.88 m got the wing tip chord as 0.266 m.

Mean aerodynamic chord:

$$\bar{c} = \frac{2}{3} \times C_r \times \left[\frac{(1 + \lambda + \lambda^2)}{1 + \lambda} \right]$$

With the C_r & C_t of 0.88 m & 0.26 m found the mean aerodynamic chord length as 0.571 m.

iv. Sweep angle

Initially we considered the wing as a rectangular box with 0° sweep angle wing, due to the lift force produced by the wing it is assumed that the wing is experiencing a bending and shear load. And in reality addition to the normal load, the wing experiences a tangential forward force which equals the leading edge suction force minus the wing drag.

Typically sweep angle has a major contribution and corresponding effects on maximum lift produced, Drag co-efficient, critical MACH no. , Structural weight & Stability.

Selection of sweep angle can be made on the flight regime, as our flight regime is subsonic and with the MACH no. of 0.12 the sweep angle is chosen as 0°[7].

v. Twist angle

As we all know **Wing twist** or **Twist angle** is an aerodynamic feature added to aircraft wings to adjust lift distribution along the wing. And with the two categories of wing twist (i.e. geometrical twist and aerodynamic twist) aerodynamic twists are most commonly used in most of the monoplanes and light aircrafts to avoid the tip stalling [7].

Considering our UAV as a light aircraft the aerodynamic twist is assumed as 2°

vi. Dihedral angle

As our selective wing type is a high wing type, and 2° of dihedral angle is been used to as it affects the roll movement of the UAV proportional to the amount of sideslip. The effect produced by the above condition is

also known as Dihedral effect. Dihedral effect is also a critical factor in the stability of an aircraft about the roll axis (the spiral mode). It is also pertinent to the nature of an aircraft's dutch roll oscillation and to maneuverability about the roll axis [7] .

vii. Selection of high lifting devices

High lift devices are movable surfaces or, in some cases, stationary components that are designed to increase lift during some phases or conditions of the flight. The most common high lift devices are flaps, slats and Krueger flaps, but the category also includes less common installations such as lead-edge root extensions.[7]

The main purpose of using the high lifting devices are:

- To allow a steeper approach without increasing the speed of the aircraft
- Reduces the distance required to take-off and land
- Reduces the speed at which the aircraft will stall
- They increase the pilot's visibility of the runway

Effects of using Flaps

▪ **Relation with Centre of pressure:**

Flap movement, up or down, will cause a change of pitching moment. This is due to Centre of Pressure (CP) movement.

Centre of pressure is a point where all the lift of the aircraft is considered to be concentrated.

▪ **Relation with lift and drag:**

Lowering flap increases both lift and drag, but not in the same proportion. Although the lift is a larger force, and proportional increase in the drag is greater, so the maximum lift/ drag ratio decreases.

In our case **fowler type flaps are used** as it is most widely used in all the military, modern aircrafts which allows our UAV will have a suitable and appropriate function to maintain the operational requirements. [7]

viii. Final design Parameters of Wing

Parameters	Values	units
Maximum cruise speed	41.6	m/s
Max. Wing loading	40	Kg/m ²
Airfoil	NACA23015	
Aspect ratio	10.75	
Wing area	3.347	m ²
Wing span	6	m
Taper ratio	0.3	
Root chord, C _r	.88	m
Tip chord, C _t	.26	m
Sweep angle	0°	
Twist angle	2°	
Dihedral angle	1°	
Material of the wing	Polyethylene terephthalate - PET	

Bending Moment Diagram

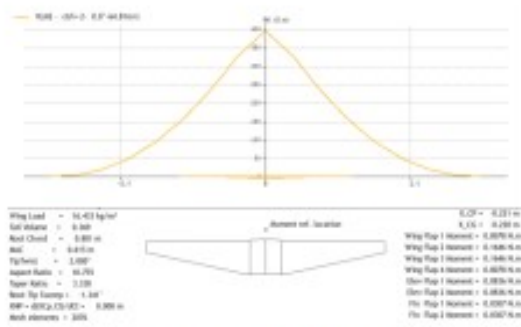


Fig. 12 Bending moment plot of 6 m span wing

Comparison of aerodynamic characteristics of 4.8 m Span wing & 6 m Span wing

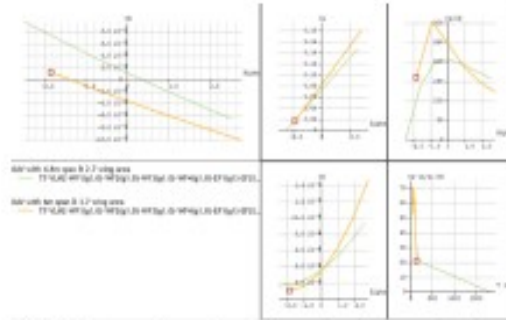


Fig. 13 Comparison of aerodynamic characteristics
From Fig 13 (C_n vs Alpha plot) we can observe that the co-efficient of moment of the wing got reduced which increases the lateral and longitudinal stability of the wing. And the minimum C_i of the wing is increased along with the decreased C_a . C_l / C_d max improved and we can get max. Lift with lesser cruise speed compared to 4.8 m span wing.

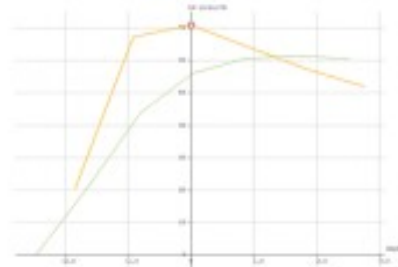


Fig. 14 C_L^{max} / C_D

From Fig. 14 we can observe that C_l / C_d max improved at 0° AOA. Therefore we can get maximum lift at lower flight speed at cruise flight. And results in less power consumption to produce forward thrust.

Sizing of the control surfaces

Elevators or Horizontal stabilisers

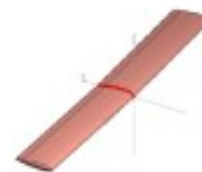


Fig. 15 Elevator

Rudders or vertical stabilizers

Parameters	values	Units
Span	0.9	m
Root chord	0.24	m
Tip chord	0.24	m
Airfoil	NACA 23015	
Position of elevator	1.5 m (from leading edge of the root chord of the wing) and 0.3 m from the neutral axis of the fuselage	
Material	Polyethylene terephthalate – PET	



Fig. 16 Rudder

Parameters	values	Units
Span	0.3	m
Root chord	0.28	m
Tip chord	0.2	m
Airfoil	NACA 23015	
Position of elevator	1.5 m (from leading edge of the root chord of the wing) at both sides of the elevator.	
Material	Polyethylene terephthalate – PET	

Sizing of the fuselage

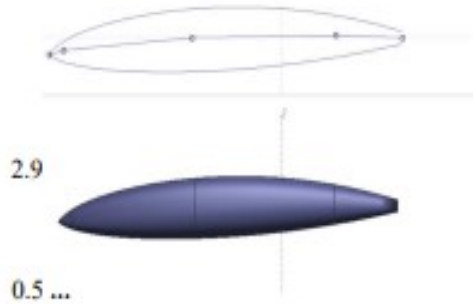


Fig. 17 Fuselage Sizing

VIII. Aerodynamic & stability analysis

Developed blended wing and body configuration



Fig.18 Preliminary UAV model

i. Pressure distribution over the UAV configuration

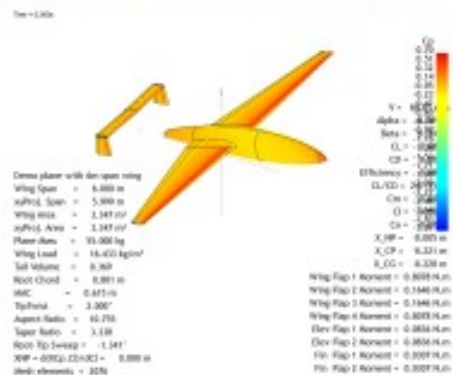


Fig. 19 Pressure Plot

ii. Trimmed conditions

Modal results

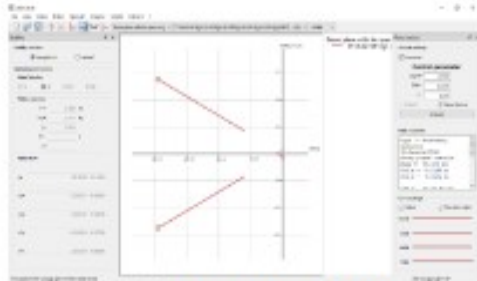


Fig. 22 Longitudinal Stability

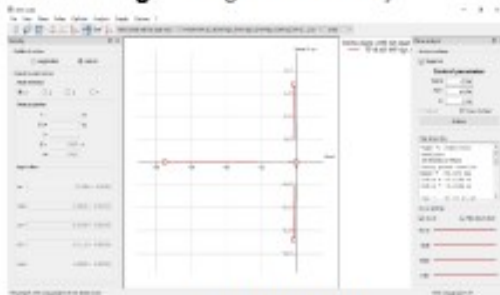


Fig. 23 Lateral Stability

Propulsion system

No. of motors: 4 + 1 (4 – VTOL & 1- cruise)

Propeller size: 30 in propeller

Power consumption breakdown

Mission Conditions	Power consumption
Take-off	648.58 W
Climbing	689.62 W
Cruise	2400 W
Descending	689.62 W (conservative)
Landing	640 W
Total power consumption	5100 (aprox.)

Batteryspecifications

Battery type: Li-po

Output voltage = 44.4 V

Power = 6000 W

C-rate = 0.5

Current 136 Ah

Weight breakdown

Components	mass (g)	Qty.	Tot. Mass (g)
motors (X-Team BLDC 100 kv 8320)	618	5	3090
ESC (Ready to sky 80A)	100	5	500
80A 200A Large current PDB	15	1	15
Battery 6s 16000 mAh	1900	4	7600
FCU, GPS, Power module, Receiver	800	1	800
propeller	200	5	1000
servo	60	5	300
Fuselage (including frame and consumables like nuts & bolts)	6000	1	6000
Main wing	15000	1	4000
Elevator	4000	1	4000
Fins	400	2	800
Landing gears (Main landing gear & Nose landing gear)	2100	1	2100
Solar charging setup	1500	1	1500
Payload	15000	1	15000
Total weight in KGs.			46.70

Solar charge control system

In order to get the maximum endurance the UAV, a solar charge control system is used.

Solar PV panels chosen: : Sun Power C-60

Mono crystalline PV cells No. of cells used: 48

(in series)

Voltage produced from each cell: 0.6 V

By connecting 48 PV cells in series we get a output voltage of 28.8 V. and to maintain the required power at a constant rate a MPPT charge controller in used and which acts in between the solar PV cells and the battery system. And this configuration helps us to increase the endurance of the UAV[5].

Performance of the UAV

V-n Diagram

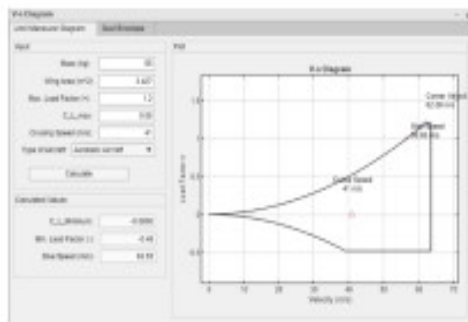


Fig. 25 V-n diagram

Gust Envelope

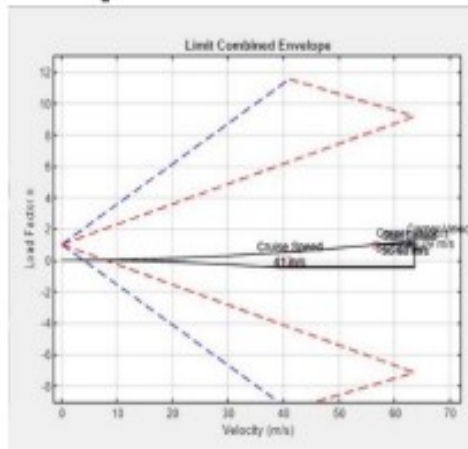


Fig. 26 Gust Envelope

IX. CONCLUSION

In this work, an approach to design a high endurance and high payload capacity unmanned air vehicle is

made. This course work demonstrates the various steps to be followed in designing of a fixed wing multirotor V-tol Configuration UAV, a CAD model is developed using X-flr software to evaluate the characteristics & performances of the generated CAD model. In order to have a high endurance and flight time along with the batteries and approach to use Solar-Hybrid method is used by using solar PV modules as discussed above. It is been found that the developed UAV model will satisfy the operational requirements mentioned in the design statements during our system level development.

X. REFERENCES

- [1]. R. Austin, Unmanned Aircraft Systems: UAVS Design, Development and Deployment, WILEY, 2010.
- [2]. "unmannedsystemstechnology.com," Aug 2019. Online. Available: <https://www.unmannedsystemstechnology.com/company/elevonx/>.
- [3]. G. o. I. DGCA, "Drone Rules 2021," 2021.
- [4]. K. A. K. a. K. E. V, "Trends in the development of the global civil drones," Eastern State Transport University, 2018.
- [5]. Liebeck, Design of the Blended Wing Body Subsonic Transport, Journal of Aircraft, Vol. 41(1), 2004, pp. 10-25.
- [6]. "The Global Drone Regulation Landscape 2018," Business Insider Intelligence, 2018.
- [7]. M. H. Sadraey, Design of Unmanned Aerial Systems, WILEY, 2020.
- [8]. xflr, "Stability Analysis with XFLR," 2017.
- [9]. xflr, "Aerodynamic Analysis with XFLR," 2018.

Cite this article as :

Dr. Balaji B, Dr. Abhishek M R, Arun V , "Design and Analysis of High Endurance Fixed Wing Multirotor UAV", International Journal of Scientific Research in Science, Engineering and Technology (IJSRSET), Online ISSN : 2394-4099, Print ISSN : 2395-1990, Volume 9 Issue 2, pp. 277-286, March-April 2022. Available at doi : <https://doi.org/10.32628/IJSRSET229249>
Journal URL : <https://ijsrset.com/IJSRSET229249>

Photos



Design & Development of Fixed wing Multirotor UAV For Quick Medical Response - 2022

